Thesis for the Degree of Doctor of Philosophy

Design and development of a novel textile-based bioreactor: Ethanol and biogas production as case studies

---

Osagie Alex Osadolor

UNIVERSITY
OF BORÅS

Design and development of a novel textile-based bioreactor: Ethanol and biogas production as case studies

Swedish Centre for Resource Recovery

Faculty of Textiles, Engineering and Business

University of Borås

SE-501 90 Borås, Sweden

ISBN 978-91-88269-80-5 (printed)

ISBN 978-91-88269-81-2 (PDF)

ISSN 0280-381X, Skrifter från Högskolan i Borås, nr. 85

Electronic version: http://urn.kb.se/resolve?urn=urn:nbn:se:hb:diva-13165

Cover page design: Suss Wilén

Printed in Sweden by Stema AB

Borås 2018

I dedicate this thesis to the Almighty God and my beloved wife Chidinma; you are a rare gem, you blossomed in the midst of the adversity we faced in the course of this PhD study.

Abstract

Bioreactors are designed to provide enabling conditions for the controlled growth of microorganisms, such as good heat and mass transfer, aeration, hydrodynamics, geometry for adequate gas holdup, pH and foaming control, conditions for optimal substrate consumption and product formation, as well as mechanisms for monitoring microbial conditions. Additionally, bioreactors are designed to handle stress that would be exerted on them by the weight of the fermenting media and by the high pressure used for sterilisation. Bioreactors are usually constructed with materials such as stainless steel, carbon steel and borosilicate glass, which must be suitable for growing the fermenting microbes, be inert and corrosion proof. In this thesis, a textile-based bioreactor was designed and developed for aerobic and anaerobic fermentation-based production processes with emphasis on mixing, mass transfer, temperature control, rheology, hydrodynamics and stress containment in the bioreactor.

Temperature control was carried out using a heat control tubing either at the bottom of the bioreactor or as a heating jacket around its vertical height. The developed temperature control system was tested anaerobically and aerobically. Under anaerobic conditions with yeast it resulted in 200 % increase in ethanol productivity in comparison with the prototype without temperature control.

A mixing system was developed for flocculating microbes and tested for anaerobic fermentation processes such as ethanol and biogas production. The developed mixing system led to the elimination of mass transfer limitation even at 30 times less bulk flow conditions. The mixing system also favoured stable bed formation, and the possibility of operating the bioreactor at a dilution rate above 1/h for ethanol production using flocculating yeast. A mixing system was also developed for aerobic fermentation and it led to improved media rheological and hydrodynamic performance of the bioreactor for fungi fermentation. The improved performance could be seen from minimised foam formation and stabilisation at an aeration rate of 1.4 VVM on a viscous, integrated first- and second-generation ethanol substrate with an initial viscosity of 93 cP.

The stress that would be exerted on the bioreactor when used for large-scale applications was simulated and validated at laboratory scale. For 100–1000 m^3 bioreactor, the tension per unit length that would be exerted on it would be between 300–20000 N/m.

In this thesis, it was found that the use of the developed textile bioreactor was effective in reducing the fermentation-associated investment cost by 21 % or more, introducing flexibility and addressing several technical problems associated with both anaerobic and aerobic fermentation-based production processes.

Keywords: bioethanol; biogas; bioreactor; bioreactor design; techno-economic analysis; membrane stress analysis; mass transfer; hydrodynamics

List of publications

Publications in this thesis

I. **Osadolor OA**, Lennartsson PR, Taherzadeh MJ. Introducing textiles as material of construction of ethanol bioreactors. Energies. 2014 Nov 18;7(11):7555-67.

II. **Osadolor OA**, Lennartsson PR, Taherzadeh MJ. Development of Novel Textile Bioreactor for Anaerobic Utilization of Flocculating Yeast for Ethanol Production. Fermentation. 2015 Nov 23;1(1):98-112.

III. **Osadolor OA**, Lundin M, Lennartsson PR, Taherzadeh MJ. Membrane stress analysis of collapsible tanks and bioreactors. Biochemical Engineering Journal. 2016 Oct 15;114:62-9.

IV. **Osadolor OA**, Nair RB, Lennartsson PR, Taherzadeh MJ. Empirical and experimental determination of the kinetics of pellet growth in filamentous fungi: A case study using Neurospora intermedia. Biochemical Engineering Journal. 2017 Aug 15;124:115-21.

V. Patinvoh RJ, **Osadolor OA**, Horváth IS, Taherzadeh MJ. Cost effective dry anaerobic digestion in textile bioreactors: Experimental and economic evaluation. Bioresource technology. 2017 Dec 1;245:549-59.

VI. **Osadolor OA**, Nair RB, Jabbari M, Lennartsson PR, Taherzadeh MJ. Effect of media rheology and bioreactor hydrodynamics on filamentous fungi fermentation of lignocellulosic and starch-based substrates under pseudoplastic flow conditions (Submitted).

Statement of contribution

My contributions to each of the publications are as follows:

Paper I: Responsible for part of the idea, performed all experimental work, analysed the data and wrote most of the manuscript.

Paper II: Responsible for the idea, performed all experimental work, analysed the data and wrote the manuscript

Paper III: Responsible for part of the idea, carried out the simulations, performed the experiments and wrote the manuscript.

Paper IV: Responsible for the idea, designed the experiments, analysed the data and wrote the manuscript.

Paper V: Responsible for the techno-economic analysis using experimentally generated data and wrote the techno-economic aspect of the manuscript.

Paper VI: Responsible for the idea, designed the experiments, performed part of the experiments, analysed the data and wrote the manuscript.

List of publications not in this thesis

Articles:

I. Patinvoh RJ, **Osadolor OA**, Chandolias K, Horváth IS, Taherzadeh MJ. Innovative pretreatment strategies for biogas production. Bioresource technology. 2016 Nov 22.

II. Jabbari M, **Osadolor OA**, Nair RB, Taherzadeh MJ. All-Polyamide Composite Coated-Fabric as an Alternative Material of Construction for Textile-Bioreactors (TBRs). Energies. 2017 Nov 21;10(11):1928.

III. Nair RB, **Osadolor OA**, Ravula VK, Lennartsson PR, Taherzadeh MJ (2017) Filamentous fungi (edible)- Neurospora intermedia for integrating lignocellulose to starch-to-ethanol process (Submitted).

Insight

From when I was young, I always loved making or doing practical things that would positively affect me and those around me. When I was in secondary school (high school), I joined a club called junior engineers scientist and technologist (JETS) club. We worked on different science projects back then; it was interesting using carbon dioxide to turn lime water milky etc. Back then I believed that it was possible to have smart or portable production facilities and various green energy sources that one could turn on or off at will (perhaps I watched way too much Dexter's Laboratory animation). This desire was part of why I chose to study Chemical engineering at bachelors and masters level. I knew I needed to get a doctorate to get good understanding of how to conduct research in Chemical engineering which is what led me to the University of Borås in Sweden.

When I discussed with Professor Mohammad Taherzadeh about doing a PhD with him, he suggested the development of a portable bioreactor made with textile-based material for bioethanol and biogas production. I was more than happy to accept it as it aligns with what I like doing. That was how my PhD journey started. My first task was to develop the bioreactor for producing bioethanol using baker's yeast. I reviewed literature and knew that I had to include basic bioreactor features including a means for temperature control and mixing for the bioreactor to work properly (**Paper I**).

The findings from the first bioreactor design were promising, and so I knew it would be interesting to see if the first basic design in which mixing is carried out with recirculation would be sufficient for fast-settling microorganisms. This was important to me because I knew it could mean that a smaller bioreactor volume could achieve improved productivity. I did some mass transfer calculations and found out that I needed to design a mixing system inside the bioreactor. I did this and found out that I could increase bioethanol productivity, reduce fermentation time and increase product yield by using the mixing system inside the bioreactor (**Paper II**)**.** Similar observations with improve bioreactor performance were obtained for aerobic fermentation (**Paper VI**).

To carry out an effective design, it is important that certain data critical for the design calculations are available. When some of the data are not available, a kinetic study comes in handy (**Paper IV**). Using the data from the kinetic study, the mixing system in the textile-based bioreactor was developed for aerobic applications. Interestingly, the bioreactor performed better than a laboratory-scale airlift or bubble column bioreactor as evidenced by minimised foaming under high aeration rates (**Paper VI**).

As promising as the results from designing and developing the textile-based bioreactor has been, I know that cost and safety among other factors are paramount if the bioreactor is to find applications where it matters the most in the real world (not in the lab). Therefore, an economic evaluation of the profitability of using the textile-based bioreactor as a means for handling solid waste from farms at small, medium and large scales via dry anaerobic digestion over other conventional methods was performed. The economic evaluation showed that using the bioreactors for dry digestion was very economical (**Paper V**). In addition, the level of safety of the bioreactor particularly for medium- to large-scale purposes was reported in **Paper III**.

In conclusion, there are some success stories from this PhD study but they did not come without several failures, hardship or sacrifices which I choose not to mention here. Those challenges were strong but my desire to excel was stronger. I know I have not yet achieved my ambition of contributing to the widespread adoption of portable reactors for energy production but I am getting closer to it.

Osagie Alex

Nomenclature

ACE	Annual capital expenditure
AD	Anaerobic digestion
APC	Annual production cost
CE	Capital expenditure
COD	Chemical oxygen demand
CSTR	Continuous stirred tank reactor
DO	Dissolved oxygen accumulation rate
IRR	Internal rate of return
NPV	Net present value
OC	Operating cost
OTR	Oxygen transfer rate
OUR	Oxygen uptake rate
PBP	Payback period
POME	Palm oil mill effluent
q_o	Specific oxygen uptake rate
TS	Total solid
VFA	Volatile fatty acids
VS	Volatile solid
VVM	Volume per volume per minute
WC	Working capacity or liquid volume fraction

Table of contents

1. Introduction

Fermentation, the breakdown of organic substrates such as monosaccharides, amino acids, and glycerol [1] by microorganisms to generate different acids, alcohols and gaseous by-products [2] usually in the absence of inorganic electron acceptors like nitrate, sulphate or oxygen [3] has long been known to man. Fermentation-based production offers several benefits over chemical production such as lower energy requirement and the use of renewable and sometimes cheaper raw materials; besides, certain products are best produced via fermentation [4]. Current examples of fermentation-based products include antibiotics, biofuels, amino acids, biopharmaceutical drugs, enzymes, proteins, biopolymers, microbial biomass and food flavours.

Despite the benefits of fermentation-based production, the design of fermentation equipment before the twentieth century was mostly empirical without the applications of chemical engineering principles like heat or mass transfer [5]. This led to difficulties in translating fermentation technologies like penicillin production to industry scale [6]. Overcoming the challenges in industry-scale penicillin manufacture by the application of chemical engineering principles in fermentation vessels (subsequently referred to as bioreactors) has been a crucial aspect that highlights the importance of structured design when making bioreactors.

Over time, several bioreactor designs such as continuous stirred tank bioreactors, bubble column and airlift bioreactors have emerged to address the technical challenges of fermentation-based production. Despite this, still several challenges associated with bioreactors exist such as the high cost of conventional bioreactors and the lack of flexibility in the applications of some bioreactor designs (for example, some bioreactor designs are not suitable for combined application for fermentation processes with high mass transfer limitation and shear-sensitive microorganisms) [7]. To address some of these challenges, for the last few decades, several biopharmaceutical and protein production facilities have started using single-use bioreactors made from polymeric materials as bioreactors due to the high investment and operational cost associated with conventional stainless steel-based bioreactors [8]. The use of this kind of bioreactors has minimised the need for other bioprocessing equipment, leading to over 60 % reduction in the fixed capital cost of plant-based bio-production facilities [9]. However, these single-use bioreactors have limited applications for several reasons such as

these bioreactors have a limited scale of application (can only be used below 2 m^3 on its own), are not suitable for continuous production and can be easily damaged [8]. Hence, the need for improvements in bioreactor technology to boost the economics and productivity of fermentation-based production still exists.

The need for the introduction of a new bioreactor design that addresses the challenges of high cost, process flexibility, ease of operations, and small-, medium- and large-scale applicability was the driving force for the introduction of the textile-based bioreactor. The design and development of this novel bioreactor was the basis of this study, and bioethanol and biogas production were the fermentation-based production investigated in this thesis.

1.1 Aim of the study

The aim of this thesis was to introduce bioreactor features in the textile bioreactor vessel so that the textile-based bioreactor can be used in a cost-effective way while also achieving safe and efficient production of fermentative products. This was done using bioethanol and biogas as examples of fermentation-based products, with emphasis on five main areas:

1. The introduction and development of a temperature control mechanism for effective heat transfer in the textile-based bioreactor (**Papers I, II, V** and **VI**)
2. Overcoming mass transfer limitation associated with aerobic and anaerobic fermentation processes (**Papers II, IV** and **VI)**
3. The introduction and development of a mixing system in the bioreactor for both aerobic and anaerobic applications (**Papers I, II** and **VI**)
4. Good fluid flow rheology in the bioreactor and vessel geometry suitable for adequate gas holdup time (**Paper VI)**
5. Ensuring safety in the application of the bioreactor particularly for medium- to large-scale purposes (**Paper III**)

1.2 Thesis structure

This thesis consists of seven main chapters as follows:

- Chapter 1 introduces the thesis, its aim and structure.
- Chapter 2 introduces flexible and deformable vessels referred to as collapsible tanks, their benefits and applications. It presents a platform for the introduction of the textile-based bioreactor as a bioreactor with all the benefits of collapsible tanks.
- Chapter 3 talks about bioreactors, their historical development, challenges of conventional bioreactors and chemical engineering theories and concepts needed for efficient bioreactor design and operations.
- Chapter 4 discusses the main bioreactor features that were designed, introduced and developed for the textile-based bioreactor for its efficient application in aerobic and anaerobic fermentation processes. It also gives some perspectives on bioethanol and biogas production.
- Chapter 5 presents the summary of findings from the economic studies performed using the textile-based bioreactor for ethanol and biogas production.
- Chapter 6 discusses about the safe application of the textile-based bioreactor particularly at medium and large scales.
- Chapter 7 gives the summary of findings and future recommendations.

1.3 Social and ethical reflections

The overall goal of research is to find out ways of making life better for mankind. This thesis adopts this idea. If we take biofuel production as an example, the cost of biofuel production is a leading challenge associated with the use of biofuels [10]; hence finding economic ways of producing biofuels would make the benefits of using biofuels to be fully appreciated and realised and using cost-effective textile-based bioreactors would help in addressing this challenge. In addition to this, the flexibility as well as the ease of transportation and installation of the bioreactor mean that it can reduce project completion time, introduce flexibility in fermentation-based production and aid the setting up of fermentation processes in areas of the world where there is lack of technical expertise needed for operating conventional bioreactors. These benefits could lead to the creation of more jobs, improved standard of living associated with increased production of fermentative products and reduction in environmental emissions

that would come from the reduced dependence on technologies that are not environmentally friendly. Further, when the bioreactor is used for biogas production in households, the produced biogas can be used for cooking, thus reducing health issues associated with old-style cooking methods used in rural areas.

2. Collapsible tanks

2.1 Collapsible tanks – portable and flexible storage

Over time, the need for storage, transportation and containment have led to the use and development of tanks. Conventionally, tanks are rigid and have a definite shape once installed. However, certain applications which require easy installation, portability, flexibility and short-term applications have led to the introduction of collapsible tanks [11]. Collapsible tanks, also called pillow or bladder tanks, are vessels made with light, easily deformable and flexible materials such as reinforced PVC, thus giving them a naturally deformable shape defined by the nature of the material contained within them [12, 13]. The benefits of collapsible tanks over rigid tanks include ease of transportation, ease of setup, portability, relatively less cost, ease of utilisation and multiplicity of application [11, 14-16]. The main drawback of collapsible tanks in comparison with rigid tanks is that they are prone to failure due to the low material strength of the polymers used for making them or from the separation of their material of construction where they are welded or joined together.

2.2 Applications of collapsible tanks

The benefits of collapsible tanks over rigid tanks have led to the application of collapsible tanks to small- and medium-scale processes [9]. Collapsible tanks are used for several applications such as specialised space-based applications, aviation-based applications, military applications, air bags in vehicles, waste storage, fuel storage, water storage, chemical storage and, more recently, as bioreactors (**Paper I–III,V**) [15-19].

In addition to the previously mentioned benefits of collapsible tanks in section 2.1, an important distinguishing feature of collapsible tanks is that they can be designed for use in non-conventional or customised applications. For example, they can be used in regions where there is space limitation, locations where access is limited or difficult and where the available space has an unusual geometry. An application of collapsible tanks for storage for up to 80 m^3 with space limitation is shown in Figure 2.1a. Other applications of collapsible tanks are shown in Figure 2.1.

Figure 2.1: Applications of collapsible tanks for different purposes in (**a**) a commercial facility with space limitation, (**b**) a food storage facility, (**c**) transportation and (**d**) a chemical production facility. Reproduced with permission from Waterplex Australia[1].

2.3 Design of collapsible tanks

Collapsible tanks are designed with an overall goal of meeting the requirements of their end-use application. Some of the key considerations before the fabrication of collapsible tanks are the area they will occupy, the properties of the material that would be contained in the collapsible tanks, the duration for which they will be used, the pressure or stress that would be exerted on the collapsible tank, and the external and internal environmental conditions at which they will be used (**Paper III**) [20-23]. The material used for constructing collapsible tanks is

[1] http://waterplex.com.au

usually joined together using different techniques like hot air welding, hot bar welding and, more recently, using adhesives to form the final product [24, 25]. When the collapsible tank has been formed, its natural morphology when filled with a fluid is similar to that of a pillow; hence, they usually called pillow tanks.

Sometimes, the fluid or material that would be contained in the collapsible tank exerts high tension on the joints of the collapsible tanks. To overcome this challenge, particularly at medium scale, the joints are usually framed or extra self-support is added to the collapsible tank using self-reinforcement of the fabricating material (Figure 2.1 A). Additionally, the natural pillow morphology can be changed by using different methods like having metallic reinforcement at the joints of the construction material, putting the collapsible tank inside a rigid material to give the shape of the material or using adhesives to join the material of construction to the desired shape (Figure 2.2).

Figure 2.2: Collapsible tanks with shapes different from the natural pillow shape. Images are reproduced with permission from Waterplex Australia[1] and FOV biogas India[2].

[1] http://waterplex.com.au
[2] fovbiogas.com

2.4 Introducing collapsible tanks as bioreactors

A reactor is a vessel in which reactants are converted to products. A bioreactor is a reactor that uses microorganisms or enzymes from microorganisms for transforming reactants to products. Conventionally, bioreactors are made using materials that are inert, non-corrosive and can provide the enabling environment needed for growing microorganisms needed for the production of the desired product [5]. Additionally, the material of construction should be able to withstand the stress exerted on the vessel by steam pressure (1–2 bar) during sterilisation or the pressure that the bioreactor fluid would exert on it. Therefore, stainless steel is typically used for the construction of bioreactors especially for medium- or large-scale applications [4, 20].

Due to the high pressure requirement during sterilisation, to safeguard against failure- or pressure-associated work hazards, bioreactors are designed as pressure vessels [20]. However, using these bioreactors increases the capital investment cost of fermentation-based facilities. For example, in ethanol production facilities, the bioreactor contributes 25–35 % of the fermentation-based capital investment cost [26], while bioreactor and aseptic bioprocessing equipment contribute over 60 % of the fixed capital cost of plant cell-based bio-production [9]. Because of this high cost, alternatives to conventional bioreactors have emerged over time and the most prominent replacement particularly for pharmaceutical or goods manufacturing practices-associated fermentation facilities are the single-use or disposable bioreactors [8].

An application of flexible materials in bioreactors can be found in lagoon bioreactors, in which a flexible material could be used to cover the lagoon or used in lining its sides to prevent leakage. Another application of flexible materials in making bioreactors is in single-use bioreactors. These bioreactors are completely made of the flexible material, giving them the natural pillow shape of collapsible tanks [8]. They can also be kept inside rigid vessels to give them the desired geometry and support [9]. However, as their name implies, they are only used once and then discarded, and this makes them unsuitable for fermentation-based production facilities with high production rates and short production cycles or for long-term continuous production applications. Further, as these bioreactors are made of plastics, disposing them poses an environmental challenge, and hence the need for alternative solutions. In 2013, a collapsible tank constructed with textile as its backbone material of construction was introduced for anaerobic fermentation for biogas production [18]. This textile-based bioreactor combines the previously mentioned advantages of collapsible tanks with improved material strength, UV resistance and ability to be sterilised either with steam or chemicals. Figure 2.3 shows a picture of one of the textile-based bioreactor vessels that was used in this thesis.

Figure 2.3: A 30 L laboratory-scale textile-based bioreactor prototype.

This thesis elaborates on the developments that have been made on the textile-based bioreactor for aerobic and anaerobic fermentation from a chemical engineering perspective using bioethanol and biogas production as case studies. Simulations were carried out to determine the stress that would be exerted on the bioreactor when used for medium- or large-scale applications and how the stress can be minimised (**Paper III**).

3. Bioreactor design and development

3.1 History and development in bioreactor technology

A bioreactor is a reactor or vessel in which microorganisms, enzymes, plant cells or mammalian cells are used for transforming substrates to product through fermentation, under controlled conditions suitable for the fermentation process. Fermentation, the basis on which bioreactors started to find applications, has been known to man since early civilisation as evidenced by the production of cheese, wine and beer which predates structured production using chemical engineering principles. During this period, emphasis was placed more on hygiene and product quality [5]. This did not change until the commercial production of acetone and butanol during the first world war [27]. The unique feature that was introduced to the acetone–butanol bioreactors back then was centred on maintaining a strict anaerobic environment [5], which was a key requirement for *Clostridium acetobutylicum* to carry out the conversion of starch or sugars to acetone and butanol [27, 28]. The creation of the anaerobic environment helped in preventing contamination and other work hazards associated with acetone–butanol production.

The next major development in the history of bioreactors was the submerged fermentative production of penicillin during the Second World War [4, 5] that introduced the use of aeration and mechanical mixing in bioreactors [29]. Due to the instability of penicillin production at small scale, a standard method of cell transfer from shake flasks to seed tanks and then submerged bioreactors was developed [29]. Additionally, a separation technique was combined with the fermentation process to improve the quality of penicillin. This method of fermentation was in turn transferred to the production of other antibodies, vitamins, amino acids and other organic compounds [4]. This was the platform that led to using continuous stirred tank bioreactors for fermentation-based production [5]. Over time, several other types of bioreactors have been introduced such as the bubble column bioreactor, airlift bioreactor, fluidised bed bioreactor, trickle bed bioreactor, tray bioreactor, rotary drum bioreactor, continuous screw bioreactor and wave bioreactor. A timeline depicting the introduction of different bioreactors is shown in Figure 3.1.

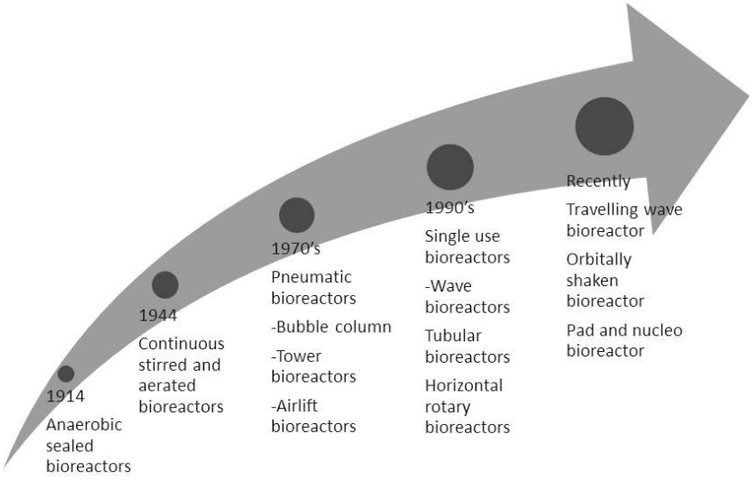

Figure 3.1: Timeline for the introduction of different bioreactor designs based on the mixing mechanism [9, 30-32].

From a technical perspective, the factors that have contributed to the introduction of different bioreactors designs include the morphology and shear sensitivity of the microorganism, mixing requirement of the fermentation process, the intended mode of operation of the bioreactor, mass transfer requirement of the fermentation process and the rheological properties of the fermentation broth. The continuous stirred tank bioreactor design was introduced to achieve good mass transfer and mixing, with mixing carried out by means of mechanical stirrers. The airlift, bubble column and fixed bed bioreactors were introduced for fermentation applications with shear sensitive microorganisms such as filamentous fungi [33]. For the bubble column bioreactor design, mixing is carried out solely by aeration occurring in one direction while the airlift design uses aeration with mixing occurring both in the riser and down-comer sections of the bioreactor. Wave or single-use bioreactors were introduced for batch-based fermentation

applications in which the growth rate or productivity is too low for continuous applications to be economical such as plant-based fermentation or shear sensitive mammalian cells fermentation [9]. The wave bioreactor design uses the rocking motion of the bioreactor to create wavelike motion of the fermentation media inside the bioreactor. The schematic representation of some bioreactor designs is shown in Figure 3.2.

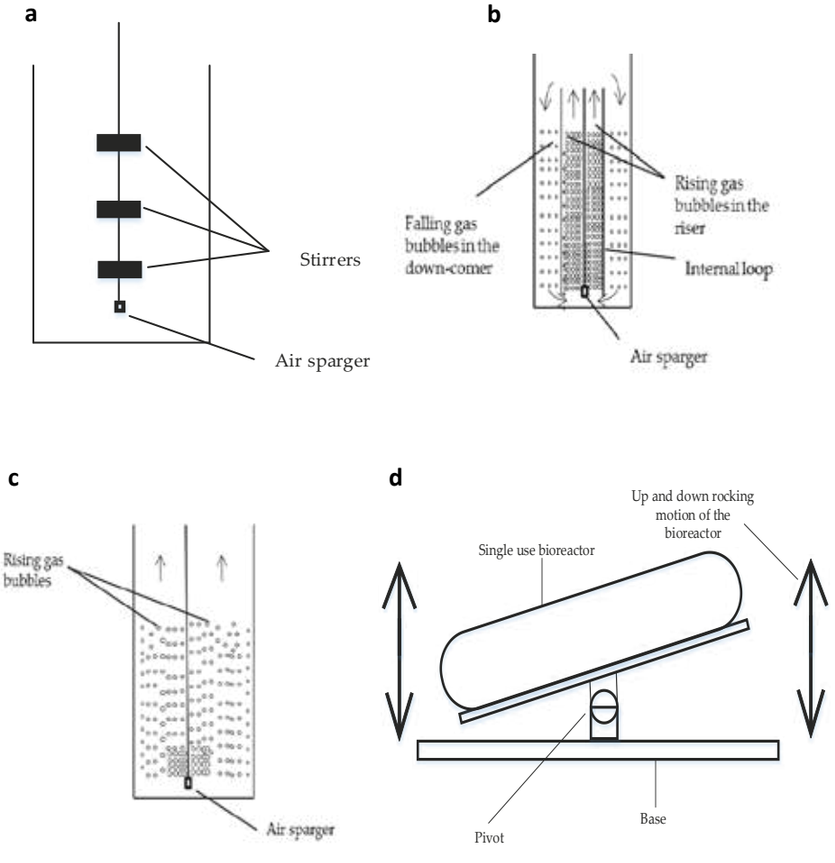

Figure 3.2: Schematic representation of different bioreactor designs showing a continuous stirred tank bioreactor (a), an internal loop airlift bioreactor (b), a bubble column bioreactor (c) and a wave bioreactor (d).

3.2 Basic requirements of a bioreactor

Although bioreactors are reactors, they have a key feature that distinguishes them from chemical reactors; bioreactors work with living microorganisms, cells or enzymes. Because of this, variations in process conditions such as temperature, pH or aeration can alter the transformation of reactants to product or the variation could lead to the death of the microorganism, thereby terminating the production process. Hence, it is important to keep the microorganisms in conditions suitable to them for producing the intended end-product.

Different microorganisms would require different conditions for growth. The conditions would depend on whether the microorganism grows aerobically or anaerobically, the strength of their cell wall or if the cells of the microorganism aggregate or not. For strictly anaerobic microorganisms such as flocculating bacteria, a bioreactor design that uses air for mixing would be lethal. Considering cell aggregation, taking a yeast strain *Saccharomyces cerevisiae* as an example, the cells could either be freely distributed throughout the bioreactor or aggregate to form flocs. *S. cerevisiae* flocs are more tolerant of inhibitory conditions than the free cells which makes *S. cerevisiae* flocs idea for second-generation ethanol production [34]. A bioreactor design that uses stirrers could break the flocs and the flocculating *S. cerevisiae* would loss its ability to tolerate inhibitors it could previously cope with. Apart from this, cell aggregation increases the mass transfer resistance that the substrate should overcome before getting inside the cells. Hence, a bioreactor design that provides good mass transfer is needed for cultivating microorganisms that form aggregates.

For substrate to be converted to product inside a bioreactor it goes through several steps, depending on whether the substrate is in a solid, liquid or gaseous phase. Let us take a gaseous substrate that should be converted to a product by a microbial cell inside the liquid phase in a bioreactor as an example. The substrate bubble must go through the gas film to leave the bulk gas phase. Then it goes through the gas liquid interface in other to enter the liquid phase. The substrate bubble then goes through the liquid film surrounding the bubble to enter the bulk liquid phase. Afterwards, it goes through the liquid film surrounding the microbial cell before reaching the surface of the cell and the conversion of the substrate to the product can begin. For the substrate to complete this movement, it would overcome some resistance (mass transfer resistance) as it moves across the different phases in the bioreactor. Hence, how this resistance and other similar important factors would be accounted for has to be incorporated into the bioreactor design. Emphasis has to be placed on important chemical engineering concepts like

mass transfer, heat transfer and hydrodynamics which describe the bioreactor performance from a macro perspective, and on the micro environmental conditions of the microorganism, like the presence of inhibitors, dissolved oxygen concentration, pH and foam formation when designing bioreactors [5, 35]. The micro environment will be directly affected by the following factors: consumption of substrates, products in the media, heat production and the formation of regions with high local cell densities or aggregates [5]. Prior to bioreactor design, a kinetic study helps to provide the data needed for designing bioreactors (**Paper IV**).

In terms of macro and micro environmental operational conditions, bioreactors can broadly be separated into aerobic or anaerobic bioreactors [4] based on the supply or utilisation of oxygen in the bioreactor. When designing or operating bioreactors, several important requirement have to be considered, such as mass transfer, heat transfer or temperature regulation, mixing, reactor geometry, aeration, means of feeding and discharging the bioreactor, dilution rate for continuous systems, mechanism for monitoring microbial conditions, process optimisation, contacting system in the bioreactor, hydrodynamic factors, process safety and the overall economy of the bioreactor [4, 5, 20, 36-40]. However, whether the bioreactor is operated aerobically or anaerobically influences which bioreactor process requirements would be given more attention when designing the bioreactor. For example, for aerobic bioreactors, the heat and mass transfer requirement is higher than for anaerobic bioreactors [4].

Heat transfer or temperature regulation, mass transfer, mixing, broth rheology, kinetics, process optimisation and safety for either aerobic or anaerobic bioreactor operational mode would be elaborated on, considering the macro and micro environmental requirements for effective bioreactor design.

3.3 Heat transfer

Heat transfer is the transfer of thermal energy, as evidenced by the temperature change, from one entity to another. Heat transfer requirements for bioreactors depend on whether the bioreactor would be operated aerobically or anaerobically, the geometry of the bioreactor, the scale of application, the predominant state of matter (i.e. solid, liquid or gas) of the fermentation media and the contacting pattern in the bioreactor [4, 41]. The mechanism of heat transfer in bioreactors could either be by conduction, convection or by radiation depending on the state of matter and contacting pattern in the bioreactor [41]. Several mathematical models have been developed to describe heat transfer in bioreactors [4, 40-42]. When bioreactors are operational,

the overall goal in terms of heat transfer is that the temperature in the bioreactor should be maintained within the range needed for growing the microorganisms in the bioreactor. How this is achieved differs and it depends on the previously mentioned factors that affect heat transfer in a bioreactor.

In general, anaerobic bioreactors require less energy for maintaining the temperature in the bioreactor within an acceptable range than aerobic bioreactors. The reasons for this include the generation of more heat energy during respiration by microorganisms, energy generation by air expansion in the bioreactor and the heat of water evaporation (as air enters the bioreactor dry but leaves saturated with water). Therefore, an aerobic bioreactor would need a mechanism for regulating heat energy of approximately 460,000 kJ/mol of oxygen consumed by the microorganisms; assuming an average oxygen uptake rate of 200 mmol/L/h, the heat transfer requirement would be 92 kJ/L/h [40]. This energy is normally added to the bioreactor using hot water for small-scale applications, whereas it is removed using cooling water for large-scale applications.

Controlling the temperature in the bioreactor based on its heat transfer requirement can be achieved either by using an external heat exchange loop, an external heating jacket or by using an internal vessel surface in the bioreactor. However, the design of such heat exchange element must be done in a way to avoid exposing the microorganisms to heat shock or oxygen deprivation (for aerobic bioreactors) [4].

3.4 Mass transfer

Mass transfer is the movement of mass from one position to another as evidenced by a concentration change. Good mass transfer in a bioreactor is important to ensure that the transformation of substrate to product in the bioreactor proceeds as planned [43]. Mass transfer in a bioreactor is affected by the factors that affect heat transfer as described in section 3.3. Additionally, mass transfer in a bioreactor is influenced by the degree of mixing, the morphology of the microorganisms, the viscosity of the fermentation medium, the aeration rate (for aerobic bioreactors) and the ease of transfer of substrate into or products out of the surface of the microorganism [44-46]. The mass transfer rate in a bioreactor is determined by two factors, diffusivity and bulk mixing, and it can be represented mathematically for non-turbulent flow as shown in Equation 3.1 where J_A is the mass flux of component A, N_A is the rate of mass transfer of component A, a is the cross-sectional area perpendicular to the direction of the transfer of component A, D_{AB} is the diffusivity of component A in a mixture of A and B, C_A is the concentration of A and U_O is the volumetric average velocity of flow of the bulk media.

$$J_A = \frac{N_A}{a} = -D_{AB}\frac{dC_A}{dy} + C_A U_O \qquad \textbf{3.1}$$

There are two factors of interest when accounting for mass transfer in bioreactors; the uniform distribution of substrate and product in the bulk fluid inside the bioreactor and the transfer of components from the bulk fluid into the microorganisms or vice versa. These two factors can be related mathematically to the right-hand side of Equation 3.1. The first part of the equation describes mass transfer by diffusion which is the only means of transfer of components from the bulk fluid to the microorganism or vice versa, while the second part describes mass transfer by bulk flow, which has to do with the uniform distribution of substrate and product in the bulk fluid inside the bioreactor. Which of the two factors would be responsible for posing mass transfer limitation in the bioreactor would depend on several factors like the solubility of the substrate or oxygen in the media (for aerobic bioreactors), the size and density of the substrates, the formation of regions of high local cell densities by the microorganism and the contacting pattern in the bioreactor [46-49].

Mass transfer for aerobic bioreactors requires more consideration than anaerobic bioreactors because the oxygen transfer rate or utilisation rate usually presents a significant mass transfer limitation [44, 45, 48, 49]. This is because even without microbial growth, the dissolved oxygen equilibrium concentration in aerobic bioreactors is only five to ten times that of the limiting concentration, and it reduces with microbial activities [5]. Bioreactors that use microorganisms that form high local cell densities (i.e. self-aggregating, flocculating or filamentous) would also experience more mass transfer limitations than those that do not [50-52]. When the solubility of the substrate is within the rate-limiting range, mass transfer limitations would also be experienced in the bioreactor if extra measures are not taken to address the mass transfer limitation [5].

3.5 Mixing and broth rheology

Mixing involves maintaining the uniformity of the substrate and product concentration in the bulk fluid inside the bioreactor with the aid of a mixing mechanism or device. Mixing also helps eliminate temperature variations in the bioreactor (**Paper I**). Mixing in a bioreactor could affect the productivity and yield in a bioreactor (**Paper II**) depending on whether the fermenting microorganism is freely uniformly distributed in the bioreactor or not. How mixing is carried out in a bioreactor depends on the state of matter in which fermentation is taking place in the bioreactor, the solubility of the substrate and product, the morphology and the thickness of the cell walls of the microorganism and whether the fermentation proceeds aerobically or anaerobically [5, 53-56]. Mixing is particularly essential when the growth of the microorganism, the substrate consumption or the product formation inside the bioreactor changes the rheological properties of the fermentation broth. Although mixing is essential for some fermentation processes, it should be within a range, as excessive mixing could be detrimental to shear-sensitive microorganisms, cause the breakup of flocculating microorganism, increase the power consumption in the facility and lead to poor bioreactor hydrodynamics conditions causing foaming and media loss [33, 57].

The development in the history of bioreactors has also impacted how mixing is carried out in bioreactors, and the transition has been from stirred mixing using mechanical devices to mixing without stirrers (**Paper II**), [4, 9, 43]. Initially with continuous stirred tank bioreactors, mixing was done using Rushton turbines, which created a staged mixing pattern inside the bioreactors [4]. Mixing with Rushton turbines have been reported to generate non-uniformity with nutrient, product, substrate and oxygen distribution in bioreactors [4, 58, 59]; so axial or radial impellers now find increasing applications in bioreactors. For applications where the microorganisms are sensitive to the shear stress exerted on their cell walls by stirrers, mixing is carried out without any mechanical devices. Examples of bioreactors without mechanical mixing devices include up-flow anaerobic sludge blanket (UASB) bioreactors, airlift bioreactors, bubble column bioreactors, different single-use bioreactors and the newly introduced textile-based bioreactor. These bioreactors employ different principles for mixing and fluidisation is one of the most used principles. Mathematical representations of the principles governing fluidisation are shown in Equations 3.2 to 3.6, with Equations 3.4 and 3.5 defining the flow conditions for Reynold's number less than 10 and Equation 3.6 must hold for fluidisation to begin and be sustained in the bioreactor (**Paper II**).

Force due to acceleration = Force due to gravity – Buoyancy force – Drag force **3.2**

Pressure force (F_p) = Force due to gravity (F_g) – Buoyancy force (F_B) **3.3**

$$V_0 = V_u = (\rho_p - \rho_f)gD_p^2\varepsilon^3/150\mu(1-\varepsilon) \quad \textbf{3.4}$$

$$V_s = (\rho_p - \rho_f)gD_p^2/18\mu \quad \textbf{3.5}$$

$$V_0 \leq V_{umax} \leq V_s \quad \textbf{3.6}$$

where V_0 is the superficial velocity, V_{umax} is the maximum fluid upward velocity, V_s is the particle or biomass settling velocity, ρ_p is the density of the particle, ρ_f is the density of the fluid, g is the acceleration due to gravity, D_p is the particle or biomass diameter, μ is the fluid viscosity and ε is the void fraction.

To achieve good mixing in a bioreactor, it is essential to understand the nature of the resistance to flow (viscosity) in the bioreactor. The viscosity in a fermentation media could either be constant or change during the duration of fermentation. The relationship between the shear stress τ (Pa) and the shear rate $\frac{dv}{dy}$ or $\acute{y}$ (1/s) when the viscosity is constant is given by Newton's law as shown in Equation 3.7.

$$\tau = -\mu\frac{dv}{dy} = -\mu\acute{y} \quad \textbf{3.7}$$

For most fermentation media, when the microorganism grows up to an extent, the fluid viscosity would start changing, and fluid would then behave as a non-Newtonian fluid. For most microbial fermentation media, the flow under this condition is pseudoplastic and it follows the relationship shown in Equation 3.8, where *K* is the fluid consistency index (Pa.s^n) and n is a number less than one [60].

$$\tau = K\acute{y}^n \quad \textbf{3.8}$$

The viscosity under non-Newtonian conditions is the apparent viscosity (μ_a) and it can be expressed by the relationship shown in Equation 3.9.

$$\mu_a = K\acute{y}^{n-1} = \frac{\tau}{\acute{y}} \quad \textbf{3.9}$$

3.6 Process optimisation and safety

Bioreactor design can be optimised with respect to several features including the vessels aspect ratio, production economics (e.g. product yield, productivity and batch completion time) and minimisation of cost and energy requirement of the bioreactor. Considering the bioreactor vessel aspect ratio, the best design would depend on whether the bioreactor would be used aerobically or anaerobically. For aerobic bioreactors, a higher height-to-diameter ratio would result in higher pressure at the bottom of the bioreactor, thereby creating a higher mass transfer driving force. Therefore, a bioreactor with a higher height-to-diameter ratio would require less aeration than one with a smaller height-to-diameter ratio. The drawback of a bioreactor with a high height-to-diameter ratio is that there would be a non-uniform distribution of nutrients and dissolved oxygen across the bioreactor and higher-pressure vessel requirements due to the high pressure at which air would be supplied to the bioreactor. Hence, it is important to design the bioreactor using an aspect ratio that provides optimal gas holdup time and a good distribution of oxygen and nutrients in the bioreactor. For anaerobic bioreactors, the optimal aspect ratio of approximately 1 provides optimal mixing; however, practical considerations such as vessel cost influences the aspect ratio to be used [4].

Safety is paramount when designing bioreactors. Failures could occur in a bioreactor when in operation from its inability to contain the stress exerted on it by the contained media [61] or from the corrosion of the material of construction of the bioreactor [62]. The stress exerted on the bioreactor can be calculated using the thin shell theory, if the ratio of its wall thickness to its radius is less than or equal to 1/20, it has a fixed geometry and the pressure inside it is constant [63]. For a bioreactor with a cylindrical geometry, the longitudinal stress (σ) exerted on it by the pressure of the fluid can be calculated using Equation 3.10, where P is the pressure, R is the radius of the bioreactor and t is the wall thickness of the bioreactor. Taking a cylindrical bioreactor with a wall thickness of 4 mm, radius of 1 m and sterilisation pressure of 2 bars, the longitudinal tensile stress that would be exerted on it would be 25 MPa. For a safety allowance factor of 1.5 [64], the material for constructing the bioreactor must have a tensile strength greater than 37.5 MPa to safeguard against failure which would occur when the stress in the vessel has exceeded the material's intrinsic tolerance values as determined by its Young's modulus [65]. This high tensile strength requirement is the reason why stainless steel is usually used for fabricating bioreactors.

$$\sigma = PR/2t \qquad \textbf{3.10}$$

3.7 Kinetics

Microbial growth, substrate consumption and the product formation rate can be investigated using a basic unstructured model.

3.7.1 Growth kinetics

Under non-limiting conditions, microbial growth can be described using Equation 3.11 as

$$\frac{dX}{dt} = \mu X, \qquad \textbf{3.11}$$

where X is the dry weight of cells (gL^{-1}), t is time (h) and μ is the specific growth rate (h^{-1}). The specific growth rate can be defined in terms of the Monod kinetic model as

$$\mu = \mu_m \frac{S}{S+K_s}, \qquad \textbf{3.12}$$

where μ_m is the maximum specific growth rate (h^{-1}), S is the substrate concentration (gL^{-1}) and K_S is the saturation constant (gL^{-1}).

Under non-limiting conditions, combining Equations 3.11 and 3.12 gives the combined microbial growth rate equation

$$\frac{dX}{dt} = \mu X = \mu_m \frac{S}{S+K_s} X. \qquad \textbf{3.13}$$

3.7.2 Aeration kinetics

For aerobic microorganisms, the supply and utilisation of oxygen in the fermentation medium is essential for microbial growth, which in turn affects substrate consumption and product formation inside the bioreactor. Oxygen supplied to a bioreactor is normally utilised in the dissolved form by microorganisms and the three important parameters influencing this are the dissolved oxygen concentration (DO), the oxygen transfer rate (OTR) and oxygen utilisation rate (OUR). The DO, OTR and OUR in a well-mixed liquid fermentation broth are related as shown in Equation 3.14.

$$DO = OTR - OUR \qquad \textbf{3.14}$$

As regards the OTR, several resistances to mass transfer are encountered when oxygen moves from the air bubbles through the liquid in the bioreactor to the surface of the microorganisms. However, it is usually assumed that oxygen transfer into microorganisms occurs through molecular diffusion and the mass transfer limitation in the gas phase can be neglected; thus,

the driving force of the OTR would be the oxygen concentration gradient between that at the bulk liquid and that at the interface [44]. Thus, the oxygen mass transfer rate per unit volume in the bioreactor can be determined using Equation 3.15 where C* is the oxygen saturation concentration in the bulk liquid in equilibrium to the bulk gas phase, k_L is the mass transfer coefficient across the liquid phase and C_L is the dissolved oxygen concentration in the bulk liquid [44].

$$N_{O_2} = aJ_{O_2} = k_La\ (C^* - C_L) \quad \textbf{3.15}$$

Because of the difficulty of measuring the interfacial surface area (a), k_La is normally used as a single parameter called the volumetric mass transfer coefficient. Several empirical correlations have been developed for estimating k_La or k_L for different types of bioreactors in which the fluid flow patterns follow either Newtonian or non-Newtonian behaviour [66-68]. The maximum OTR (OTR_{max}) can be estimated using the oxidation rate of a chemical such as sodium sulphite and several correlations have been developed for it [44, 49, 69].

The OUR can be determined by the product of the specific oxygen uptake rate of the microorganism being employed (q_o) and the biomass concentration (X). When the minimum DO threshold for microbial growth has been attained in a bioreactor, the specific oxygen uptake rate q_o has been shown to have a zero-order relationship with the DO concentration [69-71]. Hence q_o can be determined from Equation 3.14.

$$q_o = (OTR - DO)/X \quad \textbf{3.16}$$

In the case of a well-mixed bioreactor operating at the steady state, the DO in Equation (14) becomes zero [45, 48]; hence, the OUR can be approximated to equal the OTR [46]. Thus q_0 on the verge of the oxygen mass transfer limitation can be estimated as shown in Equation 3.17 **(Paper IV)** where X_t is the biomass concentration (g/L) on the verge of the oxygen mass transfer limitation.

$$q_o = OTR/X_t \quad \textbf{3.17}$$

3.7.3 Substrate consumption and product formation kinetics

When a high substrate concentration influences the observed kinetics, its influence can be included into the Monod model, as shown in Equation 3.18 [72]:

$$\frac{dX}{dt} = \mu X = \mu_m \frac{S}{S+K_s}\left(1 - \frac{S}{S^*}\right)^n X, \quad \textbf{3.18}$$

where S* is the substrate concentration (g/L) at which no growth occurs and n is the degree of the inhibition. The effect of product inhibition on the kinetics can be expressed using Equation 3.19 [73], where μ'_m is the observed maximum growth rate, P_i is the concentration of a particular product (g/L), P_i* is the concentration at which no growth occurs and a_i is the degree of product inhibition.

$$\frac{dX}{dt} = \mu X = \mu'_m \frac{S}{S+K_s}\left[\prod\left(1 - \frac{P_i}{P_{i*}^*}\right)^{a_i}\right] X \quad \textbf{3.19}$$

When both substrate and product inhibition occur, Equation 3.18 and 3.19 can be combined to describe the overall growth rate.

$$\frac{dX}{dt} = \mu X = \mu'_m \frac{S}{S+K_s}\left(1 - \frac{S}{S^*}\right)^n \left[\prod\left(1 - \frac{P_i}{P_i^*}\right)^{a_i}\right] X \quad \textbf{3.20}$$

In addition to the kinetic equations 3.13 and 3.18–3.20, the Luedeking–Piret model (Equation 3.21) is commonly used to describe the production of metabolites such as ethanol in terms of growth (dx/dt) and non-growth association [74, 75]:

$$\frac{dP_i}{dt} = \alpha_i \frac{dX}{dt} + \beta_i X, \quad \textbf{3.21}$$

where α_i is the growth-associated parameter (dimensionless) and β_i is the non-growth-associated parameter (h^{-1}).

3.8 Challenges of conventional bioreactors

Conventional bioreactors, when designed, hardly leave room for other modifications that might be interesting from the end user's perspective. For example, a continuous stirred tank bioreactor used for aerobic fermentation would not be suitable for share-sensitive microorganisms which might latter be found to be better for the fermentation production process than what was previously used after the bioreactor has been installed. Thus, it would be beneficial for bioreactors to be introduced that favour improved flexibility. Increase in the flexibility of biological-based production has been linked with several benefits that include faster batch turnover, reduced capital investment cost, reduced process installation time and the ease of transfer of focus from one high-value product to another [31]. The textile-based bioreactor developed in this thesis encompasses the concept of improved flexibility, as the same bioreactor can be used anaerobically or aerobically and for different microorganisms (**Paper I, II, V**,**VI**) [76].

For a large-scale application, the small area-to-volume ratio of stainless steel-based bioreactors (typically between 0.6–0.4) means that considerable energy would be needed for cooling them. This is because the heat loss due to evaporation and radiation increases with increasing area-to-volume ratio; a small area-to-volume ratio would reduce the heat loss to the environment and hence more cooling would be required. The developed textile-bioreactor has a higher area-to-volume ratio than conventional bioreactors and would therefore require less energy provision and energy-associated cost than conventional bioreactors.

Another challenge associated with conventional bioreactors is the high capital investment cost associated with them [26]. The high bioreactor cost translates to a high production cost, which in turn could make the product from the bio-production facility more expensive and less preferred in the market.

The operational challenges associated with different bioreactor designs are summarised in Table 3.1.

Table 3.1: Challenges associated with different bioreactor designs [77-82]

Bioreactor design type	Challenges
Stirred tank bioreactors	Uses mechanical stirrers for mixing High shear force; hence not suitable for share-sensitive microorganisms High power requirement for the stirrers
Bubble column bioreactors	Low volumetric oxygen transfer rate High risk of foam formation Extra cost associated with gas mixing for anaerobic application
Airlift bioreactors	Non-uniform distribution of bioreactor content due to higher driving force at its bottom High risk of foam formation Extra cost associated with gas mixing for anaerobic application
Fluidised bed bioreactor	Requires a density difference between media and microorganisms
Trickle bed bioreactor	High possibility of non-uniform microbial activity Low volumetric oxygen transfer rate
Tray bioreactor	Requires efficient immobilisation High possibility of non-uniform microbial activity
Rotary drum bioreactor	High power requirement for rotation when upscaled Usually designed as a horizontal vessel
Continuous screw bioreactor	High energy input for driving the screw Usually designed as a horizontal vessel
Wave bioreactor	Low volumetric oxygen transfer rate Limited to batch-related production mode Difficulty in upscaling

4. Textile bioreactor development

The textile-based bioreactor was first introduced as an economically favourable bioreactor for biogas production at small scale without any internal or external process control feature in it [18]. However, for the bioreactor to be suitable for aerobic or anaerobic fermentation-based production using different substrates and microorganisms, it is essential that process control features be introduced in the bioreactor as in other conventional bioreactors. Several process control features have been introduced and further developed in the textile-based bioreactor, including temperature control and a mixing mechanism and they will be discussed in the subsequent sub-sections. In addition, some practical considerations needed for ethanol and biogas production using different microorganisms will be discussed.

4.1 Temperature control

A means for regulating the temperature in the textile-based bioreactor that uses heat exchange tubes connected to a thermostatic recirculator wound around the bottom of the bioreactor was first introduced as shown in Figure 4.1. The temperature inside the bioreactor can be monitored continuously or when needed using a thermometer or a temperature probe connected through the top of the bioreactor. The heat exchange tubing was wound between 6–12 times to cover 75–90 % of the perimeter of the bottom part of the bioreactor. This temperature control feature was developed for anaerobic application of the bioreactor (**Paper I, II, V**) or for applications where the surface-area-to-volume ratio of the bioreactor is approximately 1 or higher.

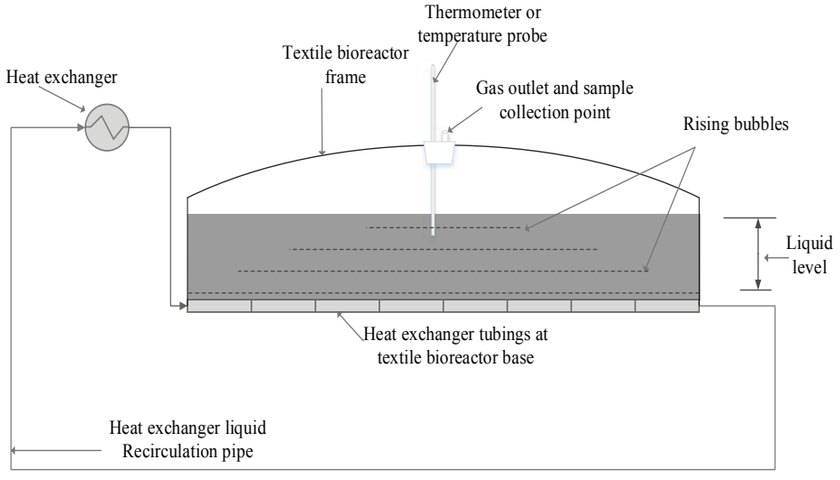

Figure 4.1: Schematic of a prototype of the textile-based bioreactor showing temperature control using heat exchange tubes at the bottom of the bioreactor.

The temperature control mechanism (shown in Figure 4.1) was tested for the anaerobic fermentation of sucrose by using baker's yeast and the result from the fermentation carried out in the textile-based bioreactor with and without this temperature control mechanism is shown in Figure 4.2 (**Paper I**). From the result, it can be seen that with temperature control, the fermentation rate was much faster as the specific ethanol productivity for the bioreactor maintained at 30 °C (which is the optimal fermentation temperature for baker's yeast) was 1.04 ± 0.01 g/L/h, which was twice that without temperature control. Additionally, the fermentation rate per gram starting yeast concentration recorded in the textile-bioreactor maintained at 30 °C is comparable with that reported for other sugar-based bioreactors [83].

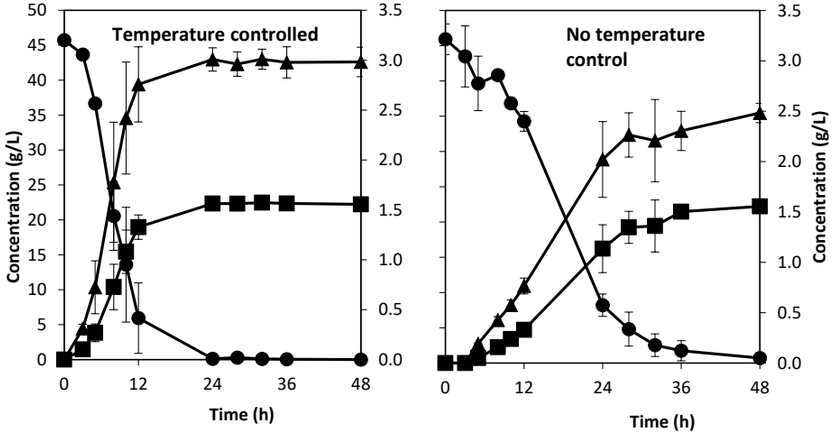

Figure 4.2: Concentration of sucrose (●) and ethanol (■) on the primary axis and glycerol (▲) on the secondary axis in the textile-based bioreactor as a function of time, with temperature controlled at 30 °C and without temperature control.

Another temperature control mechanism that was developed for the textile-bioreactor is shown in Figure 4.3. For this case, the heating tubing is wound round the vertical surface of the bioreactor or the bioreactor is put inside a heating jacket up till where the liquid height ends (**Paper VI**), [76]. This design is more suitable for aerobic fermentation with a surface-area-to-volume ratio less than 1 to increase the gas holdup time in the bioreactor. Aerobic fermentation experiments performed with this design using the fungus *Nuerospora Intermedia* as microbe, thin stillage and vinasse as substrate had similar results to that reported for conventional bioreactors [84, 85].

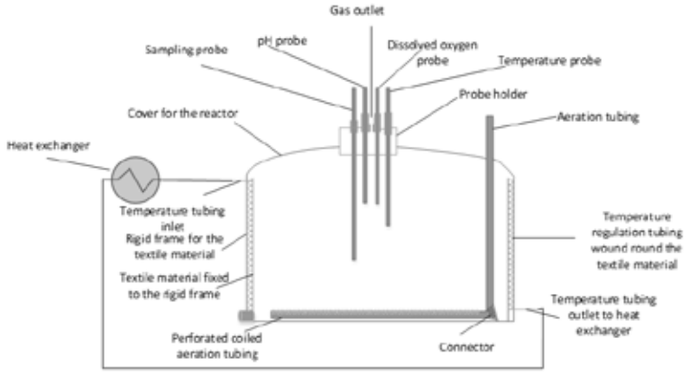

Figure 4.3: Schematic of a prototype of the textile-based bioreactor showing temperature control using heat exchange tubes or a heating jacket at the side of the bioreactor.

4.2 Mass transfer

Flocculation and pellet formation by microorganisms is associated with several benefits that include smaller bioreactor volume requirement and ease of biomass separation [43, 86-88]. However, the possibility of mass transfer limitation occurring in bioreactors that use microorganisms with morphologies that lead to self-aggregation (e.g. flocculating or pellet-forming microorganisms) or mycelial formation is usually higher than those with freely suspended cells (**Paper II, IV, VI**). This tendency for mass transfer limitation to occur has been reported for both aerobic and anaerobic bioreactors [46, 49, 89, 90]. To address chances of mass transfer limitation occurring in the textile-based bioreactor, it was developed using some fluidisation concepts to maximise the contact between the microorganisms and the substrate in the bioreactor for aerobic and anaerobic applications.

Overcoming the mass transfer limitation associated with anaerobic fermentation was investigated in the textile-based bioreactor using naturally flocculating yeast strain *S. cerevisiae* CCUG 53310 (Culture Collection University of Gothenburg, Gothenburg, Sweden) with a settling velocity of 0.01 m/s, density of 1140 kg/m^3 and particle diameter between 190 to 320 µm (**Paper II**). Mixing tubes were designed and used for re-suspending the flocculating

yeast inside the bioreactor using modified versions of Equations 3.4–3.6 specific for the bioreactor (Equations 4.1–4.4), where V_i is the velocity of the fluid going through the mixing tubing and V_h is the upward velocity with which the fluid in the mixing tubing emerges out. A schematic representation of how the mixing tube is placed in the bioreactor and the mixing pattern it created in the bioreactor is shown in Figure 4.4.

$$V_0 = Q/A = Q/(1.1\times0.34) = 2.674Q \quad \textbf{4.1}$$

$$V_i = Q/A_i = Q/(\pi\times r_i2) = 5.094\times10^4Q \quad \textbf{4.2}$$

$$V_h = 142\times V_i/1200 = 6.028\times10^3Q \quad \textbf{4.3}$$

$$V_0 \leq V_h \leq V_s \quad \textbf{4.4}$$

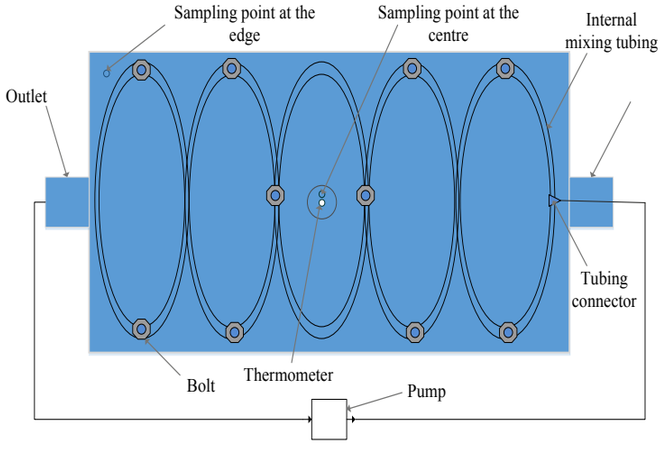

Figure 4.4a: Cross-section of the textile-based bioreactor prototype showing the internal mixing system from the top view.

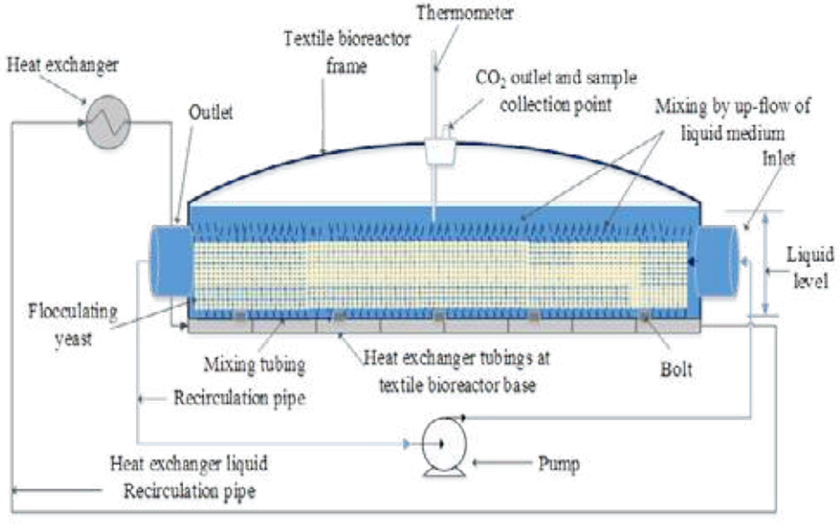

Figure 4.4b: Schematic representation of the re-suspension of flocculating yeast inside the textile-based bioreactor.

The mass transfer rate is influenced by two components, diffusivity and bulk flow (Equation 3.1). For microorganisms with self-aggregating tendencies, the mass transfer limitation experienced when they are used in bioreactors is usually based on diffusivity [91]. By increasing the contacting surface area in the textile-based bioreactor, the mass transfer limitation associated with diffusivity can be eliminated [92-94]. Results from the fermentation experiment carried out in the textile-based bioreactor using the mixing tubes showed that the mass transfer limitation associated with the use of the flocculating yeast for anaerobic ethanol production was eliminated as evidenced by the faster fermentation completion time (Figure 4.5) even when 30 times less bulk flow rate was used (**Paper II**).

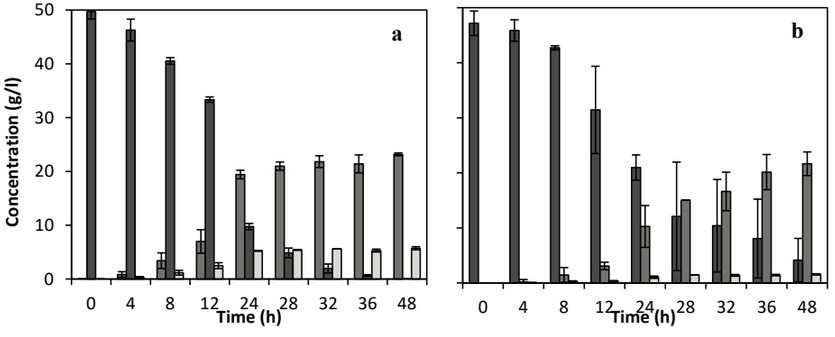

Figure 4.5: Concentration of sucrose (■), ethanol (■) and glycerol (■) in the textile-based bioreactor against time, with the developed mixing tube (a) using a fluid recirculation rate of 0.0016 VVM and without the mixing tube (b) using a fluid recirculation rate of 0.032 VVM

For aerobic bioreactors, when the substrate and nutrients in the bioreactor are well mixed, the mass transfer limitation experienced in them is usually due to oxygen transfer and utilisation rate [4, 5]. Every aerobic microorganism has a specific oxygen consumption rate within a range depending on the size distribution of the microorganism and the morphology it forms [95-97]. When the specific oxygen utilisation rate of the microorganism is known and the biomass concentration in the bioreactor is known, the oxygen mass transfer limitation can be eliminated by applying Equations 3.14–3.17 to calculate the rate at which oxygen should be supplied to the bioreactor. When the specific oxygen utilisation rate and the growth rate of the microorganism are not known, a kinetic study can be performed to determine them (**Paper IV**). Using pellet-forming fungi *Nuerospora Intermedia* as example, kinetic studies gave the specific oxygen uptake rate of the pellets as between 0.27–0.9 mmol-O_2/g-biomass/h and its maximum growth rate at pH 3.5 as 0.318/h (**Paper IV**).

4.3 Mixing

Mixing aims at achieving uniformity in temperature, nutrient, substrate and product concentration, and other bulk fluid flow properties of the fermentation media, including viscosity, inside the bioreactor. Mixing in liquid media can be achieved by agitation, with the aid of a stirrer, or by the use of a pump for recirculation, depending on the viscosity of the liquid and if the medium is single- or multi-phased [98]. For the textile-based bioreactor, mixing carried out inside it was developed based on the nature of the substrate and the fermenting microorganism and whether the bioreactor would be used aerobically or anaerobically (**Paper I**, **II** and **VI**).

The mixing requirement for the bioreactor can be estimated using the particle-settling velocity which takes into account the difference between the density of the microorganism and the liquid media inside the bioreactor (Equation 3.5). The higher the settling velocity the more the separation of the particles from the bulk fluid, indicating more mixing to achieve uniformity. For freely suspended microorganisms such as baker's yeast with density almost the same as water and substrate highly soluble in water, the settling velocity of the cells was approximately 1.15×10^{-5} m/s; hence, mixing could be carried out using recirculation of the bioreactor content without an additional mixing device (**Paper I**). Figure 4.6 shows the concentration profile of the substrate and products across the textile-based bioreactor with time from two different positions to compare the homogeneity of the fermentation broth. It can be seen from Figure 4.6 that mixing with recirculation was effective for freely suspended baker's yeast cells in the textile-based bioreactor. An analysis of variance (ANOVA) performed using a general linear model of ethanol and sucrose concentration as responses and sampling position as factor gave p-values of 0.933 for ethanol and 0.937 for sucrose, and hence the position from which the sample is drawn is not statistically significant, meaning that the mixing was uniform across the textile-based bioreactor.

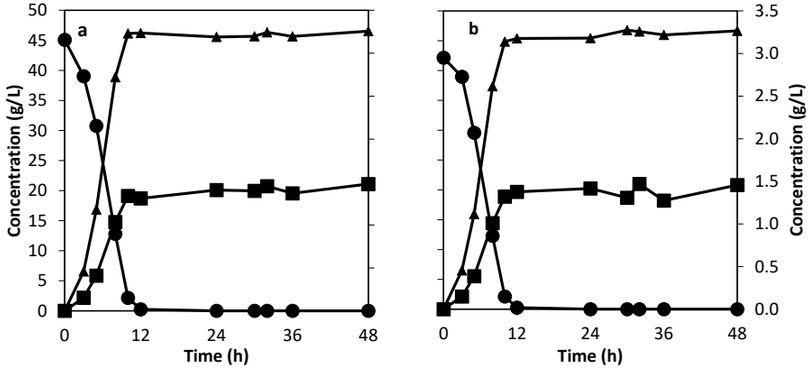

Figure 4.6: Concentration of sucrose (●) and ethanol (■) on the primary axis (left side), and glycerol (▲) on the secondary axis (right side), with samples taken from the outlet (figure a) and the centre of the reactor (figure b) as a function of time.

For microorganisms with morphologies that favour the formation of regions with high local cell densities such as flocculating yeast, flocculating bacteria, fungi pellets and fungi filaments, an additional mixing system was used inside the bioreactor (**Paper II** and **VI**). Flocculating yeast, flocculating bacteria and fungi pellets had a settling velocity of 0.01 m/s or higher in water. This high settling velocity was provided either using an upflow of the liquid media or by aeration (**Paper II**, **VI**). For anaerobic applications, with flocculating microorganisms, using Equations 4.1–4.4, a mixing system (Figure 4.4 a) that uses the liquid medium inside the bioreactor for both re-suspending the microorganisms and uniformly distributing the nutrients, substrates and product inside the bioreactor (Figure 4.4 b) was designed and tested using flocculating yeast fermentation (**Paper II**). First, the mixing system was tested by injecting bromophenol blue at one end of the bioreactor (a substance with lower diffusivity than the substrate and product [99-101]) at a different bulk flow rate (recirculation rate) to check if mixing is efficient particularly at the corners of the bioreactor. The result from this investigation (Figure 4.7) shows that the maximum time for uniformity to be achieved was 50 min when a bulk recirculation rate of 0.02VVM was used (**Paper II**). This mixing time is sufficient considering that ethanol and sucrose diffuse faster in water than bromophenol blue and also the sampling time for ethanol production is usually measured in hours [83].

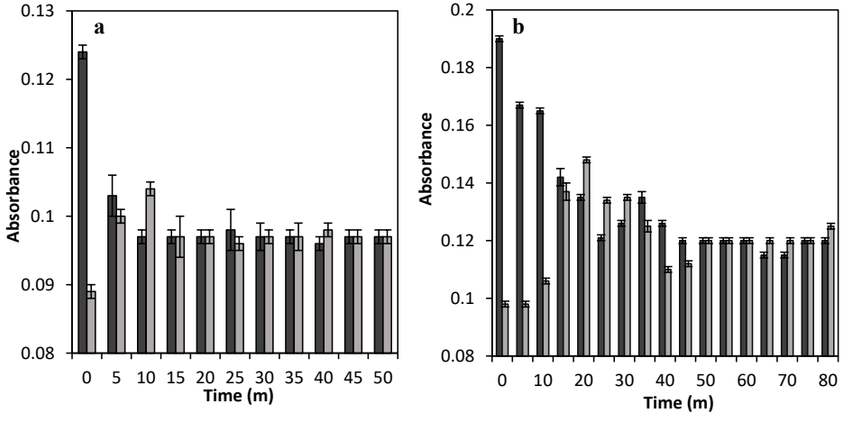

Figure 4.7: Bromophenol blue absorbance in the textile bioreactor at 0.015 VVM flow rate (a) and 0.002 VVM flow rate (b) at the injection point (■) and at the opposite rear (■)

Another feature of mixing using the internal tubing is that the tubing can be designed with different specifications such as the distance between each hole (Equation 4.3). Using an appropriate design, the upflow velocity of the fluid coming out of the tubing can be changed as shown in Equations 4.2 and 4.3. A compilation of different fluid upflow velocities at different bulk flowrates using different tubing designs is shown in Table 4.1. If the settling velocity of the microorganisms is less than the fluid upflow velocity from the mixing tubing, then the cells would be retained within the bioreactor. Taking flocculating yeast with a settling rate of 0.01 m/s as an example, with a hole spacing of 2 mm at 0.02 VVM (1.2/h dilution rate), the upflow velocity would be 0.01 m/s, and with an initial tubing length of 18 m instead of 12 m, the fluid upflow velocity would be 0.007 m/s, indicating that feeding the bioreactor with a dilution rate higher than 1/h without washout is possible. Similar analogy was used to design the aeration tubing for aerobic application of the bioreactor (**Paper VI**) but instead of liquid flow properties, gas flow properties were used.

Table 4.1: Fluid upflow velocities generated at different flow rates using different mixing tube designs in the textile-based bioreactor. VVM: volume per volume per minute; V_0: Superficial velocity; V_i: Fluid velocity; V_h: Fluid upflow velocity; V_s: Flocs settling velocity

Q (VVM)	V_0 (m/s) $\times 10^6$	V_i (m/s)	V_h at different hole spacings (m/s)			V_s (m/s)
			1-cm spacing	5-mm spacing	2-mm spacing	
0.0016	1.78	0.03	0.004	0.002	0.001	0.01
0.0120	13.37	0.25	0.030	0.015	0.006	0.01
0.0160	17.83	0.34	0.040	0.020	0.008	0.01
0.0320	35.64	0.68	0.080	0.040	0.016	0.01
0.0600	66.84	1.27	0.151	0.075	0.030	0.01

4.4 Broth rheology and hydrodynamics

Rheology is the science of fluid flow and deformation, and hydrodynamics is the study of the forces interacting between immersed bodies in the fluid, the fluid flow patterns and the deviations in fluid flow patterns caused by the immersed bodies [60]. Viscosity, the resistance to fluid motion, is extremely important for bioreactor rheological and hydrodynamics studies because it affects pumping, mixing, aeration, mass transfer, heat transfer and the overall bioprocessing economics [60]. Changes in the properties of any fluid, such as temperature or concentration, is achieved when there is motion in the fluid; hence, viscosity in bioreactors is important as submerged fermentation is carried out in the fluid inside the bioreactor. The more the viscosity, the more the force needed for fluid flow, which in turn means more power or energy would be needed to carry out the biotransformation inside the bioreactor. Further, during fermentation, the viscosity of the fermentation broth can change either because of the increase of biomass concentration, the production of viscous extracellular metabolites or a change in the consistency of the substrate (like hydrolysis of starch).

In terms of biomass, the viscosity of fermentation broths with baker's yeast cells and non-chain-forming bacteria is usually constant when the total solid in the bioreactor is less than 10 % [102-104]. However, for fermentation broth with mycelia suspension, the media viscosity changes following the pseudoplastic model (Equations 3.8 and 3.9) and there are high chances of non-uniformity of the viscosity across the bioreactor, hence it is the apparent viscosity in the

bioreactor that is measured. The biomass concentration (X) and the change in the consistency of the substrate influences the apparent viscosity of the fermentation broth [105, 106]. Empirical relations for the consistency index (K in Pa.s^n) and the flow behaviour index (n) as a function of biomass concentration were developed for aerobic filamentous fungi fermentation using an integrated media of hydrolysed wheat straw and thin stillage (Equations 4.5 and 4.6) (**Paper VI**).

$$K = 0.59\ X^{0.9} \quad \textbf{4.5}$$

$$n = 0.539 - 0.062X \quad \textbf{4.6}$$

The integrated media of hydrolysed wheat straw and thin stillage had a flow behaviour index of 0.52 because it had a total solid (TS) concentration of 7.5 % prior to fermentation, showing that its flow follows the pseudoplastic model (Equation 3.8). For substrates with high TS, the mixing and aeration requirement to achieve homogeneity or good contact between the substrate or oxygen with the microorganisms is higher than for substrates with low TS. Taking anaerobic fermentation of palm oil mill effluent (POME) using flocculating bacteria as an example, the POME had a TS of 6.6 %, a viscosity of 153 cP and density of 1017 kg/m^3, while the density of the flocculating bacteria was 1025 kg/m^3. Without aided mixing, the flocculating bacteria were floating on top of the POME, hence no proper fermentation could take place as the media was highly viscous and the density difference between the flocs and POME is not much (Equations 3.5 and 3.6).

The physical properties of the fermentation broth (such as viscosity and density), the geometry of the bioreactor, the operational conditions (such as agitation or stirring rate, aeration rate and feeding rate) and the biomass (the amount present and its growth pattern) influence the hydrodynamic conditions in a bioreactor [107, 108]. For shear-sensitive microorganisms such as filamentous fungi, the use of stirrers increases the shear force in the bioreactor which could damage their cell wall. Considering the example of aerobic fermentation with filamentous fungi, the operational hydrodynamic factors for the bioreactor design would be those related to aeration (oxygen transfer rate and foaming). For highly viscous media, a higher OTR would be needed to prevent mass transfer limitations as the OTR has an inverse relationship with viscosity [44, 69]. However, increasing the OTR increases the gas rise velocity, which has a direct relationship with the foam rise velocity in a bioreactor [109]. This is because two conditions are needed for foam formation and stabilisation: the presence of protein compounds in the substrate and a gas rise velocity higher than the liquid rise velocity [109-111]. One way

to reduce the gas rise velocity at a high OTR is to use a bioreactor design with a cross-sectional area that increases the liquid rise velocity. This was incorporated into the textile-based bioreactor design. To compare the performance of the textile-based bioreactor with other bioreactors, fermentation was carried out in different bioreactors using a 1:1 mixture of thin stillage and hydrolysed wheat straw as substrate and a mycelium-forming fungi biomass. The initial viscosity of the fermentation broth was 93 cP; hence, an aeration rate of 1.4 VVM was used for the fermentation process to prevent oxygen mass transfer limitations. The gas rise velocity for the textile bioreactor was 6.25 times less than that for the airlift and bubble column bioreactors because of the higher cross-sectional area of the textile-based bioreactor. Increase in broth viscosity increased the frequency of foam formation and stabilisation, particularly in the airlift and bubble column bioreactors where foaming led to the loss of 37 % and 54 % of the liquid from the airlift and bubble column bioreactors respectively. Foaming only occurred once during start-up for the textile-based bioreactor (**Paper VI**). This indicates that the design of a bioreactor can influence foam formation and stabilisation under operating conditions suitable for foaming in a bioreactor [112].

4.5 Perspective on bioethanol production

Ethanol can be produced biologically from fermentation (bioethanol) or from crude oil. Ethanol produced from biological processes accounts for over 95 % of global ethanol production [113]. Bioethanol is the most produced biofuel globally, accounting for 76 % of the total biofuel production in 2014 [114]. Some reasons for this include the high yield that can be attained in ethanol production, the ease of producing ethanol and government regulations or incentives [27, 113, 115]. Industrially, bioethanol is produced from glucose, fructose or sucrose from sugary raw material (e.g. sugarcane) or starchy feedstock (e.g. corn, wheat, barley etc.) using *S. cerevisiae* most times as the fermenting organism. Producing bioethanol from these feedstocks is referred to as first-generation ethanol production. Because of the food versus fuel debate and the high cost of food-based feed, considerable research has been conducted on ethanol production from lignocellulosic material [10]. Producing ethanol this way is referred to as second-generation ethanol production.

Ethanol production and utilisation has been on the increase in the past decade because of its diverse benefits, increasing environmental awareness and the need to have alternatives to fossil-based fuels [114]. Despite this, the economics of producing bioethanol still presents a

huge challenge in making it more preferable than fossil-based fuels for end users and potential investors [10]. For example, in the European Union (EU), bioethanol would only be able to compete with fossil-based fuels when crude sells for US$ 70 a barrel, while it can compete in the United States (US) when crude sells at US$ 50–60 a barrel, and in Brazil it can compete when crude sells at US$ 25–30 a barrel [116]. Currently, crude oil sells for between US$ 30–50 a barrel, making fossil-based fuels the cheapest fuel alternative in the market. The cost of bioethanol production can be separated into four main classes: the cost of the feedstock, the cost of pretreatment, the cost of the fermentation process and the cost associated with upgrading the produced bioethanol. While the costs of feedstock and pretreatment depend on the substrate (which is usually outside the control of process designers or operators), significant improvement can be made in reducing the cost associated with fermentation processes and how this can be done was considered using the textile-based bioreactor.

From a fermentation perspective, a high product yield, process development, reduction in bioreactor cost and a faster fermentation rate can help in minimising the cost of the fermentation process (**Paper II**). For first-generation ethanol production, baker's yeast and flocculating yeast were used for bioethanol production in the textile-based bioreactor (**Paper I** and **II**), while the fungi *Nuerospora Intermedia* was used for integrating first- and second-generation bioethanol production (**Paper VI**). Taking flocculating yeast as an example, using it for bioethanol production comes with several advantages such as improved inhibitor tolerance, high productivity associated with a high dilution rate and reduced bioreactor volume requirement. However, to maintain the floc size to minimise cell washout and improve mass transfer, mixing is usually carried out in the bioreactors using aeration as stirrers will break the flocs [43]. This causes two major challenges: reduced ethanol yield as aeration favours more biomass production and increased foaming tendencies [117]. Hence, mixing was carried out anaerobically in the textile-based bioreactor using the liquid medium of the fermentation broth (using the fluidisation concept shown in Equations 4.1–4.4). This resulted in an ethanol specific productivity of 0.29 ± 0.01 g-ethanol/g-biomass/h with complete substrate utilisation (**Paper II**), which compares favourably to reported ethanol specific productivity of 0.045 g-ethanol/g-biomass/h with complete substrate utilisation or 0.4 g-ethanol/g-biomass/h with significant loss of substrate [118]. Additionally, combining the benefits of lower bioreactor cost associated with the textile-based bioreactor with the elimination of the need for centrifugation (because of the high settling velocity of the flocs), the fermentation investment cost of a typical 100,000 m^3/year ethanol can be reduced by 37 % (**Paper II**).

4.6 Perspective on biogas production

Biogas is a mixture of gases consisting mainly of methane and carbon dioxide produced through anaerobic digestion (AD) of organic feedstocks. The high methane content in biogas means that it can be used as a good energy source for heating [119] or electricity generation [120]. In addition to the produced biogas, anaerobic digestion also produces fertilisers as a by-product, increasing the overall profitability of the biogas production process (**Paper V**). Biogas production has a distinct advantage over bioethanol production in that it can be produced economically at small, medium or large scales from the organic content of waste materials (**Paper V**). However, as biogas is a gaseous phase, from the perspective of transportation or storage, bioethanol production is more favourable. Another distinction between bioethanol and biogas production is that the AD process for biogas production is carried out by a consortium of microorganisms working in synergy unlike bioethanol production in which the fermentation process can be carried out by a single microorganism. The flexibility in the scale of production and the ability to produce biogas from waste, which reduces the effect of feedstock cost on biogas production, makes biogas production and utilisation a good solution in addressing both waste and energy challenges at small, medium and large scales [121].

The process of biogas production includes the preparation of the substrates for digestion [122] in addition to the AD steps, namely hydrolysis, acetogenesis, acidogenesis and methanogenesis [123]. As the AD steps are linked, any negative development on any of the preceding steps has a direct effect on the other steps involved in the biogas production process which would make the biogas bioreactor to become unstable or come to a complete halt [124]. The challenges associated with large-scale biogas production is mainly due to low biogas yield, high retention time, and high investment cost [125]. From a process perspective, these challenges can mainly be related to temperature fluctuations, foam formation, feedstock composition, feeding problems, pH changes and bioreactor cost with its associated problems [125]. Hence, a good bioreactor design, proper operations and the use of a cost-effective bioreactor was the approach with the textile-based bioreactor for biogas production. This was effective in addressing challenges due to temperature fluctuations, foam formation, feeding or mixing problems and other bioreactor-associated challenges (such as high investment cost) (**Paper V** and **VI**).

Waste, biomass and residues are considered the most abundant renewable resources globally [126]. However, the potential that lies with producing biogas from these abundant resources has not been fully realised. For example, 17 billion tons of solid waste is generated annually by people [127] with the projection estimating it to reach 27 billion tons/year from 2050 [128], while 2.5–3.75 tons of wastewater are produced for every ton of produced vegetable oil [129] and 160.59 × 10^6 MT of vegetable oil was produced in 2012 [130]. Using a methane yield of 265 Nm^3/ton-VS from municipal solid waste with a volatile solid (VS) composition of 10 % and a methane yield of 350 Nm^3/ton-VS from wastewater from vegetable oil production which contains of 4 % VS [126], a total of 4.58 × 10^{11} Nm^3 of methane could be produced if those waste materials were used for biogas production. Taking palm oil mill effluent (POME) the waste water from palm oil processing as example, the amount of biogas produced is usually below the theoretically possible value because of challenges such as the acidic pH of POME (3.4–5.2), high COD (15–150 g/L) and the release of high inhibitory concentrations of volatile fatty acids (VFA) which can hinder the methanogenesis process [131]. This challenge was addressed using a flocculating bacterial concentration of 0.625 g-COD substrate/g-VS inoculum at 37 °C or 0.313 g-COD substrate/g-VS inoculum at 22 °C. This resulted in a methane yield of 180 NmL/g-VS at 37 °C and 140 NmL/g-VS at 22 °C (unpublished data).

5. Economics of textile-based bioreactor using ethanol and biogas production as case studies

5.1 An overview on techno-economic analysis

The main goal of any production or manufacturing facility is to continue to generate profit from the entirety of its operations. Before starting a project or production facility, a techno-economic analysis is normally performed to obtain an estimate on how economical the project would be. Fermentation is the heart of biologically based production; hence, it is important that its overall economics is favourable, as the fermentation investment cost could contribute up to 30 % of the total equipment investment cost of the facility [26]. The economic parameters used for evaluating the profitability of using the textile-based bioreactor were capital or investment cost, operating cost, payback period (PBP), internal rate of return on investment (IRR) and net present value (NPV).

The investment and operation costs associated with any bioreactor directly affect the economics of choosing between using one bioreactor over another; how well the bioreactor functions as determined by factors like product yield, productivity or batch completion time affects the overall economics of the facility where the bioreactor is used. How all these factors relate to the overall production cost on a yearly basis (annual production cost: APC) is shown in Equation 5.1 [132], where Y is the product yield, FC is the feedstock cost, ACE is the annual capital expenditure, OC is the operating cost, EC is the electricity credit and Ye is the electricity yield.

$$\text{Annual production cost (APC)} = FC/Y + (ACE + OC) - Ye.EC \quad \textbf{5.1}$$

When the cost of feedstock is high and contributes the highest annual cost burden to the production facility, then it is very important that the product yield from the bioreactor is high so as to minimise the overall impact the high feedstock cost would have on the APC [133, 134]. If the production cycle time is high or the productivity is low, then it is important that the sum of the ACE and OC is low to reduce their overall contribution to the APC [135, 136]. As the feedstock cost is outside the control of bioreactor designers or operators, the goal of an economically favourable bioreactor would be that the design of the bioreactor is suitable for

attaining a high product yield from operating the bioreactor while also keeping its associated capital and operating costs low.

5.2 Economic comparison of textile-based bioreactor with conventional bioreactors

The capital expenditure needed for procuring stainless-steel vessels, the predominating material of construction for the conventional bioreactors used in the industry [20], can be estimated using Equation 5.2, where CE is the capital expenditure or investment cost ($), F_m is a material factor (2.4 for 304 stainless steel) and V is the volume (gallons) [137].

$$CE = F_m \exp[11.662 - 0.6104(\ln V) + 0.04536(\ln V)^2] \quad \textbf{5.2}$$

This capital expenditure (CE) equation can be updated to give the 2017 cost of the vessel using the projected Chemical Engineering Plant Cost Index (CEPCI) for 2017, which is 574.1, based on the current low oil price [138] as shown in Equation 5.3.

$$C_{updated} = C\,(I_{updated}/I) \quad \textbf{5.3}$$

Using Equations 5.2 and 5.3, the capital expenditure needed for any volume of stainless-steel bioreactor vessels can be estimated. Equations 5.2 and 5.3 do not include the cost associated with designing or including bioreactor features into the bioreactor vessel. The average cost needed to include bioreactor features into a stainless-steel vessel and to install it in a facility is typically 1.7 times its procurement cost [137]. Combining the installation cost with the vessel cost gave the bioreactor costs summarised for selected volumes in Table 5.1. The installed cost for a textile-based bioreactor vessel is $150/volume for small-scale applications (in volumes of 2 m^3), $100/volume for medium- to large-scale applications (volume in 100s of m^3) and $70/volume for large-scale applications (volume in 1000s of m^3) (**Paper V**). A comparison between the cost for some bioreactor volumes if they are made with stainless steel or made with the textile material is shown in Table 5.1. From the table, it can be seen that the textile-based bioreactor is at least 6.8 times less expensive than the stainless-steel bioreactor. Taking an ethanol production facility of capacity 100,000 m^3/year as an example, using a 1000 m^3 textile-based bioreactor instead of a stainless-steel bioreactor can reduce the fermentation investment cost of the facility by 21 % (**Paper I**).

Table 5.1: The installed cost of a bioreactor volume if made with stainless steel or textile material

Bioreactor size (m^3)	Procurement cost of textile based bioreactor vessel ($)	Procurement cost of 304 stainless steel bioreactor vessel ($)
100	10 000	184 000
200	20 000	234 000
300	30 000	272 000
400	40 000	308 000
500	50 000	340 000
1000	70 000	476 000

5.3 Improving the economics of fermentation processes using the textile-based bioreactor

To achieve optimal productivity with any bioreactor, it is important to maintain the bioreactor at the optimal conditions needed by the fermenting microorganism. Maintaining these conditions (such as temperature control or mixing) contributes to the operation and investment costs of a fermentation-based facility. Taking ethanol production as an example, baker's yeast would optimally produce ethanol at 30 °C, pH 4–6, and with good mixing [139]. Under optimal conditions, an ethanol specific productivity of 1.34 ± 0.02 g/L/h was attained in the textile-based bioreactor, while a specific ethanol productivity of 0.53 ± 0.02 g/L/h was obtained without temperature control or mixing (**Paper I**). Optimal ethanol productivity can be realised in non-optimal conditions by using a bioreactor volume 2.5 times that needed under optimal conditions. Doing this for a 100,000 m^3/year ethanol facility would reduce the fermentation investment cost of the facility by 26 %.

The low investment cost of the textile-based bioreactor also aids in making fermentation-based processes more attractive. For example, dry anaerobic digestion of solid waste in the textile-based bioreactor is a more economically favourable approach of handling solid waste than paying waste managers to collect the waste or composting (**Paper V**). This is evidenced by the positive net present value (NPV) and the internal rate of return (IRR) particularly at small scale.

As the scale of waste generation increased, after a biomass adaptation time of 325 days, dry anaerobic digestion in the textile-based reactor would still be preferred to composting from an economic perspective (Figure 5.1).

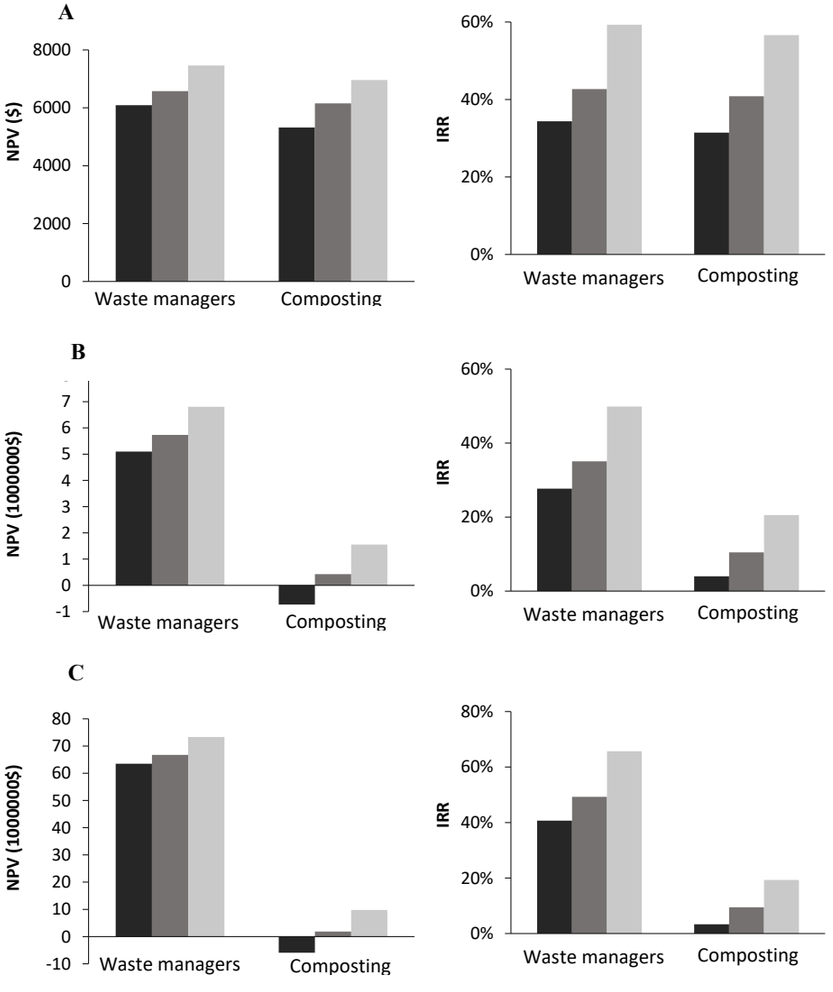

Figure 5.1: The net present value and the corresponding internal rate of return analysis for replacing waste collection by waste managers and composting with dry anaerobic digestion for small scale (A), mid-scale (B) and large scale(C) with no inoculum acclimatisation and dense feedstock (■), 234 days for inoculum acclimatisation with less dense feedstock (■) and 325 days for inoculum acclimatisation with less dense feedstock (■).

6. Upscaling the textile-based bioreactor

Despite the benefits of the textile-based bioreactor over conventional stainless steel-based bioreactors that include process flexibility, ease of transportation, installation, portability and low cost, if the bioreactor is to be used for medium- to large-scale applications, it is important that safety is assured. Conventional stainless-steel bioreactors are designed as pressure vessels, so that they can contain the pressure exerted on them during sterilisation or that exerted by the liquid contained in them [63]. This way, safety is assured when they are used. This concept of designing bioreactors as pressure vessels was extended to the textile-based bioreactor to estimate how safe it would be to use the bioreactor for medium to large-scale purposes.

Pressure vessels are either thick walled or thin walled, depending on the thickness of the material. Thin-walled pressure vessels have a wall thickness-to-radius ratio less than or equal to 1/20 [63]. This means that thin-walled pressure vessels would offer no resistance to bending, and the stress on it is distributed through its thickness, resulting in only membrane stresses. Therefore, the textile-based bioreactor is a thin-walled pressure vessel. The thin shell theory is usually used for calculating the stress in a thin-walled vessel. However, the thin shell theory cannot be directly applied in determining the stress in the textile-based bioreactor for the following reasons: the bioreactor will not have the same pressure at all points, and will not have a specific shape at all times because the shape will change with changes in pressure and the volume of fluid in the bioreactor [140].

6.1 Defining the shape of the textile-based bioreactor

To prevent failure, which would occur when the membrane stress in the bioreactor exceeds the material's intrinsic tolerance values as determined by its Young's modulus [65], it is important to be able to accurately determine the stress exerted on the bioreactor [61]. To calculate stress, it is important to be able to define the shape of the bioreactor mathematically. Defining the shape of the bioreactor is challenging because changes in pressure or liquid volume in the bioreactor always changes its shape. To overcome this challenge, the curvature (k) of the bioreactor was defined as a function of pressure, so that changes in pressure can be incorporated into defining the shape of the bioreactor (**Paper III**).

To mathematically define the shape, a reference frame was used where position and altitude were considered using the top height of the liquid level as the origin [141], so that every height below the top of the liquid level was negative. The only positive height was that due to the gas if present (Figure 6.1). The mathematical equations for defining the shape are shown in Equations 6.1–6.4, and Equation 6.4 is the differential equation that connects the curvature (k), the bioreactor strip length (x) or height (y) and the arc length of the bioreactor material in one dimension (S) together [142]. The other parameters are the directional angle of the tangent to the curve (α), the static pressure above the liquid in N/m^2 (P_0), the liquid height in meters ($y\_$) which is defined with respect to the y axis according to Equation 6.3, the acceleration due to gravity in m/s^2 (g), the fluid density in kg/m^3 (ρ) and the membrane stress force or tension per unit length in N/m (T).

$$k = \frac{d\alpha}{ds} \quad \textbf{6.1}$$

$$k = \frac{P_0 - y\_g\rho}{T} \quad \textbf{6.2}$$

$$y\_ = \begin{cases} y, y \leq 0 \\ 0, y > 0 \end{cases} \quad \textbf{6.3}$$

$$\begin{cases} \frac{d^2x}{ds^2} = k\frac{dy}{ds} \\ \frac{d^2y}{ds^2} = -k\frac{dx}{ds} \end{cases} \quad \textbf{6.4}$$

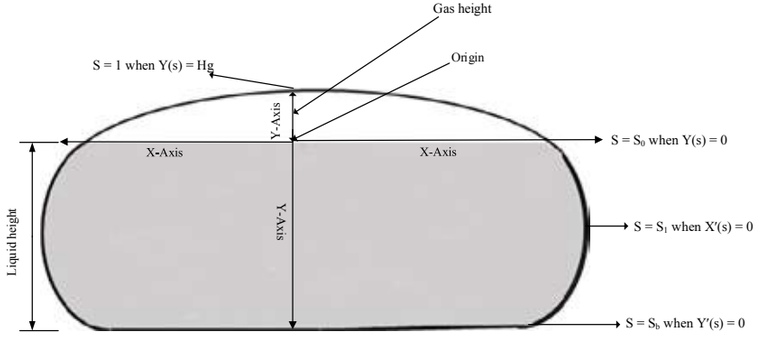

Figure 6.1: Reference frame for defining the shape of the textile-based bioreactor.

6.2 Membrane stress simulation in the textile-based bioreactor

The shape equations (Equation 6.1–6.4) were simplified to first-order differential equation forms and the resulting differential equations were solved numerically using MATLAB® ODE45 solver [143]. An iterative process was used to find the corresponding tension per unit length (T), the gas height (Hg) and the static pressure (P_0) for a given bioreactor volume, length and working capacity as shown in Table 6.1 (**Paper III**).

Table 6.1: Simulation result from numerical analysis of textile-based bioreactor volumes from 100 to 1000 m^3

Specified parameters			Final iterative values				Calculated values		
Volume of bioreactor (m^3)	Specified length (m)	Working capacity	Width of bioreactor (m)	Tension per unit length (N/m)	Gas height (m)	Static pressure (N/m^2)	Liquid height in the bioreactor (m)	Perimeter of bioreactor (m)	Flat base length of the bioreactor (m)
100	20	0.84	7	1000	0.22	58	0.63	14.57	6.63
200	23	0.80	9	1500	0.44	85	0.77	18.94	8.65
300	35	0.80	9	1500	0.44	85	0.77	18.94	8.65
400	33	0.84	11	2200	0.33	72	0.94	23.44	10.75
500	30	0.80	14	2600	0.44	73	1.02	28.21	13.04
1000	50	0.83	15	3500	0.45	92	1.18	30.20	13.87

As the simulation process can be time consuming, an equation was generated for calculating the tension per unit length (T) when the liquid height (h), gas height (Hg) and static pressure (P_0) in the bioreactor are known (Equation 6.5).

$$T = 0.5P_0(h + Hg) + 0.25\rho gh^2 \quad \textbf{6.5}$$

However, the liquid height usually changes based on the bioreactor geometry and the volume of liquid in the bioreactor. Hence, an equation for estimating the liquid height (h) for bioreactors between 100–1000 m^3 using the product of the volume per unit length (A) and the working capacity or volume fraction occupied by liquid (WC) and the width of the bioreactor (W) (Equation 6.6).

$$WC.A = 0.968W.h - 0.0755 \quad \textbf{6.6}$$

Using Equations 6.5 and 6.6 for calculating the liquid height and tension per unit length for different bioreactor volumes resulted in a maximum of 3 % deviation (i.e. overestimation or underestimation) in the value of the liquid height from simulation and 6 % maximum variation in the tension per unit length calculated from simulation (**Paper III**).

6.3 Selection of appropriate material of construction

When the bioreactor does not have an external reinforcement, the stress that would be exerted on it when in operation can be estimated using Equations 6.6 and 6.7. For any bioreactor volume, the higher the liquid height, the more the tension (**Paper III**), and one way to reduce the liquid height would be by increasing the width of the bioreactor. Taking a 1000 m^3 bioreactor with a length of 50 m as an example, for the same working capacity, if the width is 7.5 m, the tension per unit length would be 20000 N/m, while the tension per unit length can be reduced to 800 N/m by increasing the width to 30 m. Knowing the area the bioreactor would occupy can aid in designing the bioreactor with a width that minimises the stress that would be exerted on it. This can aid in selecting an appropriate material for fabricating the bioreactor.

Taking a 1000 m^3 bioreactor with calculated tension per unit length of 3360 N/m as an example, a pressure allowance factor of 1.5 times the resultant tension in both direction of the bioreactor would be needed to prevent failure [20]. If the thickness of the bioreactor is 0.75 mm, then the stress exerted on the bioreactor would be 14.2 MPa. Polymeric materials are usually used for fabricating collapsible tanks, and polyvinyl chloride (PVC) with a tensile strength between 7 and 25 MPa is the most used option [144]. The tensile strength of PVC can be increased up to 280 MPa when they are combined with some other materials to make composites [144], but making composites also increases the cost of the material. Hence, using textile which is a cheap reinforcement material is an economically favourable approach [145].

Initially, the polymeric material used in making the textile-based bioreactor was polyvinyl chloride (PVC), but recently polyamide (PA) has been introduced as a better material of construction for the textile-based bioreactor [76].

7. Conclusion and future recommendations

7.1 Major findings and conclusion

Good bioreactor design is essential for achieving optimal fermentative production. The textile-based bioreactor introduced in this thesis was designed and developed for aerobic and anaerobic fermentation and it was tested using ethanol and biogas production. The bioreactor could reduce the fermentation investment cost by 21 % or more, introducing flexibility and addressing several technical problems associated with both anaerobic and aerobic fermentation production process. The key findings from this thesis are as follows.

- With the introduction of temperature control to the bioreactor, ethanol productivity increased by 200 %. Two temperature control systems were developed for the textile-based bioreactor, one for anaerobic application suitable for bioreactors with an area-to-volume ratio of approximately 1 or higher and another aerobic application for bioreactors with an area-to-volume ratio less than 1.
- The bioreactor was designed to address the mass transfer limitation associated with microorganisms having self-aggregating tendencies, pellet and filamentous morphologies as evidenced by the reduction of the fermentation time at low bulk flowrate. This was done by increasing the contact area inside the bioreactor. Further, the oxygen mass transfer limitation was addressed.
- Mixing systems were developed for aerobic and anaerobic fermentation. Mixing time less than 1 h was obtained for limiting substrate or product condition. With the appropriate mixing system design, a dilution rate of 1/h can be used in the bioreactor without washout for microorganisms such as flocculating yeast with an average settling velocity of 0.01 m/s.
- Rheological studies showed that the textile bioreactor can be used at the high aeration rate of 1.4 VVM for viscous substrates with minimised foam formation and stabilisation tendencies.
- From the simulation of the stress that would be acting on the bioreactor from 100–1000 m^3, the tension per unit length was found to be between 300–20000 N/m, and the stress can be reduced by reducing the liquid height inside the bioreactor.

7.2 Future recommendations

Due to the limitation of time, several interesting areas which could affect the safety, economics, application and productivity of the textile-based bioreactor were not covered in this thesis. They are recommended for future research or applications of the textile-based bioreactor as follows.

- Additional safety studies. In addition to failure due to pressure from the fluid volume in the bioreactor, temperature also causes stress on the bioreactor when in application or during sterilisation. Performing a thermal stress analysis can aid both in ensuring safe applications of the bioreactor and in material selection for the bioreactor. Corrosion analysis can also be performed on the material to determine the effect of prolonged exposure of the material to corrosive fermentation media.
- Integration of fermentation processes and its economics. The flexibility of the textile bioreactor means that it can be switched from one fermentative production to another. However, several technical issues may arise from doing this and it is important understand the challenges that such a switch will pose to the bioreactor design. Additionally, a techno-economic analysis needs to be performed to quantify the profitability or otherwise of using the textile bioreactor for integration of different fermentation processes.
- Application for other fermentative products. As other fermentative production processes may have challenges different from those experienced for biofuel production, it is important that the design of the bioreactor for those applications address those challenges.
- Computational fluid dynamics. Performing a computational fluid dynamics simulation on the textile-based bioreactor can help in further improving the efficiency of mixing and the homogenisation of the content of the bioreactor, particularly for high-viscosity applications.

Acknowledgement

In the course of this PhD journey, a lot of water came under the bridge of my ability to finish as I intended. The bridge would not have held if not for the Almighty God and several people who stood with me through this journey.

First, my heartfelt gratitude goes to my supervisor Professor Mohammad Taherzadeh. As a supervisor you guided, corrected, instructed, led and gave insight to me throughout my PhD experience. As a friend you were there when I needed you and you encouraged me in the midst of difficulties. As a mentor, I learnt a lot from you, and you repeatedly taught me how to see things from different perspectives. I am most grateful.

I am grateful to Michael Tittus and Professor Vincent Ezemonye who were instrumental in the collaboration between the University of Borås and the University of Benin that led to me getting a PhD position with the University of Borås.

Patrik (my co-supervisor), thanks for your support, suggestions, encouraging words and guidance through my PhD journey. I remember how you had to micromanage me when I wrote my first manuscript. “Tack så mycket.”

I am grateful to my examiner Professor Kim Bolton. You gave insights and valuable comments that assisted in the progress I made in this PhD study.

Thanks Magnus for collaborating with me and the tremendous insight you shared with me in making my research findings better by applying statistical methods.

Regina, thanks for continually remaining a friend I could depend on. Thanks for all the collaboration we had. “o ṣeun pupọ”

Ramkumar, “Rammy my manny”, many thanks to you for being a wonderful friend and an excellent colleague. Thanks for all the collaboration we had.

Thanks Mostafa for the excellent collaboration we had in the course of my PhD studies.

My gratitude goes to all the lecturers at the University of Borås for the knowledge and technical insight you shared with me: Dr. Anitta Pattersson, Prof. Jan Nolin, Prof. Christine Räisänen, Prof. Lars Sandman and many others I did not mention by name here. Thank you all.

My appreciation goes to all past and present members of staff of the Swedish Centre for Resource Recovery: Dr. Peter Therning, Dr. Tomas Wahnström, Kristina Laurila, Marlén Kilberg, Thomas Södergren, Irene Lammassaari, Sari Sarhamo, Louise Holmgren, to name a few. Thanks to all past and present members of biogroup: Prof. Ilona Sárvári Horváth, Dr. Päivi Ylitervo, Dr. Karthik Rajendran, Dr. Maryam Kabir, Dr. Akram Zamani, Dr. Jorge Ferreira, Dr. Mofoluwake Ishola, Dr. Julius Akinbomi, Dr. Supansa Westman, Amir, Konstantinos, Veronica, Lukitawesa, Stephen, Pedro, Rebecca, Forough and Sajjad. My gratitude to past and present PhD students of the University of Borås; Dr. Fatimat Bakare, Dr. Kehinde Oluoti, Dr. Sunil Ramamoorthy, Dr. Tariq Bashir, Madumita Sadagopan, Andreas Nordin, Eboh Francis Chinweuba and many others not mentioned here.

I am most grateful to Rune and Rode Swahn who stood as parents and faithful friends over my entire family in the course of my PhD. Thanks for all the love, care, support, assistance and counsel you gave me and my family. Rune, we will continue to miss you, and your memory will live on in our hearts. Rest in peace in the presence of God.

Thanks Igbinoba Godfrey Edosa for being a wonderful friend before and during my PhD studies. I want to appreciate Johan and Sara Forsblom for being amazing friends to my entire family through the period of my PhD. Thanks for all the love, support and prayers.

I am most grateful to my mother Mabel Irhene, for all the sacrifices she made for me to be able to get a good start in life. You will forever remain my Sweet Mama. I am grateful to my aunties Belinda and Kate. Thanks for all the support. My gratitude also goes to my in-laws the Onuegbu family. Thank you for all the care and support.

Finally, I want to express my heartfelt gratitude to my immediate family. To my daughters Charis and Casiel, thank you so much for putting up with me through this period. We had to ration our play time so that Daddy could work. To my remarkable wife, friend, sister and confidant Chidinma, you have been a pillar to our family. Even though you are a psychologist by vocation, you became a chemical engineering/biotechnologist trainee. You were always in the know of my experimental findings, sharing insights with me and supporting me through very tough times. “Many daughters have done well, but you exceed them all”. Proverbs 31:29.

References

1. Angelidaki, I., et al., *Biomethanation and its potential*, in *Methods in Enzymology*. 2011. p. 327-351.
2. Atiyeh, M.R.W.a.H., *Fermentation*, in *Food and Industrial Bioproducts and Bioprocessing*. 2012, Wiley-Blackwell: Hoboken, US. p. 185 - 204.
3. Madigan, M.T., et al., *Brock biology of microorganisms*. 13 ed. 2012.
4. Benz, G.T., *Bioreactor design for chemical engineers.* Chem. Eng. Prog, 2011. **107**(2126): p. 13.
5. Blakebrough, N., *Fundamentals of fermenter design.* Pure and Applied Chemistry, 1973. **36**(3): p. 305-316.
6. American Chemical Society. *National Historic Chemical Landmarks. Penicillin Production through Deep-tank Fermentation*. 2008 [cited 2017-12-03]; Available from: http://www.acs.org/content/acs/en/education/whatischemistry/landmarks/penicillin.html.
7. Rouf, S.A., et al., *Single versus multiple bioreactor scale-up: economy for high-value products.* Biochemical Engineering Journal, 2000. **6**(1): p. 25-31.
8. Shukla, A.A. and U. Gottschalk, *Single-use disposable technologies for biopharmaceutical manufacturing.* Trends in Biotechnology, 2013. **31**(3): p. 147-154.
9. Terrier, B., et al., *Two new disposable bioreactors for plant cell culture: the wave and undertow bioreactor and the slug bubble bioreactor.* Biotechnology and bioengineering, 2007. **96**(5): p. 914-923.
10. Berni, M., et al., *Advances in biofuel production*, in *Biofuels Production*. 2013. p. 11-58.
11. Flanagan, D.T. and R.C. Hopkins, *Advanced collapsible tank for liquid containment.* 1993.
12. Kerns, N., et al., *Collapsible Storage Tank.* 2009.
13. Tuckerton, N.J., *Collapsible storage tanks.* Metal Finishing, 2000. **98**(11): p. 27.
14. Abbott, N.J., *Product- and Process-Related Coating Requirements.* Journal of Coated Fabrics, 1983. **12**(3): p. 187-193.
15. Biron, J., *An aluminum collapsible bladder tank for space systems.* AIAA Paper, 1990. **2058**.
16. Feuer, H.O. and P. Touchet, *Failure Mechanism of Urethane-Elastomer-Coated-Fabric Collapsible Fuel Tanks.* Journal of Coated Fabrics, 1991. **20**(3): p. 188-210.
17. Eibl, R., et al., *Disposable bioreactors: the current state-of-the-art and recommended applications in biotechnology.* Applied microbiology and biotechnology, 2010. **86**(1): p. 41-49.
18. Rajendran, K., et al., *Experimental and economical evaluation of a novel biogas digester.* Energy Conversion and Management, 2013. **74**(Supplement C): p. 183-191.
19. Singh, V., *Disposable bioreactor for cell culture using wave-induced agitation.* Cytotechnology, 1999. **30**(1): p. 149-158.
20. Olisti, Y., *Build better industrial bioreactors.* Chem. Eng. Prog, 1992. **1992**: p. 55-58.
21. Sharifzadeh, S., D. Verstraete, and P. Hendrick, *Cryogenic hydrogen fuel tanks for large hypersonic cruise vehicles.* International Journal of Hydrogen Energy, 2015. **40**(37): p. 12798-12810.
22. Verstraete, D., et al., *Hydrogen fuel tanks for subsonic transport aircraft.* International journal of hydrogen energy, 2010. **35**(20): p. 11085-11098.
23. Xu, W., Q. Li, and M. Huang, *Design and analysis of liquid hydrogen storage tank for high-altitude long-endurance remotely-operated aircraft.* International Journal of Hydrogen Energy, 2015. **40**(46): p. 16578-16586.

24. Jabbari, M., et al., *Introducing all-polyamide composite coated fabrics: A method to produce fully recyclable single-polymer composite coated fabrics.* Journal of applied polymer science, 2016. **133**(7).
25. Jabbari, M., et al., *Novel lightweight and highly thermally insulative silica aerogel-doped poly (vinyl chloride)-coated fabric composite.* Journal of Reinforced Plastics and Composites, 2015. **34**(19): p. 1581-1592.
26. Maiorella, B.L., et al., *Economic evaluation of alternative ethanol fermentation processes.* Biotechnology and bioengineering, 2009. **104**(3): p. 419-443.
27. Mariano, A., T. Ezeji, and N. Qureshi, *Butanol production by fermentation: efficient bioreactors*, in *The Royal Society of Chemistry*. 2016. p. 48-70.
28. Jones, D.T. and D.R. Woods, *Acetone-butanol fermentation revisited.* Microbiological reviews, 1986. **50**(4): p. 484.
29. Foster, J.W. and L.E. McDaniel, *Process for the production of penicillin*. 1948, Google Patents.
30. Ault, R.G., et al., *Biological and biochemical aspects of tower fermentation.* Journal of the Institute of Brewing, 1969. **75**(3): p. 260-277.
31. Lopes, A.G., *Single-use in the biopharmaceutical industry: A review of current technology impact, challenges and limitations.* Food and Bioproducts Processing, 2015. **93**(Supplement C): p. 98-114.
32. Schügerl, K., J. Lücke, and U. Oels, *Bubble column bioreactors*, in *Advances in Biochemical Engineering, Volume 7*. 1977, Springer Berlin Heidelberg: Berlin, Heidelberg. p. 1-84.
33. Kadic, E. and T.J. Heindel, *Concluding Remarks*, in *An Introduction to Bioreactor Hydrodynamics and Gas-Liquid Mass Transfer*. 2014, John Wiley & Sons, Inc. p. 263-266.
34. Westman, J.O., et al., *Flocculation causes inhibitor tolerance in Saccharomyces cerevisiae for second-generation bioethanol production.* Applied and environmental microbiology, 2014. **80**(22): p. 6908-6918.
35. Paek, K.Y., D. Chakrabarty, and E.J. Hahn, *Application of bioreactor systems for large scale production of horticultural and medicinal plants*, in *Liquid culture systems for in vitro plant propagation*. 2005, Springer. p. 95-116.
36. Bredwell, M.D., P. Srivastava, and R.M. Worden, *Reactor design issues for synthesis-gas fermentations.* Biotechnology progress, 1999. **15**(5): p. 834-844.
37. Kumar, S., C. Wittmann, and E. Heinzle, *Minibioreactors.* Biotechnology Letters, 2004. **26**(1): p. 1-10.
38. Nienow, A.W., *Hydrodynamics of stirred bioreactors.* Applied Mechanics Reviews, 1998. **51**: p. 3-32.
39. Nienow, A.W., *Reactor engineering in large scale animal cell culture.* Cytotechnology, 2006. **50**(1-3): p. 9.
40. Van't Riet, K. and J. Tramper, *Basic bioreactor design*. 1991: CRC Press.
41. Mitchell, D.A., O.F. von Meien, and N. Krieger, *Recent developments in modeling of solid-state fermentation: heat and mass transfer in bioreactors.* Biochemical Engineering Journal, 2003. **13**(2): p. 137-147.
42. Kantarci, N., F. Borak, and K.O. Ulgen, *Bubble column reactors.* Process Biochemistry, 2005. **40**(7): p. 2263-2283.
43. Domingues, L., et al., *Applications of Yeast Flocculation in Biotechnological Processes.* Biotechnology and Bioprocess Engineering, 2000. **5**(4): p. 288-305.
44. Garcia-Ochoa, F. and E. Gomez, *Bioreactor scale-up and oxygen transfer rate in microbial processes: an overview.* Biotechnology advances, 2009. **27**(2): p. 153-176.
45. Garcia-Ochoa, F., et al., *Oxygen uptake rate in microbial processes: An overview.* Biochemical Engineering Journal, 2010. **49**(3): p. 289-307.
46. Gomez, E., et al., *Oxygen-Uptake and Mass-Transfer Rates on the Growth of Pseudomonas p utida CECT5279: Influence on Biodesulfurization (BDS) Capability.* Energy & fuels, 2006. **20**(4): p. 1565-1571.

47. Domingues, F., et al., *The influence of culture conditions on mycelial structure and cellulase production by Trichoderma reesei Rut C-30.* Enzyme and Microbial Technology, 2000. **26**(5): p. 394-401.
48. Doran, P.M., *Chapter 10 - Mass Transfer*, in *Bioprocess Engineering Principles (Second Edition)*. 2013, Academic Press: London. p. 379-444.
49. Maier, U. and J. Büchs, *Characterisation of the gas–liquid mass transfer in shaking bioreactors.* Biochemical Engineering Journal, 2001. **7**(2): p. 99-106.
50. Ananta, I., M.A. Subroto, and P.M. Doran, *Oxygen transfer and culture characteristics of self-immobilized Solanum aviculare aggregates.* Biotechnology and bioengineering, 1995. **47**(5): p. 541-549.
51. Sousa, M.L. and J.A. Teixeira, *Reduction of diffusional limitations in yeast flocs.* Biotechnology letters, 1991. **13**(12): p. 883-888.
52. Teixeira, J.A. and M. Mota, *Experimental assessment of internal diffusion limitations in yeast flocs.* The Chemical Engineering Journal, 1990. **43**(1): p. B13-B17.
53. Cervantes, M.I.S., et al., *Novel bioreactor design for the culture of suspended mammalian cells. Part I: Mixing characterization.* Chemical Engineering Science, 2006. **61**(24): p. 8075-8084.
54. Munasinghe, P.C. and S.K. Khanal, *Syngas fermentation to biofuel: evaluation of carbon monoxide mass transfer coefficient (kLa) in different reactor configurations.* Biotechnology progress, 2010. **26**(6): p. 1616-1621.
55. Pauss, A., et al., *Liquid-to-gas mass transfer in anaerobic processes: inevitable transfer limitations of methane and hydrogen in the biomethanation process.* Applied and environmental microbiology, 1990. **56**(6): p. 1636-1644.
56. Wisniewski, C. and A. Grasmick, *Floc size distribution in a membrane bioreactor and consequences for membrane fouling.* Colloids and Surfaces A: Physicochemical and Engineering Aspects, 1998. **138**(2): p. 403-411.
57. Scardina, P. and M. Edwards, *Fundamentals of bubble formation during coagulation and sedimentation processes.* Journal of Environmental Engineering, 2006. **132**(6): p. 575-585.
58. Enfors, S.O., et al., *Physiological responses to mixing in large scale bioreactors.* Journal of biotechnology, 2001. **85**(2): p. 175-185.
59. Larsson, G., et al., *Substrate gradients in bioreactors: origin and consequences.* Bioprocess and Biosystems Engineering, 1996. **14**(6): p. 281-289.
60. Doran, P.M., *Chapter 7 - Fluid Flow*, in *Bioprocess Engineering Principles (Second Edition)*. 2013, Academic Press: London. p. 201-254.
61. Kaminski, C., *Stress Analysis & Pressure Vessels*. Lent Term. 2005.
62. Rajendran, K., S. Aslanzadeh, and M.J. Taherzadeh, *Household biogas digesters—A review*. Energies, 2012. **5**(8): p. 2911-2942.
63. Vullo, V., *Circular cylinders and pressure vessels: stress analysis and design*. 2014, Cham: Springer.
64. Olisti, Y., *Build better industrial bioreactors.* Chemical engineering progress, 1992: p. 55.
65. Ashby, M.F. and D.R.H. Jones, *Engineering Materials 1: An Introduction to Properties, Applications and Design*. Vol. 1. 2011: Elsevier.
66. Garcia-Ochoa, F. and E. Gomez, *Theoretical prediction of gas–liquid mass transfer coefficient, specific area and hold-up in sparged stirred tanks.* Chemical Engineering Science, 2004. **59**(12): p. 2489-2501.
67. Linek, V., M. Kordač, and T. Moucha, *Mechanism of mass transfer from bubbles in dispersions: part II: mass transfer coefficients in stirred gas–liquid reactor and bubble column.* Chemical Engineering and Processing: Process Intensification, 2005. **44**(1): p. 121-130.
68. Schlüter, V. and W.D. Deckwer, *Gas/liquid mass transfer in stirred vessels.* Chemical Engineering Science, 1992. **47**(9-11): p. 2357-2362.

69. Liu, Y.-S., J.-Y. Wu, and K.-p. Ho, *Characterization of oxygen transfer conditions and their effects on Phaffia rhodozyma growth and carotenoid production in shake-flask cultures.* Biochemical Engineering Journal, 2006. **27**(3): p. 331-335.
70. Hellendoorn, L., et al., *Intrinsic kinetic parameters of the pellet forming fungus Aspergillus awamori.* Biotechnology and bioengineering, 1998. **58**(5): p. 478-485.
71. Van Suijdam, J., H. Hols, and N. Kossen, *Unstructured model for growth of mycelial pellets in submerged cultures.* Biotechnology and bioengineering, 1982. **24**(1): p. 177-191.
72. Han, K. and O. Levenspiel, *Extended Monod kinetics for substrate, product, and cell inhibition.* Biotechnology and Bioengineering, 1988. **32**(4): p. 430-447.
73. Levenspiel, O., *The Monod equation: a revisit and a generalization to product inhibition situations.* Biotechnology and bioengineering, 1980. **22**(8): p. 1671-1687.
74. Feng, Y.-L., et al., *Statistical optimization of media for mycelial growth and exo-polysaccharide production by Lentinus edodes and a kinetic model study of two growth morphologies.* Biochemical Engineering Journal, 2010. **49**(1): p. 104-112.
75. Viniegra-González, G., et al., *Advantages of fungal enzyme production in solid state over liquid fermentation systems.* Biochemical Engineering Journal, 2003. **13**(2): p. 157-167.
76. Jabbari, M., et al., *All-polyamide composite coated-fabric as a replacement for material of construction of conventional textile bioreactors.* 2017.
77. Gossain, V. and R. Mirro, *Linear Scale-Up of Cell Cultures: The Next Level in Disposable Bioreactor Design.* BioProcess Int, 2010. **9**(11).
78. Kadic, E. and T.J. Heindel, *Stirred-Tank Bioreactors*, in *An Introduction to Bioreactor Hydrodynamics and Gas-Liquid Mass Transfer*. 2014, John Wiley & Sons, Inc. p. 69-123.
79. Kadic, E. and T.J. Heindel, *Bubble Column Bioreactors*, in *An Introduction to Bioreactor Hydrodynamics and Gas-Liquid Mass Transfer*. 2014, John Wiley & Sons, Inc. p. 124-167.
80. Kadic, E. and T.J. Heindel, *Airlift Bioreactors*, in *An Introduction to Bioreactor Hydrodynamics and Gas-Liquid Mass Transfer*. 2014, John Wiley & Sons, Inc. p. 168-208.
81. Kadic, E. and T.J. Heindel, *Fixed Bed Bioreactors*, in *An Introduction to Bioreactor Hydrodynamics and Gas-Liquid Mass Transfer*. 2014, John Wiley & Sons, Inc. p. 209-242.
82. Mandenius, C.-F., *Chapter 1 Challenges for Bioreactor Design and Operation.*, in *Bioreactors : design, operation and novel applications*. 2016, Weinheim, Germany : Wiley-VCH Verlag GmbH & Company KGaA.
83. Basso, L.C., T.O. Basso, and S.N. Rocha, *Ethanol production in Brazil: the industrial process and its impact on yeast fermentation*, in *Biofuel production-recent developments and prospects*. 2011, InTech.
84. Ferreira, J.A., P.R. Lennartsson, and M.J. Taherzadeh, *Production of ethanol and biomass from thin stillage by Neurospora intermedia: a pilot study for process diversification.* Engineering in Life Sciences, 2015. **15**(8): p. 751-759.
85. Nair, R.B. and M.J. Taherzadeh, *Valorization of sugar-to-ethanol process waste vinasse: A novel biorefinery approach using edible ascomycetes filamentous fungi.* Bioresource Technology, 2016. **221**: p. 469-476.
86. Liu, Y., et al., *Pelletization process to control filamentous fungi morphology for enhanced reactor rheology bioproduct formation*. 2013, Google Patents.
87. López, J.L.C., et al., *Pellet morphology, culture rheology and lovastatin production in cultures of Aspergillus terreus.* Journal of biotechnology, 2005. **116**(1): p. 61-77.
88. Saraswathy, A. and R. Hallberg, *Mycelial pellet formation by Penicillium ochrochloron species due to exposure to pyrene.* Microbiological Research, 2005. **160**(4): p. 375-383.
89. Echegaray, O.F., et al., *Fed-batch culture of Sacchoromyces cerevisiae in sugar-cane blackstrap molasses: invertase activity of intact cells in ethanol fermentation.* Biomass and Bioenergy, 2000. **19**(1): p. 39-50.
90. Fontana, A., et al., *Continuous alcoholic fermentation of sucrose using flocculating yeast. The limits of invertase activity.* Biotechnology letters, 1992. **14**(6): p. 505-510.

91. Beun, J.J., et al., *Aerobic granulation in a sequencing batch reactor.* Water Research, 1999. **33**(10): p. 2283-2290.
92. Kreutzer, M.T., et al., *Mass transfer characteristics of three-phase monolith reactors.* Chemical Engineering Science, 2001. **56**(21): p. 6015-6023.
93. Losey, M.W., M.A. Schmidt, and K.F. Jensen, *Microfabricated multiphase packed-bed reactors: characterization of mass transfer and reactions.* Industrial & engineering chemistry research, 2001. **40**(12): p. 2555-2562.
94. Ramakrishnan, D. and W.R. Curtis, *Trickle-bed root culture bioreactor design and scale-up: Growth, fluid-dynamics, and oxygen mass transfer.* Biotechnology and bioengineering, 2004. **88**(2): p. 248-260.
95. Fang, Q.H. and J.J. Zhong, *Two-stage culture process for improved production of ganoderic acid by liquid fermentation of higher fungus Ganoderma lucidum.* Biotechnology progress, 2002. **18**(1): p. 51-54.
96. Ho, C.S., L.K. Ju, and R.F. Baddour, *Enhancing penicillin fermentations by increased oxygen solubility through the addition of n-hexadecane.* Biotechnology and bioengineering, 1990. **36**(11): p. 1110-1118.
97. Tang, Y.-J. and J.-J. Zhong, *Role of oxygen supply in submerged fermentation of Ganoderma lucidum for production of Ganoderma polysaccharide and ganoderic acid.* Enzyme and Microbial technology, 2003. **32**(3): p. 478-484.
98. Paul, E.L., V.A. Atiemo-Obeng, and S.M. Kresta, *Handbook of industrial mixing: science and practice*. 2004: John Wiley & Sons.
99. Bosma, T.N.P., et al., *Mass Transfer Limitation of Biotransformation: Quantifying Bioavailability.* Environmental Science & Technology, 1997. **31**(1): p. 248-252.
100. Hayduk, W. and H. Laudie, *Prediction of diffusion coefficients for nonelectrolytes in dilute aqueous solutions.* AIChE Journal, 1974. **20**(3): p. 611-615.
101. West, J., et al., *Structuring laminar flows using annular magnetohydrodynamic actuation.* Sensors and Actuators B: Chemical, 2003. **96**(1–2): p. 190-199.
102. Deindoerfer, F.H. and J.M. West, *Rheological examination of some fermentation broths.* Biotechnology and Bioengineering, 1960. **2**(2): p. 165-175.
103. Labuza, T.P., D.B. Santos, and R.N. Roop, *Engineering factors in single-cell protein production. I. Fluid properties and concentration of yeast by evaporation.* Biotechnology and Bioengineering, 1970. **12**(1): p. 123-134.
104. Leduy, A., A.A. Marsan, and B. Coupal, *A study of the rheological properties of a non-Newtonian fermentation broth.* Biotechnology and bioengineering, 1974. **16**(1): p. 61-76.
105. Pamboukian, C.R.D. and M.C.R. Facciotti, *Rheological and morphological characterization of Streptomyces olindensis growing in batch and fed-batch fermentations.* Brazilian Journal of Chemical Engineering, 2005. **22**(1): p. 31-40.
106. Queiroz, M.C.R., M.C.R. Facciotti, and W. Schmidell, *Rheological changes of Aspergillus awamori broth during amyloglucosidase production.* Biotechnology Letters, 1997. **19**(2): p. 167-170.
107. Olmos, E., et al., *Effects of bioreactor hydrodynamics on the physiology of Streptomyces.* Bioprocess and biosystems engineering, 2013. **36**(3): p. 259-272.
108. Serrano-Carreón, L., et al., *Hydrodynamics, fungal physiology, and morphology*, in *Filaments in Bioprocesses*. 2015, Springer. p. 55-90.
109. Delvigne, F. and J.p. Lecomte, *Foam formation and control in bioreactors.* Encyclopedia of Industrial Biotechnology, 2010.
110. Flores-Cotera, L.B. and S. García-Salas, *Gas holdup, foaming and oxygen transfer in a jet loop bioreactor with artificial foaming media and yeast culture.* Journal of biotechnology, 2005. **116**(4): p. 387-396.
111. Guitian, J. and D. Joseph, *How bubbly mixtures foam and foam control using a fluidized bed.* International journal of multiphase flow, 1998. **24**(1): p. 1-16.

112. Villadsen, J., J. Nielsen, and G. Lidén, *Gas–Liquid Mass Transfer*, in *Bioreaction Engineering Principles*. 2011, Springer US: Boston, MA. p. 459-496.
113. Mussatto, S.I., et al., *Technological trends, global market, and challenges of bio-ethanol production.* Biotechnology advances, 2010. **28**(6): p. 817-830.
114. REN21, P.S., *Renewables 2015 global status report*. 2015, REN21 Secretariat Paris, France.
115. Bergeron, P., *Bioethanol market forces*, in *Handbook on bioethanol: production and utilization*, C. Wyman, Editor. 1996, CRC press. p. 61-88.
116. Demirbas, A., *Political, economic and environmental impacts of biofuels: a review.* Applied Energy, 2009. **86**: p. S108-S117.
117. Taherzadeh, M.J., et al., *Bioethanol Production Processes*, in *Biofuels Production*. 2013, John Wiley & Sons, Inc. p. 211-253.
118. Sousa, M.L., J.A. Teixeira, and M. Mota, *Comparative analysis of ethanolic fermentation in two continuous flocculation bioreactors and effect of flocculation additive.* Bioprocess Engineering, 1994. **11**(3): p. 83-90.
119. Trendewicz, A.A. and R.J. Braun, *Techno-economic analysis of solid oxide fuel cell-based combined heat and power systems for biogas utilization at wastewater treatment facilities.* J. Power Sources, 2013. **233**: p. 380-393.
120. Gebrezgabher, S.A., et al., *Economic analysis of anaerobic digestion—A case of Green power biogas plant in The Netherlands.* NJAS-Wagen. J. Life Sc., 2010. **57**(2): p. 109-115.
121. Curry, N. and P. Pillay, *Biogas prediction and design of a food waste to energy system for the urban environment.* Renewable Energy, 2012. **41**: p. 200-209.
122. Deublein, D. and A. Steinhauser, *Biogas from Waste and Renewable Resources*. 2011: Wiley-VCH.
123. Friehe, J., P. Weiland, and A. Schattauer, *Guide to Biogas From production to use* c.r.e. 5th, Gülzow, 2010 Editor. 2010.
124. Mao, C., et al., *Review on research achievements of biogas from anaerobic digestion.* Renewable and Sustainable Energy Reviews, 2015. **45**: p. 540-555.
125. Patinvoh, R.J., et al., *Innovative pretreatment strategies for biogas production.* Bioresource technology, 2016.
126. Schnurer, A. and A. Jarvis, *Microbiological handbook for biogas plants.* Swedish Waste Management U, 2010. **2009**: p. 1-74.
127. Chattopadhyay, S., A. Dutta, and S. Ray, *Municipal solid waste management in Kolkata, India–A review.* Waste Management, 2009. **29**(4): p. 1449-1458.
128. Karak, T., R.M. Bhagat, and P. Bhattacharyya, *Municipal solid waste generation, composition, and management: the world scenario.* Critical Reviews in Environmental Science and Technology, 2012. **42**(15): p. 1509-1630.
129. Chin, M.J., et al., *Biogas from palm oil mill effluent (POME): Opportunities and challenges from Malaysia's perspective.* Renew. Sust. Energ. Rev., 2013. **26**: p. 717-726.
130. Statista, *Vegetable oil production worldwide 2000-2016* *https://www.statista.com/statistics/263978/global-vegetable-oil-production-since-2000-2001/Statista Accessed 2016/09/12*. 2016: https://www.statista.com/statistics/263978/global-vegetable-oil-production-since-2000-2001/Statista Accessed 2016/09/12.
131. Ahmad, A., R. Ghufran, and Z.A. Wahid, *Bioenergy from anaerobic degradation of lipids in palm oil mill effluent.* Rev. Environ. Sci. Bio/Technol., 2011. **10**(4): p. 353-376.
132. Elander, R.T.P., V.L, *Ethanol from Corn: Technology and Economics*, in *Handbook on Bioethanol: Production and Utilization* 1996, Taylor and Francis: Washington, DC, USA. p. 329–349.
133. Green, E.M., *Fermentative production of butanol—the industrial perspective.* Current Opinion in Biotechnology, 2011. **22**(3): p. 337-343.

134. Xu, J., X. Ge, and M.C. Dolan, *Towards high-yield production of pharmaceutical proteins with plant cell suspension cultures.* Biotechnology Advances, 2011. **29**(3): p. 278-299.
135. Catapano, G., et al., *Bioreactor design and scale-up*, in *Cell and Tissue Reaction Engineering*. 2009, Springer. p. 173-259.
136. Curtis, W.R., *Achieving economic feasibility for moderate-value food and flavor additives.* Plant cell and tissue culture for the production of food ingredients. Kluwer Academic/Plenum Publishers, New York, 1999: p. 225-236.
137. Couper, J.R., et al., *COSTS OF INDIVIDUAL EQUIPMENT*, in *Chemical Process Equipment*. 2005, Elsevier Inc: Amsterdam, The Netherlands. p. 663–669.
138. Mignard, D., *Correlating the chemical engineering plant cost index with macro-economic indicators.* Chemical Engineering Research and Design, 2014. **92**(2): p. 285-294.
139. Fakruddin, M., et al., *Process optimization of bioethanol production by stress tolerant yeasts isolated from agro-industrial waste.* Intl J Renew Sustain Energy, 2013. **2**(4): p. 133-9.
140. Moss, D.R. and M.M. Basic, *Pressure vessel design manual*. 2012: Butterworth-Heinemann.
141. Koenderink, J.J. and A.J. van Doorn, *Surface shape and curvature scales.* Image and vision computing, 1992. **10**(8): p. 557-564.
142. Willmore, T.J., *An introduction to differential geometry*. 2012: Courier Corporation.
143. Shampine, L.F. and M.W. Reichelt, *The matlab ode suite.* SIAM journal on scientific computing, 1997. **18**(1): p. 1-22.
144. Budinski, K.G. and M.K. Budinski, *Engineering materials: properties and selection*. 1999, Upper Saddle River, N.J: Prentice Hall.
145. Bledzki, A.K. and J. Gassan, *Composites reinforced with cellulose based fibres.* Progress in Polymer Science, 1999. **24**(2): p. 221-274.

PAPER I

Introducing Textiles as Material of Construction of Ethanol Bioreactors.
Energies Doi:10.3390/en7117555

Energies **2014**, *7*, 7555-7567; doi:10.3390/en7117555

OPEN ACCESS

energies

ISSN 1996-1073

www.mdpi.com/journal/energies

Article

Introducing Textiles as Material of Construction of Ethanol Bioreactors

Osagie A. Osadolor *, Patrik R. Lennartsson and Mohammad J. Taherzadeh

Swedish Centre for Resource Recovery, University of Borås, SE 501-90, Borås, Sweden;
E-Mails: Patrik.Lennartsson@hb.se (P.R.L.); Mohammad.Taherzadeh@hb.se (M.J.T.)

* Author to whom correspondence should be addressed; E-Mail: alex.osagie@hb.se;
Tel.: +46-33-435-4419; Fax: +46-33-435-4003.

External Editor: Thomas E. Amidon

Received: 18 September 2014; in revised form: 4 November 2014 / Accepted: 7 November 2014 / Published: 18 November 2014

Abstract: The conventional materials for constructing bioreactors for ethanol production are stainless and cladded carbon steel because of the corrosive behaviour of the fermenting media. As an alternative and cheaper material of construction, a novel textile bioreactor was developed and examined. The textile, coated with several layers to withstand the pressure, resist the chemicals inside the reactor and to be gas-proof was welded to form a 30 L lab reactor. The reactor had excellent performance for fermentative production of bioethanol from sugar using baker's yeast. Experiments with temperature and mixing as process parameters were performed. No bacterial contamination was observed. Bioethanol was produced for all conditions considered with the optimum fermentation time of 15 h and ethanol yield of 0.48 g/g sucrose. The need for mixing and temperature control can be eliminated. Using a textile bioreactor at room temperature of 22 °C without mixing required 2.5 times longer retention time to produce bioethanol than at 30 °C with mixing. This will reduce the fermentation investment cost by 26% for an ethanol plant with capacity of 100,000 m^3 ethanol/y. Also, replacing one 1300 m^3 stainless steel reactor with 1300 m^3 of the textile bioreactor in this plant will reduce the fermentation investment cost by 19%.

Keywords: bioethanol; fermentation; bioreactor material; textile bioreactor; reactor cost

1. Introduction

We live in a world where there is an ever-increasing demand for energy. The transportation sector accounts for a high proportion of the global energy demand, which is dominated by fossil fuels [1]. There has been growing interest in alternative fuel sources and ethanol has proven to be a viable alternative to fossil fuel in the transportation sector [2,3]. As the biofuels must compete with fossil fuels, any attempt to reduce their investment and operational costs will contribute to stimulate their consumption.

Global production of ethanol, the dominating biofuel, has increased from 50 million m^3 in 2007 to 89 million m^3 in 2013 [4], the production trends across the globe for this period are shown in Table 1. Future forecast shows that global demand for ethanol will continue to increase to an estimated value of 100 million m^3 in 2015 [5]. For 10% *w/w* ethanol production in bioreactors, this will correspond to a total fermentation volume of 785 million m^3. Despite this, the relatively cheaper price of petroleum makes some ways of ethanol production uneconomical, and it is also a hindrance to the commercial introduction of 2nd and 3rd generation ethanol into the fuel market. Several research projects have been performed on ethanol production to reduce its production costs [6].

Table 1. Global ethanol production from 2007 to 2013 by country or region in million m^3 [4].

Country	2007	2008	2009	2010	2011	2012	2013
USA	24.68	35.24	41.4	50.34	52.8	50.35	50.35
Brazil	19	24.5	24.9	26.2	21.1	21.11	23.72
Europe	2.16	2.78	3.94	4.57	4.42	4.46	5.19
China	1.84	1.9	2.05	2.05	2.1	2.1	2.63
Canada	0.8	0.9	1.1	1.35	1.75	1.7	1.98
Rest of World	1.19	1.47	3.46	3.73	2.64	2.85	4.82
World total	49.68	66.79	76.86	88.24	84.81	82.57	88.69

Ethanol is nowadays produced principally by fermentation, where the excess heat of 580 kJ/kg sugar used should be continuously released [6], and the bioreactors must be cooled [7]. In addition, the cost of the fermentation process for a conventional 100,000 m^3/y ethanol facility constitutes 11% of the total fixed capital cost of the plant [8]. In other word, the fermentation process has a large direct effect on the plant investment and operational costs [8].

A reactor is a vessel where transformation of reactants to products takes place. Reactors are generally designed using the operating conditions for the reactant to product transformation in mind, while also trying to maximise profit, ensure adequate safety and minimize environmental emissions [9]. A fermentor or a bioreactor is a reactor that provides an environment suitable for the controlled growth of a microorganism which is responsible for producing a product of interest [10,11]. A bioreactor should be made of materials that are inert and do not facilitate the development of unwanted microorganisms [12]. It should provide adequate temperature control, operate well under sterilization conditions (with chemicals or temperature) [11], provide good contact area for the microbes and the substrate [9], have adequate charging inlet and discharging outlets, have a means of adequate sampling [11], and provide adequate time for the desired product to be produced [9]. Most conventional

bioreactors are designed to have very low surface area to volume ratio, which increases the cooling requirements of the bioreactor [11].

This paper introduces a novel bioreactor for producing bioethanol made from textiles. The textile bioreactor has the potential for higher flexibility in ethanol production. Its lower cost compared to stainless steel, could lead to a reduction of the cost of producing bioethanol, thereby making investments in the ethanol market more attractive.

2. Results and Discussion

The textile bioreactor used in this work is a novel bioreactor for producing bioethanol. It is made from a backbone of textile which is coated with several layers of polymers to make it resistant to chemicals, gas and liquid leakage. It is flexible, long lasting and can withstand temperatures up to 150 °C. Some of the advantages of using a textile bioreactor for bioethanol production include: it does not corrode, it can withstand the tough environmental conditions encountered during fermentation, it is a far cheaper alternative than the currently used bioethanol bioreactors, it is light, and designed for easy and safe transportation, installation and operation, and it is ultraviolet irradiations (UV) resistant, it can be sterilized with steam at 121 °C and with chemicals. It was originally developed for biogas production [13], but it was never examined for any other fermentation products. In this work, this new textile bioreactor was developed for bioethanol production, its performance was examined and the results are presented here.

2.1. Textile vs. Other Materials for Construction of Bioreactors

The materials used for constructing bioreactors must be able to withstand the physiochemical conditions encountered while running the bioreactor and during clean-up and sterilization [14]. Apart from stainless steel, other materials that could be used for making bioreactors include carbon steel, borosilicate glass, polytetrafluoroethylene (PTFE) plastic, and ceramics [14]. Only stainless steel 304 and to a lesser extent reinforced carbon steel are currently being used to make industrial ethanol bioreactors. The other materials are normally added to stainless steel bioreactors at specific points for certain purposes (e.g., borosilicate glass used in sight glasses) [14].

Bioethanol is produced by fermentation. Bioethanol fermentation takes place under slightly acidic conditions (pH between 4 and 6), temperatures ranging from 25 to 38 °C, generally without oxygen, and in a liquid medium. Ensuring that only the desired microorganism is what grows in the bioreactor is necessary to ensure the fermentable sugars are converted to the product of interest [15]. It is essential that the material used for constructing bioreactors for producing bioethanol does not affect the fermentation process and can be sterilized when needed. For all the experiments performed in the textile bioreactor, it was autoclaved for sterilization at 121 °C for 20 min and 2 bar pressure. This created a sterile working condition for the textile bioreactor. There were no incidences of bacterial contamination in all the experiments performed in the textile bioreactor, as there were no areas for harbouring unwanted microorganisms, which is one of the main reasons why stainless steel is used as the current material for making bioreactors [16]. The material of construction of the textile bioreactor has been proven to resist diverse environmental conditions (pH 3–12) [13]. In addition the material when burnt does not ignite, but rather forms a semi-solid composite which recoils inward,

making the bioreactor fire resistant. The material was designed to have high tensile strength with high flexibility to make its assembly and disassembly easy. Table 2 shows some advantages and disadvantages of using certain materials of construction for ethanol bioreactors. Considering these features and the comparison in Table 2, as a bioreactor material of construction, the textile bioreactor is an excellent choice for bioethanol production.

Table 2. Advantages and disadvantages of possible materials for construction for ethanol bioreactors [14,17,18].

Material	Modification	Advantage	Disadvantage
Textile	Layered with some polymers and UV filter	Portable. Corrosion proof. Good sterility. More cost effective than stainless steel. Can withstand high temperature. Leak proof. Long life span. Can be designed to have regions that are transparent, for easy process monitoring.	Currently a horizontal vessel.
Stainless steel 304	–	Cheapest of all the stainless steel. Leak proof. Good sterility. Can withstand high temperature and pressure. Corrosion proof. Long life span.	Quite expensive.
Carbon steel	Reinforced with stainless steel	Cheaper than 304 stainless steel. Leak proof.	Corrosion and contamination.
Borosilicate glass	–	Transparent. Inert to chemicals.	Very fragile.
Plastic	–	Very portable. Cheap.	Leaks and short life span. High chances of contamination.
Ceramics	–	Chemically stable. Wear resistant.	Brittle. Prone to thermal shock.

2.2. Reactor Cost Comparison

A major challenge facing biofuel production is its economic feasibility [19]. Bioethanol production consists of the collection of feedstock, pre-treatment of feedstock (if the feedstock is starch or lignocellulosic based), fermentation, distillation and possibly dehydration [20]. The fermentation cost of a 100,000 m^3/y ethanol production facility contributes 11% of the total plant cost, while the bioreactor cost makes up 32% of the fermentation cost [8]. In this section a comparison is made between the investment cost of stainless steel bioreactors and textile bioreactors excluding operation cost (maintenance and installation cost). Typically, the installed cost (investment and operation cost) of a stainless steel reactor is 1.7 times its purchase cost [21], while that of a textile bioreactor is 1.5 times its purchase cost [13].

The purchase cost for a 1000 m^3 textile bioreactor is $100,000. Table 3 shows the purchasing cost of different reactor sizes, for both the developed textile bioreactor and stainless steel reactors. The purchasing cost of stainless steel reactor was estimated using Equations (1) and (2) (see Section 3.5). For all reactor volumes considered, the purchasing cost of the developed textile bioreactor was far less than half the purchasing cost of the stainless steel bioreactor. Considering a 100,000 m^3/y ethanol production facility using sucrose as its raw material and having a fermentation time between 10 and 15 h [22,23], this plant will require a bioreactor volume between 1000 and 1500 m^3 for the fermentation only. If this plant has just one 1300 m^3 stainless steel bioreactor, replacing this with a 1300 m^3 textile bioreactor will reduce the fermentation investment cost by 19%, and the total plant investment cost of the facility by 2.1%.

Table 3. Purchasing cost of developed textile bioreactors and 304 stainless steel reactors.

Reactor Size (m^3)	Purchasing Cost of Developed Textile Bioreactor ($)	Purchasing Cost of 304 Stainless Steel Reactor ($)
500	66,000	201,000
1,000	100,000	282,000
1,300	130,000	325,000
1,500	150,000	352,000

2.3. Mixing and Temperature Control in the Textile Bioreactor

The mass transfer in a bioreactor affects the net productivity of the system [11,24]. The two crucial aspects of mass transfer in a bioreactor are the uniform distribution of the product and substrate in the bulk liquid, and the transfer of substrate into the cells and the products out of the cells. Mixing helps to minimize local variation of concentration and temperature in a bioreactor [11]. Mixing in liquid media can be achieved by agitation, or with the aid of a stirrer, or by the use of a pump for recirculation, depending on the viscosity of the liquid and if it media is single- or multi-phased [25]. For the textile bioreactor, mixing was performed using a recirculation pump. To determine the effectiveness of the mixing in the bioreactor and the possibility of it being used for continuous fermentation, experiments were performed where samples were collected from the sampling point at the centre of the textile bioreactor and from the exit pipes from the bioreactor. One of the basics of a continuous stirred tank reactor (CSTR) is having same concentration in the reactor as what leaves the reactor. From Figure 1, it is clearly observed that there is no significance difference between the concentration in the bioreactor (samples from the centre of the reactor) and that leaving the bioreactor (samples from the exit pipe). This shows that there is the possibility of the textile bioreactor being used for batch, fed-batch, and continuous fermentation. In addition to ensuring uniform substrate and product distribution in the textile bioreactor, the mixing also helped to provide a good transfer of substrate into and products out of the yeast (Figure 1), as the sugar was fully consumed about the same time as peak ethanol concentration was reached. Thus the mixing by recirculation in the textile bioreactor is effective.

Figure 1. Concentration of sucrose (●) and ethanol (■) on the primary axis (left side), and glycerol (▲) on the secondary axis (right side), with samples taken from the exit pipe (**a**) and centre of the reactor (**b**) with time, to determine the effectiveness of mixing by recirculation.

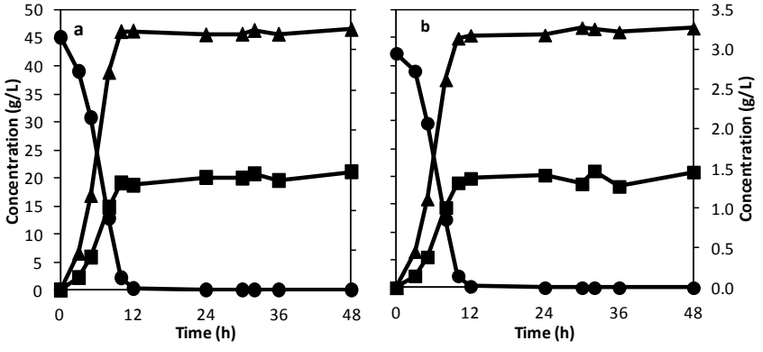

(**a**) (**b**)

Temperature control is essential for optimal product formation as every microorganism has a temperature range in which it functions optimally. For anaerobic condition that for *S. cerevisiae* is around 30 °C [15]. For lab scale production heat is normally added to the system while for the large industrial bioreactors with low surface to volume ratio, cooling is necessary [11]. Because of the nature of the material used for the developed textile bioreactor, cooling can easily be achieved by recirculation of chilled water, while heating can be achieved with hot water. The area to volume ratio of a 1000 m^3 textile bioreactor is 0.96, while that of a conventional 1000 m^3 bioreactor having a height to diameter ratio of 3 it is 0.62. The higher area to volume ratio of the textile bioreactor makes cooling (or heating) easily achievable because the heat loss (or gained) by evaporation and radiation increases with increasing area to volume ratio. Temperature control was achieved in the textile bioreactor as described in Section 3.2. In addition, the recirculation of the fluid also helped to ensure temperature uniformity in every part of the reactor. Figures 2 and 3 shows the result of the experiments performed with temperature control, while Figure 4 shows the result of the experiments without temperature control. For both cases, ethanol yields greater than 87% of the theoretical values were reached, while the experiments where temperature was maintained at 30 °C had higher fermentation rates and peak product concentrations were reached in less than 24 h. This shows that the temperature control developed for the textile bioreactor is effective.

Figure 2. Concentration of sucrose (●) and ethanol (■) on the primary axis, and glycerol (▲) on the secondary axis with time, at 30 °C and with mixing.

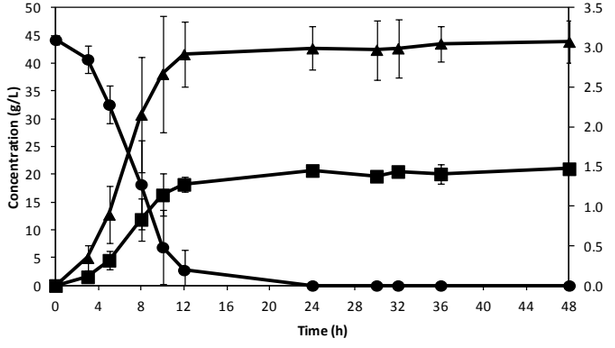

Figure 3. Concentration of sucrose (●) and ethanol (■) on the primary axis, and glycerol (▲) on the secondary axis with time, at 30 °C without mixing.

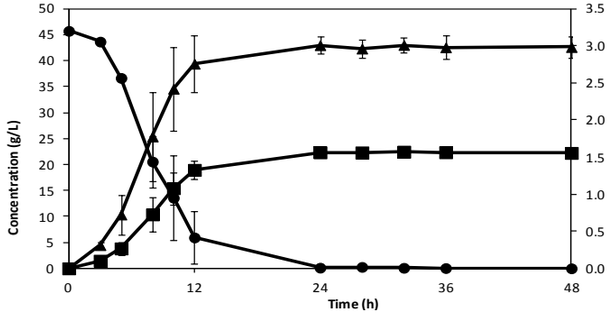

Figure 4. Concentration of sucrose (●) and ethanol (■) on the primary axis, and glycerol (▲) on the secondary axis with time, at room temperature of 22 °C (**a**) with and (**b**) without mixing.

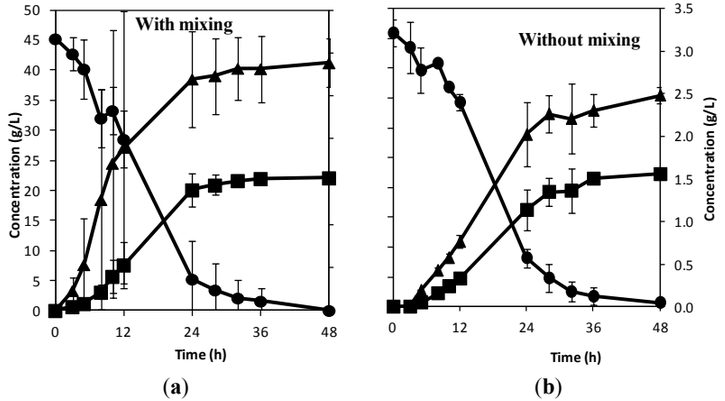

(**a**) (**b**)

2.4. Fermentation in the Textile Bioreactor and Its Economics

To determine how effective the textile bioreactor was for producing bioethanol, lab scale experiments were performed under different operating conditions. Temperature and mixing were varied, while the pH of all the experiments performed was around 6.0 ± 0.2. Figure 2 shows the result of the experiment performed in the textile bioreactor at 30 °C and with mixing. For this experiment, the yield of ethanol from the experiment (using the initial sucrose concentration of 44.2 g/L) was 0.48 ± 0.01 g/g, which is 88% of the theoretical value, and it took an average of 15 h for the yeast to consume the sugar. Comparing this fermentation time with that from a similar work were 10 g/L of yeast was used and it required a fermentation time of 10 h [22], shows that the fermentation time is good. Thus fermentation takes place effectively well and at a good rate in the textile bioreactor. From Figure 2, the average of the peak ethanol concentration was 20.04 ± 0.53 g/L, using the average fermentation time gave the specific productivity to be 1.34 ± 0.02 g $L^{-1} \cdot h^{-1}$.

Figure 3 shows the result of the experiment where temperature was fixed at 30 °C without mixing. The yield of ethanol from the experiment was 0.49 ± 0.01 g/g, and it took an average of 20 h for the yeast to consume the sugar. Comparing Figures 2 and 3 shows that mixing did not affect the fermentation rate that much when temperature is held at 30 °C without mixing, as the specific productivity for this case was 1.04 ± 0.01 g L^{-1} h^{-1} in comparison to 1.34 ± 0.02 g L^{-1} h^{-1} with mixing. To produce the same amount of ethanol as that which is produced when mixing is controlled; the textile bioreactor volume used has to be 1.29 times the one used with mixing. Taking a 1000 m^3 bioreactor operating with mixing and temperature control, this bioreactor will cost $282,000 but a 1300 m^3 textile bioreactor will cost $130,000 (see Table 3). In addition, the cost of agitation and mixing in a bioreactor accounts for 24% of the fermentation cost of a 100,000 m^3 ethanol/y production facility [8]. Using a textile bioreactor operated at 30 °C without mixing can eliminate the need for the cost of agitation and mixing, and it gives a bioreactor cost reduction of $152,000.

Figure 4 shows the result of the experiment that was performed at room temperature of 22 °C with and without mixing. The ethanol yield from the experiment with mixing was 0.49 ± 0.01 g/g, and it took an average of 40 h for the yeast to consume the sugar, while that without mixing had an ethanol yield of 0.49 ± 0.02 g/g, and it took an average of 42 h for peak ethanol concentration to be reached. Mixing did not affect the fermentation rate that much as the specific productivity with mixing was 0.55 ± 0.01 g L^{-1} h^{-1} while that without mixing was 0.53 ± 0.02 g L^{-1} h^{-1}. This result shows that there is a possibility of running the textile bioreactor without temperature control and mixing. The slower fermentation rate from producing bioethanol at 22 °C can be accommodated by increasing the retention time and the bioreactor volume. Comparing Figures 2 and 4, the same amount of ethanol per hour will be produced in both cases if the volume of the textile bioreactor for the production without temperature control and mixing is 2.53 times that with temperature control and mixing. Taking a 1000 m^3 bioreactor with temperature control and mixing, the purchasing cost of a 1000 m^3 bioreactor is $282,000 while that of a 2530 m^3 textile bioreactor (consisting of one 1000 m^3 reactor and one 1500 m^3 reactor) is $250,000 (see Table 3). In addition, operating the textile bioreactor without temperature control and mixing also reduces the total fermentation cost, as the cost of temperature control, mixing and agitation accounts for 26% of the fermentation cost in a 100,000 m^3/y ethanol production plant [8]. For the same bioethanol production rate it is more economical to use a larger

volume of the textile reactor without temperature control and mixing than a smaller bioreactor volume with temperature control, mixing and agitation.

Comparing the scenario where there is mixing but the textile bioreactor is operated at 22 °C, the size of the reactor in this case would be 2.44 times the size of that operated at 30 °C. Using a 1000 m^3 bioreactor at 30 °C will cost $282,000 while a 2440 m^3 textile bioreactor running at 22 °C will cost $250,000. However running the textile bioreactor at 22 °C with mixing will only reduce the fermentation cost by 2%, which is not as economical as 26% cost reduction obtained by running it at 22 °C without mixing [8].

For all experiments performed in the textile bioreactor there were no incidences of bacterial contamination. From the results, experiments performed at 30 °C had faster fermentation rates than the ones performed at room temperature. For a continuous process, both temperature control and mixing will be essential to achieve high dilution rate. The results of the experiments show that the textile bioreactor can be used for bioethanol production at different conditions of temperature and mixing.

3. Experimental Section

3.1. Microorganism

Dry ethanol red yeast (*Saccharomyces cerevisiae*) from Fermentis (Strasbourg, France) was used for the fermentation. A starting concentration of 1 g/L of the dry yeast was used.

3.2. Textile Bioreactor

A schematic of the lab scale prototype of the developed bioreactor is shown in Figure 5. The material of construction (MOC) was a textile backbone coated with several layers to protect against pressure, chemicals in the reactor, weather conditions and to be gas proof. The material was developed by FOV Fabrics AB (Borås, Sweden) primarily for biogas reactors and it was welded to form a reactor by Kungsäter Industri AB (Kungsäter, Sweden). The lab scale bioreactor had a total volume of 30 L and a working volume of 25 L. The dimensions of the bioreactor were 100 cm length, 50 cm breadth, and 6 cm width. It had an opening of 4 cm diameter, which serves for sample collection; probe stand, thermometer stand, and gas exit. The dimensions of the outlet and inlet tapered from 9 to 4 cm at the bioreactor entrance, to allow for easy loading of the bioreactor. The dimension of the tubes connected to the inlet and outlet were 8 mm.

The means for temperature control was made using Poly(vinyl chloride) (PVC) tubing of 50 m length and a woollen blanket; the PVC tubing was connected to a GD120 grant thermostatic circulator (GD Grant Instruments Ltd., Cambridge, UK). The tubing was wound 14 times, covering the whole perimeter of the textile bioreactor at the bottom, as such, *Saccharomyces cerevisiae* was not exposed to thermal shocks [12]. The tubing and the textile bioreactor were enclosed by the woollen blanket. The temperature of the thermostatic circulator was set at 33 °C. A 200 rpm Watson Marlow compact peristaltic pump (W-M Alitea AB, Stockholm, Sweden) was used for recirculation of the fluid in the reactor for mixing.

Figure 5. Schematic diagram of the textile bioreactor lab scale prototype setup.

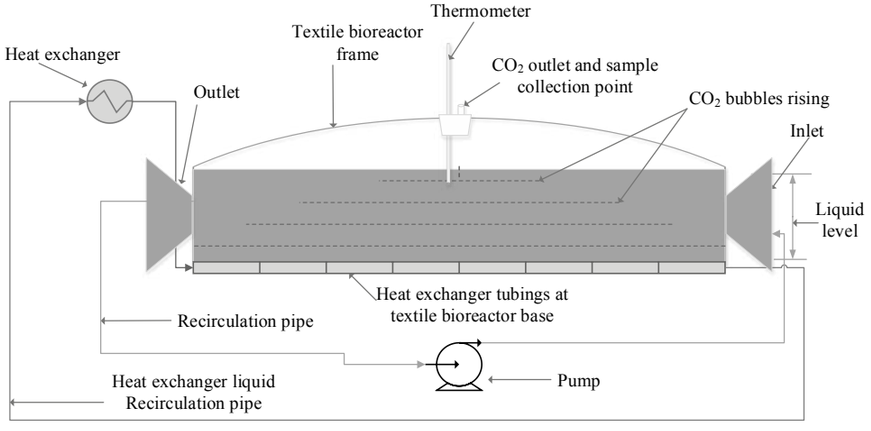

3.3. Experimental setup

Experiments with temperature (30 °C and room temperature of 22 °C) and (with and without) mixing using recirculation as process variables were carried out in the textile bioreactor. Sucrose (50 g/L) was used as the carbon and energy sources, supplemented with 7.5 g/L $(NH_4)_2SO_4$, 3.5 g/L KH_2PO_4, 0.75 g/L $MgSO_4 \cdot 7H_2O$ and 1.0 g/L yeast extract. The total liquid volume in the reactor was 25 L for all experiments. The flow rate used for recirculation of the fluid for the experiments with mixing was 0.924 L/min. Sucrose concentration dropped between 44 and 47 g/L when the feed stream used for each experiment was autoclaved. Each experiment was performed in duplicate.

To determine the effectiveness of the mixing in the bioreactor, samples were taken from the recirculation pipe and from the centre of the reactor.

3.4. Analytical Method

Liquid samples from the textile bioreactor were analysed using high-performance liquid chromatography (HPLC) with a hydrogen-based ion exchange column (Aminex HPX-87H, Bio-Rad, Hercules, CA, USA) at 60 °C and 5 mM 0.6 mL/min H_2SO_4 eluent. A refractive index detector (Waters 2414, Waters Corporation, Milford, MA, USA) and a UV detector (Waters 2487) were used with the HPLC. The samples used for the HPLC analysis were centrifuged for 10 min at 10,000 ×*g* and the liquid portion stored for analysis. The samples were stored at −20 °C prior to HPLC analysis. All reported error bars and interval represents two standard deviations. The yield for each experiment was calculated using the concentrations measured by the HPLC after autoclaving.

3.5. Cost Estimation

The purchasing cost of 500, 1000, 1300 and 1500 m^3 versions of the developed textile bioreactors were provided by FOV Fabrics AB, and compared with those of 304 stainless steel reactors.

The purchasing cost of a 304 steel reactor was estimated using Equation (1) [21], where V is the reactor volume in gallons and F_m is 2.4 for 304 stainless steel [21]. The Chemical Engineering Plant Cost Index (CEPCI) as at when Equation (1) was developed is 325.8 [21]. The capital cost was then updated to January 2014 values using Chemical Engineering Plant Cost Index (CEPCI) of 572.8 [26]. The updated cost was computed using Equation (2):

$$C = F_m \exp[11.662 - 0.6104(\ln V) + 0.04536(\ln V)^2] \quad (1)$$

$$C_{updated} = C\,(I_{updated}/I) \quad (2)$$

4. Conclusions

In this work, a novel bioreactor for bioethanol production was introduced. The bioreactor has textile as its core material of construction. For the experiments performed on a lab scale prototype textile bioreactor, the optimum result for possible continuous production of bioethanol was that obtained from the experiment performed at 30 °C and with mixing, having a yield of 0.48 ± 0.01 g/g and it took an average of 15 h for all the sugar to be fermented and peak bioethanol production level to be reached. For the same ethanol production rate, the need for mixing and temperature control can be eliminated by using a textile bioreactor 2.5 times the volume of that needed with temperature and mixing control. Doing this For a 100,000 m^3/y bioethanol production facility will reduce the fermentation investment cost by 26%, while replacing a 1300 m^3 stainless steel reactor with a 1300 m^3 textile bioreactor running at 30 °C and with mixing will reduce the fermentation investment cost by 19% and the total plant investment cost by 2.1%.

Acknowledgments

The textile bioreactor material used for this work was kindly supplied by FOV Fabrics AB, Borås, Sweden. The authors will like to appreciate Ramkumar Nair and Mostafa Jabbari for assisting in making the heat exchanger for the textile bioreactor.

Author Contributions

Osagie A. Osadolor did the experimental design and performed all the experiments, wrote most of the manuscript and was responsible for part of the idea. Patrik R. Lennartsson was responsible for part of the idea and manuscript. Mohammad J. Taherzadeh was responsible for part of the idea and manuscript. All authors have given their approval to the final version of the manuscript.

Conflicts of Interest

The authors declare no conflict of interest.

References

1. Wyman, C.E. Ethanol production from lignocellulosic biomass: Overview. In *Handbook of Bioethanol: Production and Ultilization*; Wyman, C.E., Ed.; CRC Press: Boca Raton, FL, USA, 1996; pp. 1–3.

2. Balat, M.; Balat, H. Recent trends in global production and utilization of bio-ethanol fuel. *Appl. Energy* **2009**, *86*, 2273–2282.
3. Americano da Costa, M.; Normey-Rico, J.E. Modeling, control and optimization of ethanol fermentation process. *World Congr*. **2011**, *18*, 10609–10614.
4. Licht, F.O. Ethanol Industry Outlook 2008–2013 Reports, 2014. Available online: http://www.ethanolrfa.org/pages/annual-industry-outlook (accessed on 23 July 2014).
5. Sarkar, N.; Ghosh, S.K.; Bannerjee, S.; Aikat, K. Bioethanol production from agricultural wastes: An overview. *Renew. Energy* **2012**, *37*, 19–27.
6. Palacios-Bereche, R.; Ensinas, A.; Modesto, M.; Nebra, S.A. New alternatives for the fermentation process in the ethanol production from sugarcane: Extractive and low temperature fermentation. *Energy* **2014**, *70*, 595–604.
7. Magazoni, F.; Monteiro, J.B.; Colle, S.; Cardemil, J.M. Cooling of ethanol fermentation process using absorption chillers. *Int. J. Thermodyn.* **2010**, *13*, 111–118.
8. Maiorella, B.L.; Blanch, H.W.; Wilke, C.R.; Wyman, C.E. Economic evaluation of alternative ethanol fermentation processes. *Biotechnol. Bioeng.* **2009**, *104*, 419–443.
9. Hess, W.T. *Kirk Othmer Encyclopedia of Chemical Technology*; John Wiley & Sons: Hoboken, NJ, USA, 1995.
10. Leib, T.M.; Pereira, C.J.; Villadsen, J. Bioreactors: A chemical engineering perspective. *Chem. Eng. Sci*. **2001**, *56*, 5485–5497.
11. Blakebrough, N. Fundamentals of fermenter design. *Pure Appl. Chem.* **1973**, *36*, 305–316.
12. Benz, G.T. Bioreactor design for chemical engineers. *Chem. Eng. Prog.* **2011**, *107*, 21–26.
13. Rajendran, K.; Aslanzadeh, S.; Johansson, K.; Taherzadeh, M.J. Experimental and economical evaluation of a novel biogas digester. *Energy Convers. Manag*. **2013**, *74*, 183–191.
14. Olisti, Y. Build better industrial bioreactors. *Chem. Eng. Prog.* **1992**, *1992*, 55–58.
15. Fakruddin, M.; Islam, M.A.; Ahmed, M.M.; Chowdhury, N. Process optimization of bioethanol production by stress tolerant yeasts isolated from agro-industrial waste. *Int. J. Renew. Sustain. Energy* **2013**, *2*, 133–139.
16. Santos, N.M.; Amorim, J.; Nascente, P.A.P.; Freire, C.M.A.; Cruz, N.C.; Rangel, E.C. Enhancement of corrosion resistance AISI 304 steel by plasma polymerized thin films. *Mater. Res. Soc. Symp. Proc*. **2013**, *1499*, doi:10.1557/opl.2013.442.
17. Ashby, M.F.; Jones, D.R.H. *Engineering Materials 1: An Introduction to Properties, Applications and Design*; Elsevier: Amsterdam, The Netherlands, 2012.
18. Baddoo, N.R. Stainless steel in construction: A review of research, applications, challenges and opportunities. *J. Construct. Steel Res*. **2008**, *64*, 1199–1206.
19. Berni, M.; Dorileo, I.L.; Prado, J.M.; Forster-Carneiro, T.; Meireles, M.A.A. Advances in biofuel production. In *Biofuels Production*; Scrivener Publishing LLC: Beverly, MA, USA, 2013; pp. 11–58.
20. Taherzadeh, M.J.; Lennartsson, P.R.; Teichert, O.; Nordholm, H. Bioethanol production processes. In *Biofuels Production*; John Wiley & Sons: Hoboken, NJ, USA, 2013; pp. 211–253.
21. James, R.; Couper, W.R.P.; Fair, J.R.; Walas, S.M. Costs of individual equipment. In *Chemical Process Equipment*; Elsevier Inc.: Amsterdam, The Netherlands, 2005; pp. 663–669.

22. Basso, L.C.; Basso, T.O.; Rocha, S.N. Ethanol production in Brazil: The industrial process and its impact on yeast fermentation. In *Biofuel Production—Recent Developments and Prospects*; InTech: Rijeka, Croatia, 2011; pp. 85–100.
23. Richard, T.; Elander, V.L.P. Ethanol from corn: Technology and economics. In *Handbook on Bioethanol: Production and Utilization*; Wyman, C.E., Ed.; CRC press: Boca Raton, FL, USA, 1996.
24. Shupe, A.M.; Liu, S. Effect of agitation rate on ethanol production from sugar maple hemicellulosic hydrolysate by Pichia stipitis. *Appl. Biochem. Biotechnol.* **2012**, *168*, 29–36.
25. Paul, E.L.; Atiemo-Obeng, V.; Kresta, S.M. *Handbook of Industrial Mixing: Science and Practice*; John Wiley & Sons: Hoboken, NJ, USA, 2004.
26. Mignard, D. Correlating the chemical engineering plant cost index with macro-economic indicators. *Chem. Eng. Res. Des*. **2014**, *92*, 285–294.

PAPER II

Development of Novel Textile Bioreactor for Anaerobic Utilization of Flocculating Yeast for Ethanol Production. *Fermentation* Doi:10.3390/fermentation1010098

Fermentation **2015**, *1*, 98-112; doi:10.3390/fermentation1010098

OPEN ACCESS

fermentation

ISSN 2311-5637

www.mdpi.com/journal/fermentation

Article

Development of Novel Textile Bioreactor for Anaerobic Utilization of Flocculating Yeast for Ethanol Production

Osagie A. Osadolor *, Patrik R. Lennartsson and Mohammad J. Taherzadeh

Swedish Centre for Resource Recovery, University of Borås, SE 50190 Borås, Sweden;
E-Mails: Patrik.Lennartsson@hb.se (P.R.L.); Mohammad.Taherzadeh@hb.se (M.J.T.)

* Author to whom correspondence should be addressed; E-Mail: Alex.Osagie@hb.se;
Tel.: +46-33-435-4620; Fax: +46-33-435-4008.

Academic Editor: Ronnie G. Willaert

Received: 17 September 2015 / Accepted: 19 November 2015 /Published: 23 November 2015

Abstract: Process development, cheaper bioreactor cost, and faster fermentation rate can aid in reducing the cost of fermentation. In this article, these ideas were combined in developing a previously introduced textile bioreactor for ethanol production. The bioreactor was developed to utilize flocculating yeast for ethanol production under anaerobic conditions. A mixing system, which works without aerators, spargers, or impellers, but utilizes the liquid content in the bioreactor for suspending the flocculating yeast to form a fluidized bed, was developed and examined. It could be used with dilution rates greater than 1.0 h^{-1} with less possibility of washout. The flow conditions required to begin and maintain a fluidized bed were determined. Fermentation experiments with flow rate and utilization of the mixing system as process variables were carried out. The results showed enhanced mass transfer as evidenced by faster fermentation rates on experiments with complete sucrose utilization after 36 h, even at 30 times lesser flow rate.

Keywords: flocculating yeast; textile bioreactor; ethanol; mass transfer; mixing; fluidization

1. Introduction

Increasing energy demand and environmental awareness have influenced the progressive rise in the production and utilization of bioethanol as a transportation fuel [1]. To boost the competitiveness of bioethanol to fossil fuel, particularly with the current low prices of fossil fuels, there is the need to

continue increasing the productivity of the ethanol production process while reducing the production cost. Flocculation has proven to be advantageous in improving the productivity of the bioethanol production process [2]. Some of its benefits include production at high dilution rate, improved inhibitor tolerance, longer reuse of cells, reduced contamination tendencies at high dilution rate, reduced bioreactor cost because of smaller reactor volume [3], and ease of separating cell flocs from liquid medium in the bioreactor [4].

To effectively utilize flocculation, the size of the flocs and their settling characteristics need to be well understood. It is important that the floc size is large enough to prevent washout while being small enough to allow effective passage and mass transfer of the substrate into the cells and product out of the cells. To avoid washout, mechanical stirrers that break down the flocs are not usually used in bioreactors utilizing flocculating organisms [3]. Depending on the settling rate of the flocs, the contacting pattern that they would make in a bioreactor could result in fixed or fluidized bed. Fixed or fluidized bed systems have their benefits, but for optimal mass transfer and faster production rate, fluidized bed systems are more advantageous because of the larger contacting area of the flocs [5]. To create a stable fluidized bed, the flow rate has to be between the minimum to initiate fluidization and the maximum to prevent the flocs from being carried away from the bioreactor [5]. For these reasons, the design and operation of the bioreactor to be used for propagating flocculating microorganisms is quite important. Fluidization in bioreactors can be achieved either by aeration or by utilizing high flow liquid streams [6]. Currently, airlift bioreactors are the main type of bioreactor being used for utilizing flocculating yeast for bioethanol production [3].

Aeration is required when flocculating yeast is used in an airlift bioreactor for ethanol production [3]. This reduces the ethanol yield as ethanol is optimally produced anaerobically. Besides this, bioreactor cost is high, including aeration, generating more operation cost. Bioreactors for ethanol production have to be designed in a way that they do not hinder the activity of the microorganism within them, withstand the corrosive nature of fermentation media, and provide suitable environment and control needed to optimally produce the desired product(s) [7]. The overall goal in their design is to deliver the required functions and to be economical [8]. Conventional bioreactors for ethanol production are made using stainless steel as the major material of construction and constitute 32% of the fermentation investment cost in a typical 100,000 m^3/year plant [9]. Reducing the cost of ethanol bioreactors will reduce the cost of ethanol production. Some polymeric materials (*e.g.*, polyaniline) have good corrosion-resistance properties [10] and are cheaper than stainless steel, so they could be options for making ethanol bioreactors. However, some challenges regarding their use include their tensile strength and the effectiveness of mixing in the bioreactors made with them. A novel bioreactor with textile as its material of construction was recently introduced as a cheaper alternative to bioreactors made with stainless steel [11]. The textile bioreactor has textile as its backbone material of construction which improves its strength [11]. In this paper, the conditions needed to maintain optimal contact of the flocculating yeast in the bioreactor were determined, and the textile bioreactor was developed accordingly. This enabled anaerobic production of ethanol with the flocculating yeast, while also maintaining good mixing in the bioreactor, thus creating optimal production conditions.

2. Methods

2.1. Microorganism

Naturally flocculating yeast strain *S. cerevisiae* CCUG 53310 (Culture Collection University of Gothenburg, Gothenburg, Sweden) was used for the experiments. The flocculating yeast cells were maintained on a yeast extract peptone dextrose (YPD) agar plate containing 20 g/L agar, 20 g/L D-glucose, 20 g/L peptone, and 10 g/L yeast extract at 4 °C. Before being used for fermentation, the flocculating cells were added into 800 mL YPD media containing 20 g/L D-glucose, 10 g/L yeast extract, and 20 g/L peptone in a 2 L cotton-plugged flask. Three flasks were incubated in a shaking water bath (Grant OLS 200, Grant instrument Ltd., Cambridge, UK) at 125 rpm and 30 °C for 48 h. The supernatant liquid from two of the flasks were discarded, and the sedimented flocculating yeast were rinsed with distilled water into the textile bioreactor for fermentation. The content of the third flask was used to determine the yeast concentration in the bioreactor. A starting concentration of 2 g/L dry weight of the flocs was used for all fermentation experiments.

The average particle diameter for this yeast strain was measured using the optical density and sedimentation technique [12] and it was found to be between 190 to 320 μm. This was done by transferring samples of the cell culture to a tube in which the optical density was measured using a spectrophotometer at a wavelength of 660 nm for the various samples at different times. The optical density readings from the spectrophotometer were proportional to the flocculating yeast concentration. When all the flocculating yeast had settled (settling time), the optical density read from the spectrophotometer gave constant readings, which corresponded to the concentration of the free cells. Dividing the distance from which the flocculating yeast cells fell by the settling time gave the settling velocity. The average diameter of the flocs was calculated from Stokes' law (see equation 4), using flocculating yeast density of 1140 kg/m^3, viscosity of 0.798×10^{-3} Ns/m^2 (*i.e.*, viscosity of water at 30 °C) and acceleration due to gravity of 9.81 m/s^2.

2.2. Textile Bioreactor and Its Development

The bioreactor used for this work (Ethanolic textile lab reactor ETLRII, FOV Fabrics AB, Borås, Sweden), was a 30 L laboratory scale reactor with a working volume of 25 L. Its dimensions were 110 cm length, 8 cm depth, and 34 cm width (Figure 1a). The inlet and outlet diameter were 5 cm. It had a 4 cm opening at the middle that served as a sample collection point, a gas outlet, and a thermometer stand. Tubing was connected to the inlet and outlet of the bioreactor for recirculation.

A 12 m silicone peroxide tubing with 5 mm internal diameter and 8 mm external diameter (VWR International, Leuven, Belgium) was used as the internal mixing tubing in the bioreactor. Holes of 0.42 mm at 1 cm intervals were made in the tubing. The tubing was wound around the perimeter of the bioreactor twice and then joined into five elliptical ribbons by plastic fasteners (Figure 1b). The tubing was kept in the liquid phase by means of ten stainless steel bolts, each having internal and external diameters of 2.4 and 3.5 cm respectively, and weighing 94.6 g. The two ends of the tubing used for mixing were connected to the inlet tubing from the pump. A peristaltic pump (405U/L2 Watson-Marlow, Stockholm, Sweden) was used for recirculation, feeding, and discharging the content of the bioreactor.

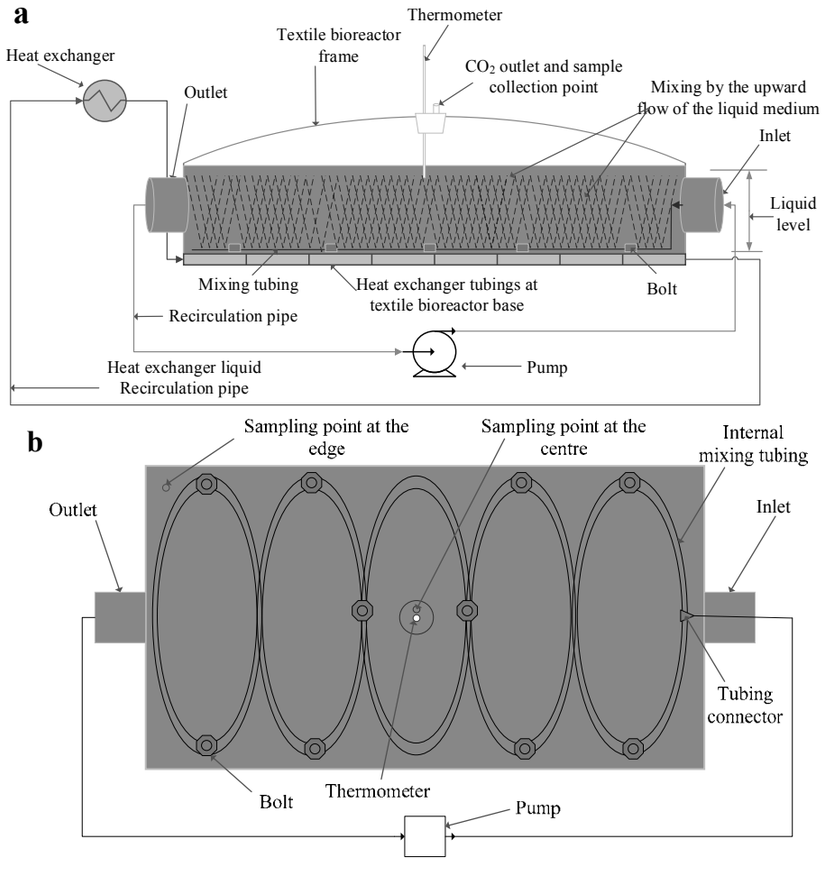

Figure 1. Developed textile bioreactor showing internal mixing inside the bioreactor from (**a**) a side view, and (**b**) a top view of the internal mixing system inside the bioreactor.

2.3. Mixing in the Bioreactor

First 20 L distilled water was fed to the bioreactor. Then, 90 ± 5 mL of 100 ppm bromophenol blue solution was added to the bioreactor at one of its ends (hereafter referred to as the injection point). The content of the bioreactor was recirculated through the internal mixing tube at flow rates of 0.002 and 0.015 volume per volume per minute (VVM). Samples were taken from the two opposite rear edges of the bioreactor. The absorbance of the samples was measured by a spectrophotometer (Biochrom Libra S60, Cambridge, UK) at 592 nm [13]. Mixing during fermentation was carried out by recirculation. To determine the effectiveness of mixing in experiments performed with internal mixing tubing, samples were taken from two sampling points, one at the center of the bioreactor and another at its edge. The samples were taken at a depth of 8 cm and from the surface of the liquid medium in the bioreactor.

2.4. Analytical Methods

Biomass was rinsed with distilled water and dried in an oven at 70 °C for 24 h, and its concentration was reported in g/L. Samples from the bioreactor were analyzed using a hydrogen-based ion exchange column (Aminex HPX-87H, Bio-road, Hercules, CA, USA) in a high performance liquid chromatography (HPLC) at 60 °C and 5 mM 0.6 mL/min H_2SO_4 eluent. A refractive index detector (Waters 2414, Waters Corporation, Milford, MA, USA) was used with the HPLC. Before being used for HPLC analysis, the samples were centrifuged for 5 min at 10,000× *g* and the liquid portion stored at −20 °C. Concentrations reported for all fermentation experiments were the amount determined by HPLC.

Scanning for the highest peak was used to determine the best wavelength for measuring the absorbance of bromophenol blue samples from the bioreactor. The settling rate of the flocculating yeast used for the experiment was determined using a sedimentation column. Biomass concentration of 2 g/L dry weight was released into a sedimentation column that was filled to 10 cm with the media for fermentation, and the content was mixed. The time taken for the flocs to settle to the base of the column was recorded as the settling time. The distance that the flocs settled from was divided by the settling time to give the settling velocity (V_s).

2.5. Experimental Setup for Fermentation

Fermentation experiments with and without internal mixing tubing and different flow rates (0.0016–0.06 VVM) as process variables were carried out anaerobically in the textile bioreactor. Sucrose (50–55 g/L) was used as the energy and carbon source for the flocculating yeast. It was supplemented with 1.0 g/L yeast extract, 7.5 g/L $(NH_4)_2SO_4$, 3.5 g/L KH_2PO_4, and 0.75 g/L $MgSO_4$ $7H_2O$. The liquid volume in the reactor for all experiments was 25 L. Sucrose concentration dropped between 51–45 g/L after the feed to the textile bioreactor was autoclaved. Each experiment was performed in duplicate. The error bars shown on all figures represent standard deviation values generated from the duplicated experiments.

2.6. Fluidization of the Flocs in the Bioreactor

The four forces exerted on a particle during free settling are shown in Equation (1) [14]. On the verge of fluidization, the drag force becomes equal to the pressure force acting on the flocs, and the force due to acceleration becomes zero [14]. The resulting force balance equation is shown in Equation (2). The minimum flow rate to establish this condition occurs when the superficial velocity (V_0) is equal to the fluid upwards velocity (V_u). To prevent the flocs from be carried away from the bioreactor, the maximum fluid upwards velocity (V_{umax}) should be equal to the flocs' settling velocity (V_s) [15]. For Reynolds numbers less than 10, these velocities can be obtained from Equations (3) and (4) [15]. Where ρ_p is the density of the particle, ρ_f is the density of the fluid, g is acceleration due to gravity, D_p is the particle diameter, μ is the viscosity, and ε is the void fraction.

$$\text{Force due to acceleration} = \text{Force due to gravity} - \text{Buoyancy force} - \text{Drag force} \quad (1)$$

$$\text{Pressure force } (F_p) = \text{Force due to gravity } (F_g) - \text{Buoyancy force } (F_B) \quad (2)$$

$$V_0 = V_u = (\rho_p - \rho_f) g D_p^2 \varepsilon^3 / 150\ \mu\ (1 - \varepsilon) \quad (3)$$

$$V_{umax} = V_s = (\rho_p - \rho_f)gD_p^2/18\ \mu \quad (4)$$

For the textile bioreactor prototype used in this work, the superficial velocity is defined in Equation (5), where Q is the liquid flow rate in m^3/s and A is the surface area. The velocity of the fluid (V_i) going through the mixing tubing is defined in Equation (6), where A_i is the internal area of the tubing. Using the continuity principle, the velocity at which the fluid leaves the small holes in the tubing is 142 (*i.e.*, $2.5^2/0.21^2$) times higher than that at which it enters [15]. However, as the tubing is 12 m long and the holes are spaced 1 cm apart, there were 1200 holes. So, the upward velocity (V_h) with which the fluid emerges would split accordingly. This is shown in Equation (7). For fluidization to begin and be sustained in the developed textile bioreactor, Equation (8) shows the governing criteria:

$$V_0 = Q/A = Q/(1.1 \times 0.34) = 2.674Q\ (m/s) \quad (5)$$

$$V_i = Q/A_i = Q/(\pi \times r_i^2) = 5.094 \times 10^4 Q\ (m/s) \quad (6)$$

$$V_h = 142 \times V_i/1200 = 6.028 \times 10^3 Q\ (m/s) \quad (7)$$

$$V_0 \leq V_h \leq V_s \quad (8)$$

2.7. Statistical Analysis

All statistical analyses were performed with the MINITAB® software package. Results were analyzed with ANOVA (analysis of variance), using general linear model, and factors were considered significant when they had *p*-value less than 0.05. The analysis was performed on the results obtained from samples measured from the start of the experiment up until the 32nd hour, when stationary phase was reached. Ethanol and sucrose concentrations were used as the response variables, the position from which the sample was taken was used as the main factor, while time and number of runs served as blocking factors.

3. Results and Discussion

Possible ways to reduce the fermentation cost in a bioethanol plant includes process development, utilizing new and cheaper bioreactors, and making the separation process more efficient. This work combines these ideas in developing the textile bioreactor. The newly developed textile bioreactor has the high flexibility, ease of operation and installation, good mechanical strength, high thermal tolerance, low purchase cost, resistance to corrosive fermentation media, and ease of transportation of its previous prototype [11]. It has a new mixing system that eliminates the need for mixing by using either axial flow impellers or aeration spargers. This removes the purchasing and operational cost associated with the maintenance of those devices. A highly flocculating yeast strain with a settling rate of 1 cm/s was used to examine the performance of the developed textile bioreactor for bioethanol production. The efficiency of mixing (a measure of the mass transfer efficiency) in the developed textile bioreactor and the flow rate needed to maintain optimal contact between the flocculating yeast and bioreactor content were investigated in this work.

3.1. Maintaining Optimal Flocs Contact in the Textile Bioreactor

Increasing the surface contact area of enzymes or catalyst in the form of a fluidized bed generally increases the speed at which a chemical reaction takes place [14]. Thus, flocculating yeast retained in a bioreactor in the form of fluidized particles would result in more rapid utilization of the substrate in the bioreactor. Using Equations (5) to (7), different fluid upflow velocities and superficial velocities for different flow rates were generated, and their values are shown in Table 1. As seen in this table, the required velocity needed to begin fluidization is low. This is because the textile bioreactor prototype used for this analysis has a high surface area to volume ratio of 12.5 m^2/m^3. The superficial velocity reduces with increasing surface area to volume ratio, so the upflow velocity needed on the verge of fluidization would be less for bioreactors having a higher surface area to volume ratio.

Table1. The fluid upflow velocity generated at different flow rate in the textile bioreactor. VVM: volume per volume per minute; V_0: Superficial velocity; V_i: Fluid velocity; V_h: Fluid upflow velocity; V_s: Flocs settling velocity.

Q (VVM)	V_0 (m/s) × 10^6	V_i (m/s)	V_h at Different Hole Spacing (m/s)			V_s (m/s)
			1 cm Spacing	5 mm Spacing	2 mm Spacing	
0.0016	1.78	0.03	0.004	0.002	0.001	0.01
0.0120	13.37	0.25	0.030	0.015	0.006	0.01
0.0160	17.83	0.34	0.040	0.020	0.008	0.01
0.0320	35.64	0.68	0.080	0.040	0.016	0.01
0.0600	66.84	1.27	0.151	0.075	0.030	0.01

For continuous production of bioethanol using flocculating yeast, it is desirable to carry out the production at a high dilution rate and at the same time prevent washout. From Equation (8), washout could occur when the fluid upflow velocity (V_h) exceeds the flocs settling velocity (V_s). From Table 1, it can be observed that washout would occur in this textile bioreactor prototype if operated on a dilution rate greater than 0.72 h^{-1} (*i.e.*, $Q \geq 0.012$ VVM), as V_h is greater than V_s. One way to increase the dilution rate would be to increase the number of holes by reducing the space between consecutive holes in the mixing tubing. From Table 1, reducing the space between the tubes to 2 mm would allow the bioreactor to be operated at a dilution rate of 1 h^{-1} with lesser tendency for washout, as V_h equals V_s with this condition. Another possibility of increasing the dilution rate would be to use mixing tubing of a length longer than 12 m. For example, using 18 m long tubing at 2 mm spacing, from equation 7, at Q = 0.02 VVM (dilution rate of 1.2), V_h becomes 0.007 m/s, which is less than the settling velocity of 0.01 m/s. Normally, at a dilution rate greater than the growth rate, washout would occur, but with this type of configuration for the mixing tubing, even with dilution rate higher than growth rate, washout would not occur.

3.2. Mixing as a Means of Reducing Mass Transfer Limitations

Efficient mass transfer is important for optimal performance in any bioreactor, as it helps to facilitate transfer of substrate into and product out of the microorganism, and prevent improper cell growth in the bioreactor [7]. Mass transfer is influenced by two factors: the diffusional flux between the cells and

the liquid media, and the bulk flow of the liquid media. The first factor is influenced by the diffusivity of the product or substrate into the liquid media. The second is enhanced by the mixing system in the bioreactor, like agitation, aeration, or the use of stirrers [16]. With the theoretical understanding of how the flow rate can influence good contacting pattern in the previous section, experimental verifying the theoretical concepts are presented in this section.

For bioreactors utilizing flocculating yeast, mass transfer limitations need to be adequately considered. There needs to be a balance between having flocs of large sizes, favorable for the enhancement of cell retention in the bioreactor, and reducing the size of the flocs, which is necessary for the reduction of the mass transfer limitations. Characterizing solute transport into and out of the flocs is challenging because of the fragile nature of the flocs and the difficulty in deciding the geometry the flocs actually have inside the bioreactors [3]. The approach in this article was to relate the mass transfer due to diffusion to the coefficient of diffusivity, and the flow rate of the liquid media being recirculated as a measure of that due to the bulk flow of the liquid [17].

Figure 2 shows the result of the absorbance of bromophenol blue measured across the textile bioreactor at different flow rates. At 0.015 VVM, equilibrium was reached in the textile bioreactor in 15 min. At a flow rate of 0.002 VVM, equilibrium was reached in 50 min. At 25 °C, the diffusion coefficient of bromophenol blue in water is 3×10^{-10} m^2/s [18], that of ethanol in water is 1.24×10^{-9} m^2/s, that of sucrose in water is 5.24×10^{-10} m^2/s, and that of water in water is 2.45×10^{-9} m^2/s [19]. The lower diffusivity of bromophenol blue than that of the product and substrate serves as a benchmark for understanding the influence of diffusivity on mass transfer under limiting product or substrate conditions [20]. Achieving equilibrium in 50 min at a flow rate of 0.002 VVM is sufficient, as the sampling time for experiments on bioethanol production is usually measured in hours [21].

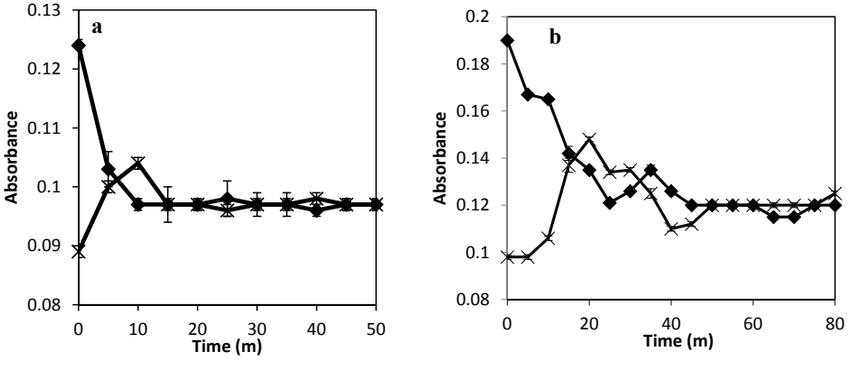

Figure 2. Bromophenol blue absorbance variation in the textile bioreactor at (**a**) a flow rate of 0.015 VVM, and (**b**) at a flow rate of 0.002 VVM at the injection point (♦) and at the opposite end (×).

3.2.1. Mass Transfer Enhancement by Internal Mixing Tubing in the Textile Bioreactor

The internal tubing had holes of 0.42 mm diameter which were 1 cm spread apart all through the textile bioreactor. Both ends of the tubing were connected to the input stream from the pump. The size of the holes and the continuous inflow of the liquid medium generate a pressure difference between the input stream and the fluid inside the tubing. A diameter of 0.42 mm was used because using a larger diameter would result in the incoming fluid leaving the tubing only from the entrance, and a smaller size would generate high back pressure on the pump.

The holes in the internal tubing create upward flow of the liquid stream, which helps in re-suspending the settling flocs, thus improving the mass transfer rate inside the textile bioreactor. To test this idea, fermentation experiments were carried out in the textile bioreactor. Figure 3a shows the result with internal tubing to aid mixing at 0.0016 VVM, while Figure 3b shows the result when mixing is not aided at a flow rate of 0.032 VVM. A lower flow rate was used for the case with aided mixing to show that the result obtained was not due to the flow rate but due to the mixing system itself—as demonstrated in Figure 2a, higher flow rate has been shown previously to improve mass transfer. The same starting concentration of 2 g/L dry weight flocculating yeast was used in both cases. For the aided mixing case (Figure 3a), the fermentation process and sucrose consumption was complete after 36 h, while the unaided mixing experiment (Figure 3b) still had more than 4 g/L of unconsumed sucrose after 48 h. The longer time in Figure 3b is attributable to the settling of the flocs at the bottom of the textile bioreactor, which causes uneven consumption of the substrate in the reactor. The superficial velocity for Figure 3b from Table 1 is 3.6×10^{-5} m/s, which can be met by the velocity of the CO_2 gas bubbles rising from the bottom of the reactor, at the onset of the fermentation experiment. This could explain the higher substrate consumption during the first 28 h of fermentation than in the latter part. However, when the sucrose at the bottom of the reactor is consumed, there will no longer be CO_2 bubbles to re-suspend the settled flocs, so the flocs at the bottom of the reactor, because of the mass transfer limitation, would go into the stationary phase faster, resulting in longer fermentation time or incomplete utilization of the substrate. In Figure 3a, the upward flow of the liquid stream helped to keep the flocs uniformly distributed in the textile bioreactor through the duration of the fermentation experiment. This shows that the developed mixing system for the textile bioreactor is effective in preventing ineffective substrate utilization and increasing the fermentation rate. From Figure 3a, the average peak ethanol concentration was 22.13 ± 0.93 g/L. Using the average fermentation time gave the specific ethanol productivity in the developed textile bioreactor with aided mixing at 0.0016 VVM as 0.29 ± 0.01 g-ethanol/g-biomass/h. The best specific productivity from a gas lift reactor with recycle was reported as 0.045 g-ethanol/g-biomass/h with no sugar loss, and 0.43 g-ethanol/g-biomass/h with significant sugar loss [22]. For an airlift reactor, optimum specific productivity of 0.4 g-ethanol/g-biomass/h with significant sugar loss has been reported [23]. Comparing the reported specific productivity of different bioreactors for ethanol production from literature with that of the developed textile bioreactor, it can be seen that for an optimal combination of high specific productivity and complete sugar utilization, the developed textile bioreactor performs better.

3.2.2. Higher Flow Rate with and without Internal Tubing

The mass transfer rate can be enhanced to an extent by increasing the bulk flow of the liquid media [16]. The effect of higher flow rate on the fermentation rate was investigated. For the textile bioreactor with internal mixing tubing, a flow rate of 0.012 VVM (7.5 times higher than the previously examined flow rate) was used as the recirculation rate in the textile bioreactor with internal mixing tubing. Figure 4a shows the result of this experiment. From Figure 4a, the fermentation rate was slightly faster in the first 32 h of fermentation in comparison to the experiment with a recirculation rate of 0.0016 VVM. However, the substrate was fully consumed after 36 h in both cases. This shows that mixing is not the rate limiting step in both cases, but rather sucrose hydrolysis and slow fructose utilization [22]. This limitation can be handled in several ways such as operating the reactor in a fed-batch mode [24], or by maintaining a high concentration of flocs in the bioreactor [22]. However, for continuous production, using a flow rate of 0.012 VVM at 1 cm hole spacing would cause washout to occur much faster than that at a flow rate of 0.0016 VVM (Table 1). This did not affect the fermentation rate in the experiment performed at a flow rate of 0.012 VVM because the cells were recycled back into the textile bioreactor.

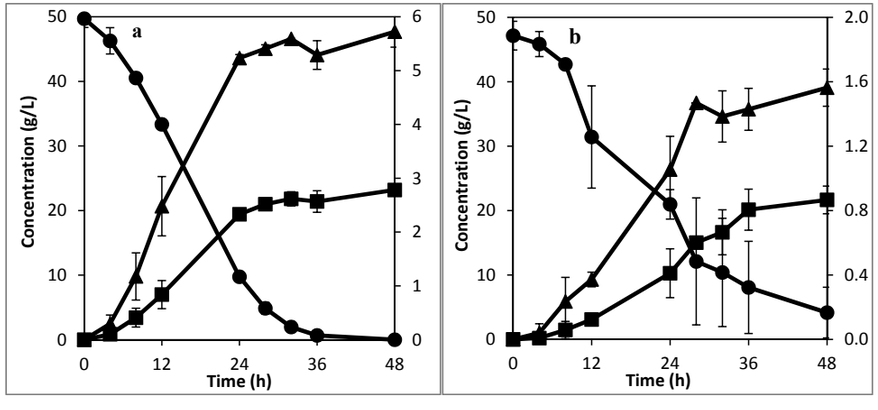

Figure 3. Experiment with enhanced mixing at (**a**) a recirculation rate of 0.0016 VVM , and (**b**) without enhanced mixing at 0.032 VVM, showing ethanol (■) and sucrose (●) concentration in the primary axis (right hand side), and glycerol concentration (▲) in the secondary axis.

For the case without the mixing tubing, a flow rate of 0.06 VVM (1.9 times higher than the previously examined flow rate) was used as the recirculation rate. The result of this experiment is shown in Figure 4b. Comparing the experiment performed at 0.06 VVM with that at 0.032 VVM shows that the higher recirculation flow rate increased the fermentation rate. However, the higher flow rate was not sufficient to cause complete utilization of the sucrose within 48 h because the settling rate of the flocs is higher than the turbulence created by the high flow rate. Comparing the experiment performed at 0.0016 VVM with that performed at 0.06 VVM shows that the developed mixing system is much more effective in overcoming mass transfer limitations associated with mixing, even with 30 times slower flow rate.

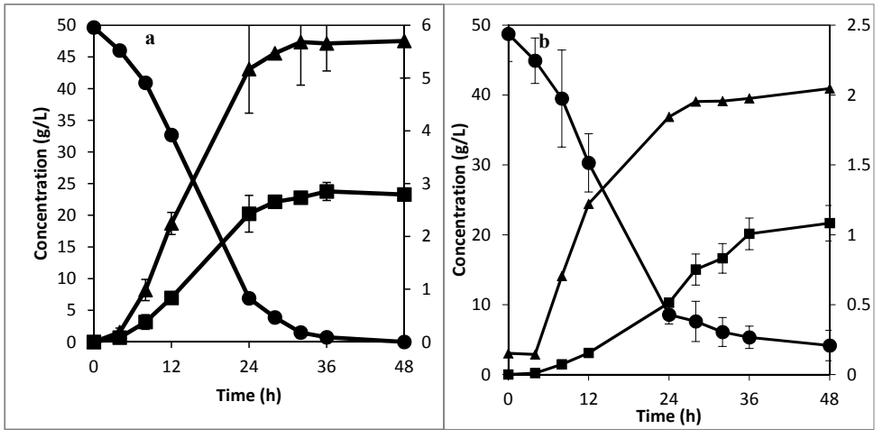

Figure 4. Experiments with (**a**) enhanced mixing at 0.012 VVM, and (**b**) without enhanced mixing at a recirculation rate of 0.06 VVM , showing ethanol (■) and sucrose (●) concentration in the primary axis (right hand side), and glycerol concentration (▲) in the secondary axis (left hand side).

3.3. Mixing along the Edges of the Textile Bioreactor

One of the limitations of a rectangular reactor is the possibility of it having poor mixing, especially at the edges [25]. Ethanol and sucrose concentrations across different sampling positions in the developed textile bioreactor at a recirculation rate of 0.0016 VVM are shown in Table 2. From Table 2 it can be seen that the concentrations of ethanol and sucrose from different sampling points and depths are similar. ANOVA using a general linear model of ethanol and sucrose concentration as responses and sampling position as factor gave *p*-values of 0.861 for ethanol and 0.733 for sucrose, so the position from which the sample is drawn is not statistically significant, meaning that the mixing is uniform at all points in the textile bioreactor. This uniformity in the textile bioreactor implies that the flocs responsible for the conversion of substrate to product is uniformly distributed across the developed textile bioreactor. From this it can be seen that the developed textile bioreactor does not have regions with significant ethanol or sucrose concentration variation, so there will be efficient and fast utilization of the substrate across it.

Table 2. Ethanol and sucrose concentrations from different sampling point in the textile bioreactor.

Time (h)	Run	Ethanol Concentration (g/L)				Sucrose Concentration (g/L)			
		Edge 8 cm Deep	Edge Surface	Centre 8 cm Deep	Centre Surface	Edge 8 cm Deep	Edge Surface	Centre 8 cm Deep	Centre Surface
0	1	0.00	0.00	0.00	0.00	48.96	48.46	48.75	48.75
4	1	0.86	0.45	0.51	0.47	46.22	44.97	44.84	44.84
8	1	2.39	2.30	2.15	2.38	43.61	41.91	40.97	40.97
12	1	5.14	5.41	5.23	5.44	36.16	38.04	36.01	33.70
24	1	17.91	18.24	18.87	18.85	11.61	5.52	12.11	9.34
28	1	20.46	19.95	20.60	20.44	3.21	2.13	3.14	5.50
32	1	21.20	21.25	21.68	21.04	1.35	1.35	1.38	1.39
0	2	0.00	0.00	0.00	0.00	48.19	50.40	50.68	50.68
4	2	1.18	1.18	1.27	1.21	46.86	46.86	47.72	47.72
8	2	4.56	4.41	4.41	4.44	40.87	39.94	40.10	40.10
12	2	8.60	8.27	8.23	8.53	32.41	30.77	31.84	32.98
24	2	20.03	19.94	20.01	19.98	10.00	10.14	10.03	10.16
28	2	21.93	21.65	21.88	21.52	4.34	4.16	4.31	4.22
32	2	22.60	22.05	22.65	22.59	2.30	2.82	2.87	2.55

3.4. Ethanol Production Process Development and Cost Reduction

Ethanol could be produced by batch, fed-batch, or continuous modes of production. Conventionally, ethanol is produced anaerobically, and the yeast cells are centrifuged and either recycled or channeled somewhere else [26]. However, for a 100,000 m^3/year ethanol production facility, the centrifuge accounts for 18% of the fermentation investment cost [9], excluding the energy cost. This can be eliminated by using flocculating yeast. Mixing in bioreactors using flocculating yeast is carried out using aeration (so the bioreactor is operated as a bubble column or an airlift reactor) as stirrers breaks the flocs [3]. Despite the Crabtree effect that favors ethanol production by *S. cerevisiae* under aerobic conditions [27], aerobic conditions cause more biomass production, which reduces the amount of ethanol that can be produced [28]. The developed textile bioreactor has been shown to both anaerobically use flocculating yeast for ethanol production and maintain good mixing, thus it can combine the benefits of optimal ethanol production and elimination of centrifugation cost.

Using the same volume of textile bioreactor in place of a stainless steel reactor has been previously shown to reduce the fermentation investment cost by 19% [11]. Combining this with the savings obtained by not using a centrifuge would result in 37% reduction in the investment cost of a 100,000 m^3/year ethanol production facility [9].

4. Conclusions

The developed textile bioreactor showed a better combination of specific ethanol productivity and complete sugar utilization than both gas lift bioreactors with recycle and airlift bioreactors when using flocculating yeast for ethanol production. The results of the anaerobic mixing efficiency with high settling flocculating yeast showed excellent mixing in comparison with the previous prototype. This makes it possible to combine optimal anaerobic ethanol production rates and the process benefits of using flocculating yeast for ethanol production. Additionally, for yeast flocs having average particle diameter between 190 to 320 μm, there is the possibility of operating the bioreactor at a dilution rate of more than 1 h^{-1} with less chances of washout by using mixing tubing configurations that makes the fluid upflow velocity less than the flocs settling velocity. Using flocculating yeast as the fermenter in the same volume of the developed textile bioreactor as the conventionally used bioreactor in a 100,000 m^3/year ethanol production facility can give a 37% reduction in fermentation investment cost.

Acknowledgments

The authors would like to appreciate Magnus Lundin, Peter Therning, and Regina Patinvoh for their technical assistance and valuable discussions. The textile bioreactor used for this article was kindly provided by FOV Fabrics AB (Borås, Sweden).

Author Contributions

Osagie A. Osadolor did the experiment design, performed all the experiment, wrote most of the manuscript and had the idea. Patrik R. Lennartsson was responsible for part of the manuscript. Mohammad J. Taherzadeh was responsible for part of the manuscript. All authors have given their approval for this final version of the manuscript.

Conflicts of Interest

The authors declare no conflict of interest.

References

1. Balat, M.; Balat, H. Recent trends in global production and utilization of bio-ethanol fuel. *Appl. Energ.* **2009**, *86*, 2273–2282.
2. Mussatto, S.I.; Dragone, G.; Guimarães, P.M.R.; Silva, J.P.A.; Carneiro, L.M.; Roberto, I.C.; Vicente, A.; Domingues, L.; Teixeira, J.A. Technological trends, global market, and challenges of bio-ethanol production. *Biotechnol. Adv.* **2010**, *28*, 817–830.
3. Domingues, L.; Vicente, A.A.; Lima, N.; Teixeira, J.A. Applications of yeast flocculation in biotechnological processes. *Biotechnol. Bioprocess. Eng.* **2000**, *5*, 288–305.
4. Verstrepen, K.J.; Klis, F.M. Flocculation, adhesion and biofilm formation in yeasts. *Mol. Microbiol.* **2006**, *60*, 5–15.
5. Ergun, S.; Orning, A.A. Fluid flow through randomly packed columns and fluidized beds. *J. Ind. Eng. Chem.* **1949**, *41*, 1179–1184.
6. Muroyama, K.; Fan, L.S. Fundamentals of gas-liquid-solid fluidization. *AIChE. J.* **1985**, *31*, 1–34.
7. Blakebrough, N. Fundamentals of fermenter design. *Pure Appl. Chem.* **1973**, *36*, 305–316.
8. Mark, R.; Wilkins, A.H.A. Fermentation. In *Food and Industrial Bioproducts and Bioprocessing*; John Wiley & Sons: Hoboken, NJ, USA, 2012.

9. Maiorella, B.L.; Blanch, H.W.; Wilke, C.R.; Wyman, C.E. Economic evaluation of alternative ethanol fermentation processes. *Biotechnol. Bioeng.* **2009**, *104*, 419–443.
10. Wei, Y.; Wang, J.; Jia, X.; Yeh, J.-M.; Spellane, P. Polyaniline as corrosion protection coatings on cold rolled steel. *Polymer* **1995**, *36*, 4535–4537.
11. Osadolor, O.A.; Lennartsson, P.R.; Taherzadeh, M.J. Introducing textiles as material of construction of ethanol bioreactors. *Energies* **2014**, *7*, 7555–7567.
12. Van Hamersveld, E.H.; van der Lans, R.; Luyben, K. Quantification of brewers' yeast flocculation in a stirred tank: Effect of physical parameters on flocculation. *Biotechnol. Bioeng.* **1997**, *56*, 190–200.
13. Nagai, Y.; Unsworth, L.D.; Koutsopoulos, S.; Zhang, S. Slow release of molecules in self-assembling peptide nanofiber scaffold. *J. Control. Release* **2006**, *115*, 18–25.
14. Kunii, D.; Levenspiel, O. *Fluidization Engineering*; Elsevier: Amsterdam, The Netherlands, 2013.
15. McCabe, W.L.; Smith, J.C.; Harriott, P. *Unit Operations of Chemical Engineering*; McGraw-Hill: New York, NY, USA, 1993; Volume 5.
16. Benitez, J. *Principles and Modern Applications of Mass Transfer Operations*; John Wiley & Sons: Hoboken, NJ, USA, 2011.
17. Bergman, T.L.; Incropera, F.P.; Lavine, A.S. *Fundamentals of Heat and Mass Transfer*; John Wiley & Sons: Hoboken, NJ, USA, 2011.
18. West, J.; Gleeson, J.P.; Alderman, J.; Collins, J.K.; Berney, H. Structuring laminar flows using annular magnetohydrodynamic actuation. *Sensor Actuator B* **2003**, *96*, 190–199.
19. Hayduk, W.; Laudie, H. Prediction of diffusion coefficients for nonelectrolytes in dilute aqueous solutions. *AIChE. J.* **1974**, *20*, 611–615.
20. Bosma, T.N.P.; Middeldorp, P.J.M.; Schraa, G.; Zehnder, A.J.B. Mass transfer limitation of biotransformation: Quantifying bioavailability. *Environ. Sci. Technol.* **1996**, *31*, 248–252.
21. Elander, R.T.; Putsche, V.L. *Ethanol from Corn: Technology and Economics*; Taylor and Francis: Washington, DC, USA, 1996; pp. 329–349.
22. Fontana, A.; Ghommidh, C.; Guiraud, J.P.; Navarro, J.M. Continuous alcoholic fermentation of sucrose using flocculating yeast. The limits of invertase activity. *Biotechnol. Lett.* **1992**, *14*, 505–510.
23. Sousa, M.L.; Teixeira, J.A.; Mota, M. Comparative analysis of ethanolic fermentation in two continuous flocculation bioreactors and effect of flocculation additive. *Bioprocess. Eng.* **1994**, *11*, 83–90.
24. Echegaray, O.F.; Carvalho, J.C.M.; Fernandes, A.N.R.; Sato, S.; Aquarone, E.; Vitolo, M. Fed-batch culture of sacchoromyces cerevisiae in sugar-cane blackstrap molasses: Invertase activity of intact cells in ethanol fermentation. *Biomass Bioenergy* **2000**, *19*, 39–50.
25. Oca, J.; Masaló, I. Design criteria for rotating flow cells in rectangular aquaculture tanks. *Aquacult. Eng.* **2007**, *36*, 36–44.
26. Basso, L.C.; Rocha, S.N.; Basso, T.O. Ethanol Production in Brazil: The Industrial Process and its Impact on Yeast Fermentation; Intech: Rijeka, Croatia, 2011.
27. Verduyn, C.; Zomerdijk, T.P.L.; van Dijken, J.P.; Scheffers, W.A. Continuous measurement of ethanol production by aerobic yeast suspensions with an enzyme electrode. *Appl. Microbiol. Biotechnol.* **1984**, *19*, 181–185.

28. Taherzadeh, M.J.; Lennartsson, P.R.; Teichert, O.; Nordholm, H. Bioethanol production processes. *Biofuels Prod.* **2013**, 211–253, doi:10.1002/9781118835913.ch8.

PAPER III

Membrane stress analysis of
collapsible tanks and bioreactors.
Biochemical Engineering Journal
Doi.org/10.1016/j.bej.2016.06.023

Biochemical Engineering Journal 114 (2016) 62–69

Contents lists available at ScienceDirect

Biochemical Engineering Journal

journal homepage: www.elsevier.com/locate/bej

Regular article

Membrane stress analysis of collapsible tanks and bioreactors

Osagie A. Osadolor*, Magnus Lundin, Patrik R. Lennartsson, Mohammad J. Taherzadeh

Swedish Centre for Resource Recovery, University of Borås, SE 50190, Borås, Sweden

ARTICLE INFO

Article history:
Received 12 March 2016
Received in revised form 13 June 2016
Accepted 20 June 2016
Available online 22 June 2016

Keywords:
Pressure vessel
Collapsible tank
Bioreactor
Stress calculations
Stress relation
Curvature analysis

ABSTRACT

Collapsible tanks, vessels or bioreactors are finding increasing usage in small/medium scale processes because they offer flexibility and lower cost. However, if they are to be used at large scale, they need to be shown capable of handling the physical stress exerted on them. Because of their nonconventional shape and non-uniform pressure distribution, thin shell analysis cannot be used in calculating their stress. Defining curvature in terms of pressure addressed these challenges. Using curvature and numerical analysis, the membrane stress in collapsible tanks designed as bioreactors of volumes between 100 to 1000 m^3 were calculated. When the liquid/gas height and static pressure are known, an equation for calculating tension per length was developed. An equation that could calculate the liquid height from the bioreactor's volume, dimensions and working capacity was generated. The equation gave values of liquid height with a maximum deviation of 3% from that calculated by curvature analysis. The stress values from the liquid height and tension equations had a maximum deviation of 6% from those calculated by curvature analysis. The calculated tensile stress in a 1000 m^3 collapsible tank was 14.2 MPa. From these calculations, materials that optimize both cost and safety can be selected when designing collapsible tanks.

1. Introduction

Collapsible tanks or vessels are vessels made from materials that are flexible, easily deformable, and light. Without a rigid supporting system collapsible tanks normally take the shape of a pillow when filled with fluid, so they are also called pillow or bladder tanks. Collapsible tanks are used as water storage vessels, fuel storage vessels, transportation vessels, sewage tanks, food storage vessels, chemical storage vessels, bioreactors for e.g. ethanol [1] or biogas production [2] etc. The benefits of using collapsible tanks over rigid tanks include process flexibility, ease of transportation, installation, portability and low cost. Collapsible tanks come in sizes suitable for use at small, medium [3] and large scale. Collapsible tanks are usually designed with their end use in view. One common question when using these collapsible tanks especially at larger scale is if the materials used for constructing them can tolerate the stress caused by the high pressure and the large liquid volume. Despite their wide application, there is no scientific publication on how to calculate the stress in these containers to safeguard against failure.

When collapsible tanks are used for storing or processing fluids, they can be designed as pressure vessels. A pressure vessel is a vessel that can withstand the internal pressure that is acting on it [4]. According to its wall thickness, pressure vessels can be classified as thick or thin walled. A pressure vessel is thin walled if the ratio of its wall thickness to its radius is less than or equal to 1/20 [4] . Thin walled vessels offer no resistance to bending, so the stress on it is distributed through its thickness, resulting in only membrane stresses, while thick walled vessels offer resistance to bending, so they have both membrane stresses and bending stresses [4]. Thus, collapsible tanks are thin-walled pressure vessels. Thin shell theory is normally used for calculating the stress in thin walled pressure vessels under constant internal pressure [4]. Using the thin shell theory in calculating the membrane stress in collapsible tanks would not give accurate values. Some reasons for this are; collapsible tanks will not have the same pressure at all points, and they will not have a specific shape at all times because their shape will change with changes in pressure and the volume of fluid in them [5].

Accurate determination of the stresses in any pressure vessel is essential to safeguard against failure [6] which could occur when the membrane stress in the vessel has exceeded the material's intrinsic tolerance values as determined by its Young's modulus [7]. One challenge why the thin shell theory cannot be used to calculate the stress that would act on collapsible tank is that their

Abbreviations: DEs, differential equations; WC, working capacity.

* Corresponding author.
E-mail addresses: Alex.Osagie@hb.se (O.A. Osadolor), Magnus.Lundin@hb.se (M. Lundin), Patrik.Lennartsson@hb.se (P.R. Lennartsson), Mohammad.Taherzadeh@hb.se (M.J. Taherzadeh).

http://dx.doi.org/10.1016/j.bej.2016.06.023
1369-703X/

Nomenclature

k	Curvature
s	Arc length
P_0	Static pressure
h	Y_ liquid height
Hg	Gas height
α	Directional angle of the tangent to the curve
T	Membrane stress force or tension per unit length
W	Width of collapsible tank
L	Length of collapsible tank
p	Perimeter of collapsible tank
A_L and A	Liquid and total cross sectional area of collapsible tank

shape would change with variations in the pressure and volume of the fluid in these tanks. Defining their curvature as a function of the fluid property of interest, which in this case is pressure, helps to overcome this challenge. This also helps in handling the second challenge of non-uniform pressure distribution in collapsible tanks. In this work, the membrane stress associated with collapsible tanks and their geometry was determined using their curvature and numerical analysis. The results gotten from the analysis performed on collapsible tanks can assist in determining their strength, how suitable they would be for large scale purposes, how they can be designed to minimize the stress in them, and what materials are suitable for making them.

2. Methods

The geometry of a collapsible tank as determined by curvature is shown in Fig. 1. The stress analysis performed in the direction of the width of a collapsible tank is termed circumferential, while that one performed in the direction of the length is termed longitudinal. The key assumptions used for the analysis performed in this work are; (a) the weight of the material used for constructing the collapsible tank can be neglected, (b) the material is infinitely flexible in the direction of curvature, (c) the collapsible tank membrane stress can be analysed using one plane at a time, and (d) the sum of the static pressures generated by the two directions of curvature gives the overall static pressure acting on the collapsible tank. As failure due to tensile stress has a higher chance of occurring in areas with less material reinforcement [7], curvature analysis performed in this paper best describes regions far from the edges of the collapsible tanks. In these areas, it can be assumed that there would be no interaction of the two orthogonal axes and the joints in the collapsible tank to increase its strength.

2.1. The shape of a collapsible tank as defined by its curvature

To find the shape of a collapsible tank, a reference frame was chosen in which position and altitude were considered using the top height of the liquid level as the origin [8]. Every height below the top of the liquid level was negative, while only the gas height (if present) was positive (Fig. 2).

The curvature (k) of any shape or line was defined using Eq. (1), where α is the directional angle of the tangent to the curve and s is the arc length [9]. However, as the pressure is the source of the curvature, the curvature was expressed in terms of the pressure according to Eq. (2), where P_0 is the static pressure above the liquid (N/m^2), y_ is the liquid height (m) which is defined with respect to the y axis according to Eq. (3), g is gravity (m/s^2), ρ (rho) is density (kg/m^3) and T is the membrane stress force or tension per unit length (N/m). The differential equations (DEs) relating the curvature, the arc length and the x and y coordinate functions for the curve are shown in Eq. (4) [10].

$$k = \frac{d\alpha}{ds} \tag{1}$$

$$k = \frac{P_0 - y\_g\rho}{T} \tag{2}$$

$$y\_ = \begin{cases} y, y \le 0 \\ 0, y > 0 \end{cases} \tag{3}$$

$$\begin{cases} \frac{d^2x}{ds^2} = k\frac{dy}{ds} \\ \frac{d^2y}{ds^2} = -k\frac{dx}{ds} \end{cases} \tag{4}$$

2.2. Numerical analysis

A system of 4 first order DEs ($U_1(s)$:$U_4(s)$), were defined to reduce the 2 second order DEs in Eq. (4) to their first order forms [11]. The defined functions are shown between Eq. (5)–(8).

$$U_1(s) = x(s) \tag{5}$$

$$U_2(s) = y(s) \tag{6}$$

$$U_3(s) = \frac{dU_1}{ds} = \frac{dx}{ds} \tag{7}$$

$$U_4(s) = \frac{dU_2}{ds} = \frac{dy}{ds} \tag{8}$$

The DEs generated by substituting the defined functions (Eq. (5):(8)) and Eq. (2) into Eq. (4) results in a system of first order DEs as shown in Eq. (9). The resulting system of DEs (see Eq. (10)) was solved numerically using MATLAB® ODE45 solver. The calculations were performed using initial values of $U_1(0) = 0$, $U_2(0) = Hg$, $U_3(0) = 1$, and $U_4(0) = 0$.

$$\begin{cases} \frac{dU_3}{ds} = \frac{d^2x}{ds^2} = k\frac{dy}{ds} = kU_4(s) = \frac{P_0 - U_2g\rho}{T}U_4(s) \\ \frac{dU_4}{ds} = \frac{d^2y}{ds^2} = -k\frac{dx}{ds} = -kU_3(s) = -\frac{P_0 - U_2g\rho}{T}U_3(s) \end{cases} \tag{9}$$

$$\begin{cases} \frac{dU_1}{ds} = U_3(s) \\ \frac{dU_2}{ds} = U_4(s) \\ \frac{dU_3}{ds} = \frac{P_0 - U_2g\rho}{T}U_4(s) \\ \frac{dU_4}{ds} = -\frac{P_0 - U_2g\rho}{T}U_3(s) \end{cases} \tag{10}$$

2.3. Stress and shape determination

The numerical results from equation 10 was used to analyse the relationship between the membrane stress (T), the static pressure (P_0), the gas height (Hg) and the shape of the collapsible tank. The stress (T), static pressure (P_0) and gas height (Hg) (see Eq. (10)) were used as control parameters to generate the corresponding collapsible tank shape (x,y). From this shape, other properties of the collapsible tank such as width, liquid depth, and cross sectional area were calculated. The width (W) of the collapsible tank was determined as shown in Eq. (11), when carrying out the circumferential stress analysis.

$$W = 2x(s) \text{ at the point where } \frac{dx}{ds} = 0 (s_1 \text{ in Fig. 2}) \tag{11}$$

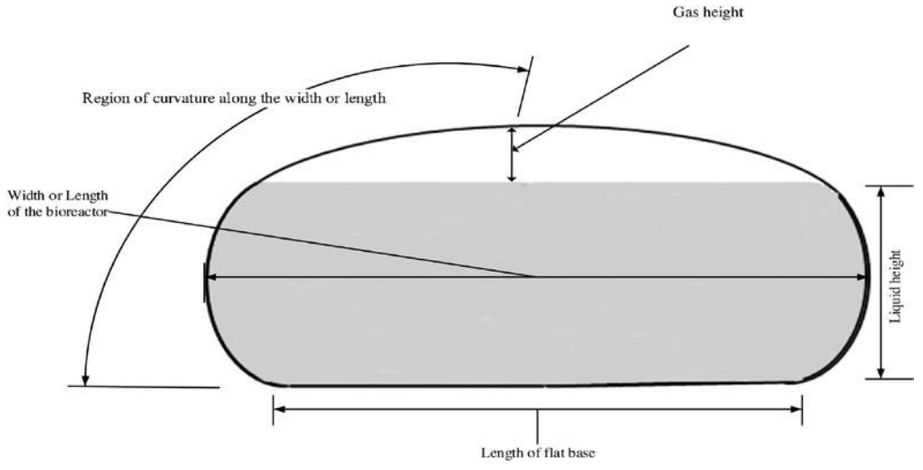

Fig. 1. The geometry of a collapsible tank.

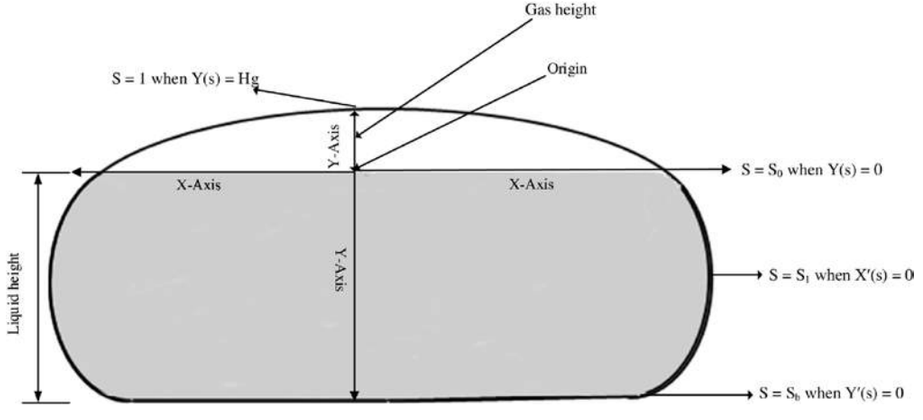

Fig. 2. The reference frame used to analyse the collapsible tank.

When the longitudinal stress analysis was carried out, the length of the collapsible tank (L) was determined as shown in Eq. (12).

$$L = 2x(s) \text{ at the point where} \frac{dx}{ds} = 0 \tag{12}$$

The liquid depth (h) for both circumferential and longitudinal stress analysis was calculated using Eq. (13).

$$h = -y(s) \text{ at the point where} \frac{dy}{ds} = 0 \ (s_b \text{in Fig. 2}) \tag{13}$$

The length of the flat base (L_{base}) of the collapsible tank for both circumferential and longitudinal stress analysis was determined using Eq. (14).

$$L_{base} = 2x(s) \text{ at the point where } \frac{dy}{ds} = 0 (s_b \text{in Fig. 2}) \tag{14}$$

The perimeter (p) of the collapsible tank was calculated by summing the arc length (s_b) from the top to the base (i.e. from Hg or s = 1 to s_b in Fig. 2) with the base length (L_{base}).

$$p = 2(Ls + L_{base}) \tag{15}$$

The volume per unit length or width of the collapsible tank was determined as the cross sectional area (A) inside the (x,y) curve calculated according to Eq. (16). The last form of Eq. (16) was what was used for the calculations in MATLAB (see Table 1)

$$A = 2\int_{-h}^{Hg} xdy = -2\int_{Hg}^{-h} xdy = -2\int_{1}^{sb} x(s)y'(s)ds \tag{16}$$

The volume of the tank occupied by liquid per unit length or width was determined as the liquid cross sectional area (A_L) from

Table 1
Result from numerical analysis in the width direction of collapsible tanks from 100 to 1000 m³ and a 30 L bioreactor.

Specified parameters				Final iterative values			Calculated values		
Volume of bioreactor (m^3)	Specified length (m)	Working capacity	Width of bioreactor (m)	Tension per unit length (N/m)	Gas height (m)	Static pressure (N/m^2)	Liquid height in the bioreactor (m)	Perimeter of bioreactor (m)	Bioreactor's flat base length (m)
100	20	0.84	7	1000	0.22	58	0.63	14.57	6.63
200	23	0.80	9	1500	0.44	85	0.77	18.94	8.65
300	35	0.80	9	1500	0.44	85	0.77	18.94	8.65
400	33	0.84	11	2200	0.33	72	0.94	23.44	10.75
500	30	0.80	14	2600	0.44	73	1.02	28.21	13.04
1000	50	0.83	15	3500	0.45	92	1.18	30.20	13.87
0.03	1.1	0.82	0.40	6	0.02	10	0.05	0.84	0.37

where the liquid region began (y(s) = 0 i.e. where s = s_0 in Fig. 2) to the base of the collapsible tank (y(s) = − h or s = s_b).

$$A_L = 2\int_{-h}^{0} x\,dy = -2\int_{s0}^{Sb} x(s)y'(s)\,ds \quad (17)$$

The working capacity of the collapsible tank (WC) was defined as the ratio of liquid cross-sectional area to the total cross-sectional area as shown in Eq. (18).

$$WC = A_L/A \quad (18)$$

Eq. (11), (12),(14)–(17) were multiplied by 2 because the solutions were calculated for the right half of the laterally symmetric cross section (Fig. 2).

The numerical analysis was performed using MATLAB ODE45 solver. Details about how the solver works is not presented here but can be found from literature [12] . The steps taken to perform the analysis from Eq. (7) –(18) in MATLAB are shown in Fig. 3.

2.4. Iterative calculation of the stress, static pressure and gas height from specified collapsible tank

For a given cross-sectional area of a collapsible tank (i.e. its volume per unit length or width) and its working capacity, an iterative process was used to find the corresponding tension per unit length or width (T), the gas height (Hg) and the static pressure (P_0). T, Hg, and P_0 were used as input variables in the iterative process. After determining the solution to the DEs in Eq. (7)–(10), a plot of the solution (x,y) was drawn to ensure the collapsible tank shape was as expected, before the other values (from Eq. (11)–(18)) were calculated. Fig. 3 shows how the analysis was performed with MATLAB. When the cross-sectional area used for the analysis is the volume of the collapsible tank per its length, the analysis is termed circumferential, while when the cross-sectional area is the volume per unit width of the collapsible tank the analysis it is termed longitudinal. Dimensions of collapsible tanks used by FOV Fabrics AB (Borås, Sweden) for making flexible and easily deformable bioreactors were used for the calculations.

For the circumferential membrane stress analysis; the length was assumed constant and the target volume per unit length was calculated. T, Hg and P_0 values were defined for target values of A, A_L and W. The steps shown in Fig. 3 as discussed above were placed inside a least square iterative solver of MATLAB (lsqcurvefit), which continued to change the values of T, Hg and P_0 until the volume per unit length, the working capacity and width generated were same as the target values. The value of T in the final iterative calculation was the circumferential membrane tension per unit length. The collapsible tank width under these conditions was calculated from Eq. (11) and used for the longitudinal analysis.

For the longitudinal membrane stress analysis; the width was constant and the volume per unit width was calculated. The liquid height (gotten from Eq. (13)) and Hg were additional constrains to the ones used for the circumferential analysis. Iterative steps described for the circumferential stress analysis were performed to give the mean longitudinal tension per unit width.

2.5. Calculating the stress in a collapsible tank with known parameters

When the liquid height, gas height and static pressure in a collapsible tank are known, the tension per unit length acting on the collapsible tank can be calculated by integrating the first part of Eq. (9). This part of Equation can be rewritten as;

$$\frac{d^2x}{ds^2} = f[y(s)]\frac{dy}{ds} \quad \text{Where } f[y(s)] = \frac{P_0 - U_2 g\rho}{T} = \frac{P_0 - y(s)g\rho}{T} \quad (19)$$

Multiplying Eq. (19) by ds and integrating gives Eq. (20)

$$\int_{sb}^{s=1} \frac{d^2x}{ds^2}ds = \int_{sb}^{s=1} F[y(s)]\,ds = \int_{-h}^{Hg} f[y(s)]\,dy \quad (20)$$

The left hand side (LHS) of equation 20 gives −2 (as X′(s) = 1 @ s = 1 and −1 @ s = s_b see Fig. 2). The integral of the right hand side is shown in Eq. (21)

$$F[y(sb)] - F[y(s=1)] = \frac{-2P_0h - (-h)^2 g\rho}{2T} - \frac{P_0Hg}{T} \quad (21)$$

Combining Eq. (21) with the LHS of Eq. (20) and making T subject of the formula gives Eq. (22).

$$T = 0.5P_0(h + Hg) + 0.25\rho gh^2 \quad (22)$$

2.6. Comparison of the stress determined by curvature analysis with experimentally measured values from a laboratory scale collapsible tank

The calculated stress value in a 30 L collapsible tank (which is used as a bioreactor) with 1.1 m length was used to compare with the result from numerical curvature analysis. The bioreactor was filled with 25 L of water and sparged with air. The curvature was measured halfway between the top of the bioreactor and the top of the liquid in the bioreactor (i.e. where the curvature is constant) using a flexible retractable measuring tape to measure the change in arc length and a folding ruler used to measure the change in inclined height (which gave the directional change in the angle of the tangent to the curve). The curvature was calculated by dividing the directional change in the angle of the tangent to the curve at the specified point by the corresponding change in the arc length (see Eq. (1)). The static pressure and total pressure were measured using a laboratory made u-tube manometer. The static pressure was the pressure measured on top of the liquid in the bioreactor, while the total pressure was measured at the base of the bioreactor. The gas and liquid height in the bioreactor, and the bioreactor's width and length were measured using a retractable measuring tape. The


```
% rho, and g were specified

rho = 1000; g = 9.81;

% values for T, Hg, P0 were specified

T = 1000; Hg = 0.2; P0 = 100;

% a nameless function holder f, was created to simplify equation 10 and 11

f = @(s,y) [y(3); y(4); (P0/T-rho*g/T*y(2)*(y(2)<0))*y(4); - (P0/T-
rho*g/T*y(2)*(y(2)<0)) * y(3)];

[s y] = ode45(f,[0:0.0001:25],[0,Hg,1,0]);

plot(y(:,1),y(:,2))

% the point at which the curve touches the base

sb = find(y(:,4)>0,1)

% the arc length to the point at which the curve touches the base

s1 = s(sb)

% half the length of the flat base

xb = y(sb,1)

perimeter = 2*(s1+xb)

baselength = 2*xb

% the point on the curve with the maximum width or length

sw = find(y(:,3)<0,1);

Width or length = 2* y(sw,1)

liquidheight = -y(sb,2)

% the point on the curve where the liquid region begins

s0 = find(y(:,2)<0,1);

% Liquid volume per unit length

AL = -2*sum(y(s0:sb,1).*y(s0:sb,4))*0.0001

% The volume per unit length

A = -2*sum(y(1:sb,1).*y(1:sb,4))*0.0001

Working capacity = liqVol/TotVol
```

Fig. 3. Numerical analysis with Matlab.

average of the curvature values calculated was used for determining the stress in the bioreactor from Eq. (2). The stress calculated from the previously mentioned experimentally measured parameters in the 30 L bioreactor was compared with the value gotten from the numerical curvature analysis.

3. Results and discussion

Collapsible tanks find application in different industries and processes. In the biotechnology industry, they are used for making bioreactors used for biogas production [2], bioethanol production [13], biological production using plant cells [3] etc. especially at small and medium scale. These bioreactors offer flexibility, low cost, easy installation and customized applicability to bio-based production [13]. If these and other benefits derived from using these types of bioreactors can be translated from small and medium scale to the large scale production of bio-products like biofuels, it could assist in increasing the economic competitiveness of the biofuels against fossil based fuels. However, in order to apply these bioreactors or any type of collapsible tank for large scale purposes they need to be able to handle the stresses exacted on them while in operations [14] and during cleaning if needed [15]. The membrane stresses of collapsible tanks meant to be used as bioreactors and that of a 1000 m^3 water storage vessel were investigated using curvature and numerical analysis and the results are presented in this section.

3.1. Shape and stress determination in collapsible tanks designed as bioreactors

Collapsible tanks of volumes between 100–1000 m^3 designed as bioreactors for large scale applications were used for stress calculations using numerical analysis.

3.1.1. Circumferential analysis

The results of the analysis performed in the width direction of collapsible tanks from 100 to 1000 m^3 are shown in Table 1. The tension per unit length values in the width direction for the collapsible tanks considered were between 1000 N/m and 3500 N/m. It can be observed from Table 1 (see the 200 and 300 m^3 collapsible tanks) that collapsible tanks having the same liquid height, static pressure and gas height would have the same tension irrespective of the volume of the collapsible tank or its length, which agrees with Eq. (22). However, the volume, width and length of a collapsible tank or bioreactor are important parameters for its design, cost, and plant layout planning. Because of this and the possibility of controlling the liquid height, static pressure and gas height in the collapsible tank by the volume and dimension of the collapsible tank, a relation between the width, liquid height, volume and working capacity of the bioreactor was calculated from the plot of the results in Table 1. The relation is shown in Eq. (23). It can be seen from the relation that there is a linear relationship between the product of the volume per unit length (A) and the working capacity (WC) of the collapsible tank (i.e. the liquid cross-sectional area in the collapsible tank) and the product of the width (W) and liquid height (h) in the collapsible tank.

$$WC.A = 0.968W.h - 0.0755 \quad (23)$$

From Eq. (23), the liquid height can be calculated from collapsible tanks with specified volume, length, width and working capacity. The calculated liquid height can then be used to determine the tension per unit length acting in the bioreactor using Eq. (22) when P_0 and Hg are known.

3.1.2. Longitudinal analysis

The mean tension per unit width in the length direction of collapsible tanks considered was between 1050–4000 N/m. The results from this analysis plotted against those from the circumferential analysis are shown in Fig. 4. There was a linear relationship between the circumferential tension per unit length and the mean longitudinal tension per unit width (Fig. 4). The relation between both stresses is shown in Eq. (24). For the collapsible volumes and dimensions considered, the mean longitudinal tension was higher than the circumferential tension. This is because collapsible tanks tend to have more curvature along their width than along their length, and from Eq. (2) there is an inverse relationship between tension and curvature.

$$T_{Longitudinal} = 1.16 \times T_{Circumferential} - 177.21 \quad (24)$$

3.2. Comparing relation equation values with values from numerical analysis

The liquid height relation in Eq. (23) was generated using initially specified length, width, and working capacity values for a specific collapsible tank volume. This relation was examined to determine how well it could estimate the liquid height in different collapsible tanks. For a specified collapsible tank volume, dimensions different from the ones used for generating it were put in it and the liquid height values calculated with it were compared with the values gotten from curvature analysis. Additionally, tension per unit length values was calculated both from Eq. (22) (by using liquid height values from Eq. (23)) and from curvature analysis. The generated liquid height and tension per unit length values from the relations and from curvature analysis for different collapsible tank volumes are shown in Table 2. A maximum difference of 3% (i.e. overestimation or underestimation) in the value of the liquid height calculated from the curvature analysis and from the height relation can be seen (Table 2). In addition, the maximum difference in tension for all cases examined is approximately 6%. This small difference both for the liquid height and tension shows that the height relation estimates very well what the height of liquid would be in a collapsible tank from the dimensions of the collapsible tank.

3.3. Comparing experimentally measured values with that from numerical curvature analysis

The stress in a 30 L laboratory scale collapsible tank (that is used as a bioreactor) was calculated from experimentally measured values using its curvature. The average curvature of the bioreactor from its measured directional change in tangent and the change in arc length was 1.78 m^{-1}, while the static pressure in the bioreactor was 10 Pa. Using Eq. (2) , the tension per unit length of the bioreactor was calculated to be 5.62 N/m. Performing the numerical analysis for a theoretical 30 L bioreactor as previously described gave the tension per unit length of the bioreactor to be 6 N/m (see Table 1). The liquid height measured from the experimental bioreactor was 5 cm, while that from the numerical curvature analysis was 4.81 cm. The width of the experimental bioreactor was measured to be 36 cm, the corresponding value from the numerical curvature analysis was 39.6 cm. The liquid volume fraction or working capacity in the laboratory bioreactor was 0.833, while numerical analysis gave it as 0.815. Comparing these values shows how well the result from the curvature analysis agrees with the experimentally measured values. From this, it can be expected that numerical curvature analysis can be used to determine the shape and stress in collapsible tanks or bioreactors.

3.4. Operating the collapsible tank under different conditions

The collapsible tank or bioreactor can be operated under different conditions. When the collapsible tank is operated at static pressures between 10 and 100 Pa, width to liquid height ratio between 13 and 20, and working capacity between 0.6–1, it can be said to be in a relaxed condition (i.e. normal operating conditions specified by its manufacturer). When operated at static pressure between 1100 and 5000 Pa and with a width to liquid height ratio between 1 and 5, it can be said to be pressurized. When operated at working capacity less than or equal 0.5, static pressure between 15 and 50 Pa and width to liquid height ratio greater than 20, it can be said to be deflated. How these changes can affect the tension and total pressure in the collapsible tank is shown in Table 2 and Fig. 5. The total pressure (used in Fig. 5) was calculated by summing the static pressure with pressure due to liquid height in the same collapsible tank. The results show that the tension per unit length profile (from numerical curvature analysis) and the total pressure profile are similar for the same operating condition in the collapsible tank. This is because the pressure and the liquid height in the collapsible tank are the sources of the tension (Eq. (22)).

Considering the 100 m^3 collapsible tank, changing the operating conditions from relaxed to pressurized resulted in 430% increase in tension, while the change from relaxed to deflated resulted in 60% decrease in tension. Considering the 400 m^3 collapsible tank, changing from relaxed to pressurized conditions resulted in 430% increase in tension, while changing from relaxed to deflated conditions reduced the tension by 60%. For the 1000 m^3 collapsible tank, changing from relaxed to pressurized conditions resulted in 530% increase in tension, while changing from relaxed to deflated conditions resulted in 64% reduction in tension. Using these values, if a bioreactor or collapsible tank would be operated or sterilized at a static pressure up to 5000 Pa, the ultimate tensile strength of its material of construction must be at least 6 times the calculated tension values under normal conditions plus a security margin. If this cannot be attained, the bioreactor or collapsible tank should not be operated or sterilized under these conditions.

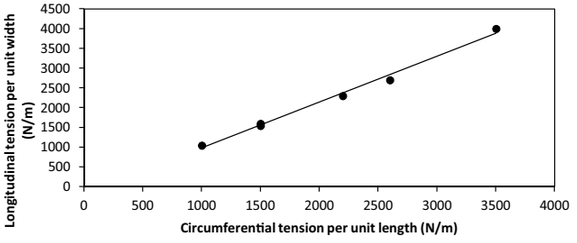

Fig. 4. Longitudinal tension against circumferential tension at a particular collapsible tank volume for volumes between 100–1000 m^3.

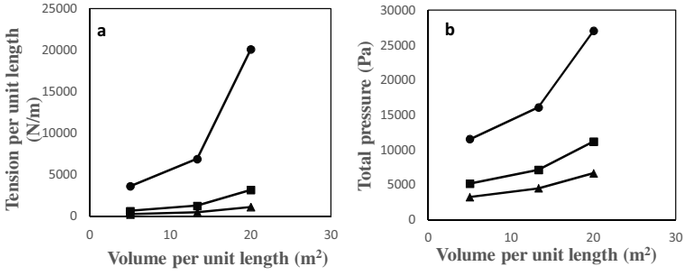

Fig. 5. A plot of Tension per unit length from numerical curvature analysis (a) and total pressure (b) against the volume per unit length of collapsible tanks when operated at deflated (▲), relaxed (■) and pressurized (●) conditions.

Table 2
Comparison results gotten from the generated relation and from numerical analysis for different bioreactor volumes.

Volume of bioreactor (m^3)	Specified length (m)	Working capacity	Specified width (m)	Liquid height from relation (m)	Liquid height from analysis (m)	Tension per unit length from relation (N/m)	Tension per unit length from numerical analysis (N/m)	Change in liquid height (%)	Change in tension per unit length (%)
100	20	0.80	8	0.526	0.523	689.97	680.97	−0.67	1.32
100	10	0.80	8	1.043	1.044	2862.33	2867.54	0.10	0.18
100	20	0.50	8	0.333	0.329	279.60	273.43	−1.15	2.26
100	20	0.80	4	1.053	1.040	3713.23	3642.92	−1.17	1.93
400	30	0.80	15	0.740	0.726	1351.91	1301.39	−1.93	3.88
400	15	0.80	15	1.474	1.479	5545.10	5580.81	0.33	−0.64
400	30	0.50	15	0.464	0.455	537.84	517.39	−1.98	3.95
400	30	0.80	7.5	1.480	1.526	6557.12	6920.36	3.01	−5.25
1000	50	0.82	15	1.142	1.132	3255.33	3201.64	−0.84	1.68
1000	50	0.50	15	0.694	0.673	1221.87	1150.63	−3.14	6.19
1000	25	0.83	15	2.278	2.205	13731.72	12905.74	−3.31	6.40
1000	50	0.82	7.5	2.269	2.324	19369.92	20098.94	2.35	−3.63
1000	50	0.82	30	0.567	0.584	790.14	836.92	2.84	−5.59

3.5. Selection of material for construction of collapsible tanks

The tensile strength of general purpose plastics ranges between 1 and 50 MPa. The tensile strength of plastics can be increased up to 280 MPa when they are combined with some other materials like silicone in the form of composites [16]. Turning conventional plastics into composites increases their strength but also increases their cost. One of the driving forces behind the use of collapsible tanks is their cheap cost in comparison to rigid vessels. To be able to maintain this edge, a good trade-off would be needed so that one can combine less expensive materials with plastics to increase their tensile strength, and ensure the strength of the collapsible tank is optimized to prevent failure. Apart from using composites, other materials can also be used for making collapsible tanks as long as they have properties that meet the tank end use requirement. If the area the collapsible tank is going to occupy is known, the tension that would be acting in the bioreactor can be estimated using Eq. (22) and (23), with the known tension, the type of material that satisfies both the cost and tension criteria can be selected for designing the collapsible tank.

Considering a 1000 m^3 collapsible tank that would be used for water storage, if because of area constraint the tank should have a length of 40 m, width of 20 m and working capacity of 0.9, then the liquid height in the tank would be 1.2 m (Eq. (23)) while the circumferential tension per unit length would be 3360 N/m (Eq. (22)) and the mean longitudinal stress would be 3720 (Eq. (24)). If the tank would be made of plasticized polyvinylchloride (PVC) as the base

polymeric material then a pressure allowance of factor of 1.5 [14] needs to factored into the calculated stress to prevent failure. If this factor is included and the thickness of the tank is 0.75 mm then the required tensile stress would be 14.2 MPa. However, the ultimate tensile strength of plasticized PVC is between 7 and 25 MPa [16] . If the PVC is plasticized with a material of low cost (e.g. textile) [17] which can increase the tensile strength of the composite higher than 14.2 MPa then failure can be prevented while also reducing cost.

4. Conclusion

Curvature analyses performed on collapsible tanks used as bioreactors of volumes between 100 m^3 to 1000 m^3 gave their shape, and the tension in these tanks was found to be between 300 N/m to 20000 N/m. For the bioreactor volumes considered a relation which could give the liquid height in the bioreactor from the properties of the bioreactor was found. The liquid height calculated by the relation had a maximum deviation of 3% from that calculated from curvature analysis. The tension in a collapsible tank can be minimized by minimizing the static pressure and liquid height in the tank taking the area it would occupy into consideration.

Acknowledgement

The authors would like to appreciate FOV Fabrics AB (Borås, Sweden) for providing the bioreactor used for the experimental part of this work.

References

[1] O.A. Osadolor, P.R. Lennartsson, M.J. Taherzadeh, Introducing textiles as material of construction of ethanol bioreactors, Energies 7 (2014) 7555–7567.
[2] K. Rajendran, S. Aslanzadeh, M.J. Taherzadeh, Household biogas digesters—a review, Energies 5 (2012) 2911–2942.
[3] B. Terrier, D. Courtois, N. Hénault, A. Cuvier, M. Bastin, A. Aknin, J. Dubreuil, V. Pétiard, Two new disposable bioreactors for plant cell culture: the wave and undertow bioreactor and the slug bubble bioreactor, Biotechnol. Bioeng. 96 (2007) 914–923.
[4] V. Vullo, Circular Cylinders and Pressure Vessels: Stress Analysis and Design, Springer, Cham, 2014.
[5] D.R. Moss, M.M. Basic, Pressure Vessel Design Manual, Butterworth-Heinemann, 2012.
[6] C. Kaminski, Stress Anal. Pressure Vessels (2005).
[7] M.F. Ashby, D.R.H. Jones, Engineering Materials 1: An Introduction to Properties, Applications and Design, Elsevier, 2011.
[8] J.J. Koenderink, A.J. van Doorn, Surface shape and curvature scales, Image Vision Comput. 10 (1992) 557–564.
[9] H. Liu, L.J. Latecki, W. Liu, A unified curvature definition for regular, polygonal, and digital planar curves, Int. J. Comput. Vision 80 (2008) 104–124.
[10] T.J. Willmore, An Introduction to Differential Geometry, Courier Corporation, 2012.
[11] J. Stoer, R. Bulirsch, Introduction to Numerical Analysis, Springer New York, New York, NY, 2002 (SpringerLink).
[12] L.F. Shampine, M.W. Reichelt, The matlab ode suite, SIAM J. Sci. Comput. 18 (1997) 1–22.
[13] O. Osadolor, P. Lennartsson, M. Taherzadeh, Development of novel textile bioreactor for anaerobic utilization of flocculating yeast for ethanol production, Fermentation 1 (2015) 98.
[14] Y. Olisti, Build better industrial bioreactors, Chem. Eng. Prog. (1992) 55.
[15] Y. Chisti, M. Moo-Young, Fermentation technology bioprocessing, scale-up and manufacture, in: Biotechnology-The Science and the Business, CRC Press, 1999, pp. 177.
[16] K.G. Budinski, M.K. Budinski, Engineering Materials: Properties and Selection, Prentice HallUpper Saddle River, NJ, 1999.
[17] A.K. Bledzki, J. Gassan, Composites reinforced with cellulose based fibres, Prog. Polym. Sci. 24 (1999) 221–274.

PAPER IV

Empirical and experimental determination of the kinetics of pellet growth in filamentous fungi: A case study using *Neurospora intermedia*. *Biochemical Engineering Journal*
Doi.org/10.1016/j.bej.2017.05.012

Biochemical Engineering Journal 124 (2017) 115–121

Contents lists available at ScienceDirect

Biochemical Engineering Journal

journal homepage: www.elsevier.com/locate/bej

Regular article

Empirical and experimental determination of the kinetics of pellet growth in filamentous fungi: A case study using *Neurospora intermedia*

Osagie A. Osadolor*, Ramkumar B. Nair, Patrik R. Lennartsson, Mohammad J. Taherzadeh

Swedish Centre for Resource Recovery, University of Borås, SE50190 Borås, Sweden

ARTICLE INFO

Article history:
Received 24 January 2017
Received in revised form 9 May 2017
Accepted 14 May 2017
Available online 16 May 2017

Keywords:
Neurospora intermedia
Fungi pellets
Kinetic parameters
Growth inhibition
Fermentation

ABSTRACT

Pellet morphology formation by filamentous fungi has gained a lot of attention because of its multiple benefits such as the ease of separation and smaller bioreactor volume requirement. Most reported kinetics studies on fungal pellet growth are centred on aeration, despite the experimental results pointing to the importance of other factors such as pH, substrates and product concentration etc., influencing the pellet formation. Hence a kinetic study on the effect of multiple factors such as aeration, substrate and product concentration and pH was done in this paper using *Neurospora intermedia* as a model organism, whose ability to form mycelial pellets was recently reported. The maximum growth rate of the pellets under uninhibited conditions at its optimal growth pH was 0.318 h^{-1}. The pellets were found to be inhibited by high product (ethanol) concentration with no growth occurring at 70 g L^{-1} and above. High substrate concentration favoured the formation of loose fur-like fluffy pellets. The specific oxygen uptake rate of the pellets was between 0.27–0.9 mmol-O_2 g-biomass$^{-1}h^{-1}$ depending on the pellet average diameter. The results from this kinetic study can be used for bioreactor design, operations and optimization of fermentation processes utilizing *N. intermedia*.

1. Introduction

Filamentous fungi are versatile group of microorganisms that are conventionally used in the industry for a wide array of commercial value-added products ranging from bulk chemicals to medicines. The manipulation of filamentous fungal growth is a critical aspect in the industrial fermentation process; difficult than that of the other microbial species because of their different morphologies and the presence of tangled mycelia under different cultivation condition [1]. The phenomenon of pellet formation is a one of the most studied area in the filamentous fungal research because of the advantages of pellets over filamentous forms such as the ease of separation and less bioreactor volume requirement, particularly the fungal species with industrial applications [2–4]. Several factors such as pH, oxygen level, temperature, medium composition, nutrients, ions etc. have been associated with the change from filamentous to pellet morphology and vice versa [1].

The growth kinetics of some pellet forming filamentous fungi have been investigated in literature with different kinetic models such as logistic growth law [5], exponential law [6], cube root law [7,8], Gompertz's model [9] and Monod kinetics [10–12]. In a research study, Van Suijdam, Hols and Kossen [12] compared some of the previously mentioned models and used the Monod's equation in describing the growth of mycelium pellet because of the ease of introducing substrate and oxygen mass transfer limitations into it. As aeration is essential for the growth of fungi pellets, most kinetics study of fungi pellet are centred on oxygen mass transfer limitation investigation [10–12]. However, experimental investigation of pellet formation from filamentous fungi have found that certain fungi form pellets only within a pH range with aeration only important for biomass growth [13–15]. Additionally, certain substrates (such as potato dextrose or soybean peptone) or products (such as ethanol) influence the growth or formation of pellets by filamentous fungi [16–18]. Thus, there is need to include the influence of these other parameters when investigating the kinetics of pellet formation by the filamentous fungi.

Neurospora intermedia, used as a model organism in the present study, show much morphological and genetic similitude with *Neurospora crassa*, a model organism for genetic and molecular research studies for decades. *N. intermedia* has been traditionally used for the preparation of an indigenous Indonesian food, *oncom* [19] and they are categorized as 'generally regarded as safe' (GRAS). During the 1980's and 90's genetics and molecular level studies with both

* Corresponding author.
E-mail addresses: alex.osagie@hb.se (O.A. Osadolor), ramkumar.nair@hb.se (R.B. Nair), patrik.lennartsson@hb.se (P.R. Lennartsson), mohammad.taherzadeh@hb.se (M.J. Taherzadeh).

http://dx.doi.org/10.1016/j.bej.2017.05.012
1369-703X/

the *N. crassa* and *N. intermedia* strains have also been carried out extensively [20–22]. Considering the edible nature of the fungus, our research group has recently established an *'integrated biorefinery'* concept using this fungus for valorising various industrial waste streams such as the stillage from starch-to-ethanol process, lignocellulosic waste such as the straw or bran, sugar-to-ethanol process waste-vinasse, etc., by producing ethanol and protein rich fungal biomass for feed applications [23–25].

Kinetic study of *N. intermedia* either in pellet or filamentous forms has not been reported in literature and research based on an industrial scale application of this fungus is also scarce. Using experimental data and empirical relationships, a kinetic study of the effect of aeration, pH, substrate and product concentration for pellet formation, growth, and inhibition was performed in this paper using *N. intermedia* as the model organism, whose ability to form pellets was recently observed [13]. The present study is hence the first of its kind to describe the kinetics of fungi pellet growth and inhibition considering a range of factors for the pellet formation in filamentous fungi with *N. intermedia* as the model organism The findings from this kinetic study are important for efficient reactor design and operations using filamentous fungi in submerged fermentation industrial processes such for ethanol production or protein rich biomass feed production.

2. Methods

2.1. Fungal strain

An edible ascomycete fungus, *Neurospora intermedia* CBS 131.92 (*Centraalbureau voor Schimmelcultures*, Netherlands) was used in this kinetic study as a model organism. The fungal culture was maintained on potato dextrose agar (PDA) slants containing (in g/L): potato extract 4, D-glucose 20, agar 15 and the slants were renewed every six months. For the regular experimental purpose, the fungus was transferred to fresh PDA plates containing (in g/L): potato extract 4, D-glucose 20 and agar 15. The fungal plates were then incubated aerobically for 3–5 days at 30 °C. For preparing spore suspension, plates with fully grown fungal mycelia were flooded with 20 mL sterile distilled water and the spores were released by gently agitating the mycelia with a disposable spreader. Generally, an inoculum of 20 mL spore suspension per L medium with a spore concentration of 5.8–6.3 × 10^5 spores/mL was used for the cultivations.

2.2. Standard fungal cultivation – shake flask

The fungal cultures were carried out aerobically in a liquid semi-synthetic potato dextrose medium (containing 20 g/L glucose and 4 g/L potato extract), unless otherwise specified. Cultivations were made in 100 mL volume (in 250 mL Erlenmeyer flasks), for 96–120 h in an orbital shaking water bath (Grant OLS-Aqua pro, UK) at 35 °C and 150 rpm (with an orbital shaking radius of 9 mm and a flask diameter of 85 mm), with samples taken every 24 h, unless otherwise specified. The pH was adjusted with either 2 M HCl or 2 M NaOH. For kinetics experiments, fungal cultivations were made on semi-synthetic media with pH (range: 3–10); substrate concentration (range: 10–200 g/L); and product concentration (10–100 g/L).

2.3. Standard fungal cultivation – airlift bioreactor

Fungal cultivations were carried out in a 4.5-L bench scale airlift bioreactor (Belach Bioteknik, Sweden), with a working volume of 3.5 L. An internal loop with cylindrical geometry with a diameter 58 mm, height 400 mm and thickness 3.2 mm was used to achieve the airlift-liquid circulation. The bioreactor and the draft tube were made of transparent borosilicate glass. Aeration at the rate 0.71 vvm ($volume_{air}/volume_{media}$/min) was maintained (unless otherwise specified) throughout the cultivation, using a sintered stainless steel air-sparger with a pore size of 90 μm. Filtration of the inlet air was achieved by passing it through a polytetrafluoroethylene (PTFE) membrane filter (0.1 μm pore size, Whatman, Florham Park, NJ, USA).

2.4. Analysis

Initial spore concentration was measured using a Bürker counting chamber (with a depth of 0.1 mm) under a light microscope (Carl Zeiss Axiostar plus, Germany). Fungal biomass concentration (dry weight) was determined at the end of the cultivation by washing the pellet or mycelial biomass with deionized water followed by drying at 105 °C for 24 h before weighing. A digital Vernier caliper (Limit, Sweden) with the resolution of 0.01 mm was used to measure the pellet diameter. The viscosities of the samples were determined using a Brookfield digital viscometer-model DV-E (Chemical Instruments AB, Sweden). High Performance Liquid Chromatography (HPLC) system (Waters 2695, Waters Corporation, USA) was used to analyse all liquid fractions from the fungal cultivations. A hydrogen-based ion-exchange column (Aminex HPX-87H, Bio-Rad Hercules, CA, U.S.A.) at 60 °C with a Micro-Guard cation-H guard column (Bio-Rad) and 0.6 mL/min 5 mM H_2SO_4 (eluent), was used for the analyses of glucose, ethanol, glycerol and total sugars. All experiments and analyses were carried out in duplicate and results are reported with error bars and intervals representing two standard deviations.

3. Kinetics

Microbial growth, substrate consumption and product formation rate can be investigated using basic unstructured model. Under non-limiting conditions, fungal pellet growth can be described using the Eq. (1):

$$\frac{dX}{dt} = \mu X \tag{1}$$

where, X is the dry weight of cells (gL^{-1}), t is time (h) and μ is the specific growth rate (h^{-1}). The specific growth rate can be defined in terms of the Monod kinetic model as:

$$\mu = \mu_{max}\frac{S}{S + K_s} \tag{2}$$

where μ_{max} is the maximum specific growth rate (h^{-1}), S is the substrate concentration (gL^{-1}) and K_S is the saturation constant (gL^{-1}).

The kinetic study performed in this article was carried out using the assumptions that the fungal pellets follow the Monod growth kinetics; at low pellet and substrate concentrations the media properties are same as that of water, as the measured viscosity of the PDB media was 1.01 ± 0.09 cP at 25 °C; oxygen transfer into the pellets occur only through molecular diffusion and at the threshold of dissolved oxygen accumulation limitation the oxygen transfer rate into the media is equal to the oxygen uptake rate by the mycelial pellets. The kinetic parameters in the proposed kinetic models were determined using experimental data obtained from a series of batch shake flask experiments, by minimizing the squared sum of errors between the experimental data and the model predictions. Estimation of the parameters in the kinetics equation and curve fittings were done using "Cftool" in MATLAB® R2013b.

3.1. The effect of aeration

Under non-limiting concentration, the fungal pellet growth rate can be described by combining Eqs. (1) and (2):

$$\frac{dX}{dt} = \mu X = \mu_{max}\frac{S}{S + K_s}X \tag{3}$$

As *Neurospora intermedia* is strictly aerobic fungus, dissolved oxygen needs to be available for pellet growth to occur. The dissolved oxygen concentration accumulation rate (DO) in a media can be defined using Eq. (4) as

$$DO = OTR - OUR \tag{4}$$

where OTR is the oxygen transfer rate (mg-O_2 or mmol-O_2 L^{-1} h^{-1}) into the media and OUR is the oxygen uptake rate (mg-O_2 or mmol-O_2 g-L^{-1} h^{-1}) by the microorganisms. The OUR is defined as the product of the specific oxygen uptake rate of the microorganism being employed (q_o), in this case *N. intermedia*, and the biomass concentration (X).

Using the assumption that oxygen transfer into the pellets occurs through molecular diffusion, the mass transfer limitation in the gas phase can be neglected, thus the driving force of the OTR would be the oxygen concentration gradient between that at the bulk liquid and that at the interface [26]. This assumption agrees with the Reynold's number ($Re = \rho N D^2/\mu$) that was from 120 to 210, calculated using the D as the orbital shaking diameter (9 mm), ρ as fluid density (1000 kg/m^3), μ as the viscosity of the PDB media (1.01 cP) which was in the laminar range for the different shake flask frequency N. At low biomass concentrations, OUR can be neglected from Eq. (4), so the maximum OTR (OTR_{max}) can be estimated using oxidation rate of a chemical such as sodium sulphite [26–28]. The OTR_{max} can be estimated using a modified version of the OTR empirical relationship developed by Auro, Hodge and Roth [29] when the shake flask frequency difference is accounted for [27,30].

$$OTR_{max} = 8.46(f/f_o)^{0.88}\ [bi(10^{miVF})\ (10^{-bsV_L V_F^{ms}})] \tag{5}$$

where f is the shake flask frequency (rpm), f_o is the reference shake flask frequency (96 rpm), bi = 1.468, mi = 7.9 × 10^{-5}, V_F is the volume of the flask (mL), ms = − 0.94, V_L is the liquid volume in the flask (mL) and bs = 1.657.

The specific oxygen uptake rate (q_o) has been shown to have a zero order relationship with dissolved oxygen for the fungi pellets and other microbial growth as long as the minimum DO threshold needed for growth has been reached [10,12,27]. Thus, at the DO threshold, q_0 can be estimated from Eq. (6):

$$q_o = (OTR - DO)/X \tag{6}$$

In a well-mixed bioreactor operating at steady state, DO in Eq. (4) becomes zero [30,31]. Using similar analogy and with the OTR in a shake flask fixed, as the biomass concentration increases up to the verge of aeration limitation, the DO approaches zero [32], so OUR can be approximated to equal OTR, thus q_0 on the verge of aeration limitation can be estimated as:

$$q_o = OTR/X_t \tag{7}$$

where X_t is the biomass concentration (g/L) on the verge of aeration mass transfer limitation in the shake flask.

3.2. The effect of product and substrate concentration

When high substrate concentration influences the observed kinetics, its influence can be included into the Monod model, this is shown in eq. (8) [33]:

$$\frac{dX}{dt} = \mu X = \mu_m\frac{S}{S + K_s}\left(1 - \frac{S}{S*}\right)^n X \tag{8}$$

where S* is the substrate concentration (g/L) that no growth occurs and n is the degree of the inhibition. The effect of product inhibition on the kinetics can be expressed using Eq. (9) [34], with μ'_m as the observed maximum growth rate, P_i the concentration of a particular product (g/L), P_i* is the concentration at which no growth occurs and a_i is the degree of product inhibition.

$$\frac{dX}{dt} = \mu X = \mu'_m\frac{S}{S + Ks_s}\left[\prod\left(1 - \frac{P_i}{P_i**}\right)^{a_i}\right]X \tag{9}$$

When both substrate and product inhibition occurs, Eqs. (8) and (9) can be combined to describe the overall growth rate

$$\frac{dX}{dt} = \mu X = \mu'_m\frac{S}{S + K_s}\left(1 - \frac{S}{S*}\right)^n\left[\prod\left(1 - \frac{P_i}{P_i*}\right)^{a_i}\right]X \tag{10}$$

In addition to the kinetic Eqs. (3), (8)–(10), the Luedeking-Piret model (Eq. (11)) is commonly used to describe the production of metabolites such as ethanol in terms of growth (dx/dt) and non-growth association [7,35]:

$$\frac{dP_i}{dt} = \alpha_i\frac{dX}{dt} + \beta_i X \tag{11}$$

where α_i is the growth associated parameter (dimensionless) and β_i is the non-growth associated parameter (h^{-1}).

3.3. The effect of pH

Within the non-lethal pH region, the pH of a medium influences the maximum growth rate and the inhibitory potential of growth inhibiting organic compounds present in the medium [36,37]. When the pH affects only the maximum growth rate, its effect can be accounted for using Eq. (12) [36]. When there is a strong interaction between pH and the un-dissociated form of the organic compounds present in the media, the pH and inhibitor effect follows the Hendersson-Hasselbach equation [37]:

$$\mu'_{max} = \frac{\mu_{max}}{1 + \frac{H^+}{K_H} + \frac{K_{OH}}{H^+}} \tag{12}$$

where H^+ is the hydrogen ion concentration, K_H and K_{OH} are constants.

4. Results and discussion

The ability of filamentous fungi to form pellets is interesting for the reasons such as; the formation of more anoxic regions (which results in more production of anaerobic products like ethanol), easy separation of the fungi from the bioreactor because the filamentous forms of fungi are sometimes attached to the metallic surface of the bioreactor, smaller bioreactor volume requirement which results in lower fermentation investment cost, and higher resistance to inhibitory conditions due to less cell exposure to the inhibitory environment. Despite these benefits, the growth rate of fungi pellets, substrate consumption and product formation rate can vary from the theoretically expected rate for different reasons, as shown in Fig. 1 [28,34]. When oxygen transfer rate into the microbial medium is not sufficient, irrespective of the nutrient availability or other enabling conditions, the fungi pellet growth rate observed would be impeded by the oxygen mass transfer deficiency, which will in turn affect both the substrate consumption rate and the product formation rate [28]. Similar analogy applies to the influence of product concentration, substrate concentration and the pH of the media on fungi pellet growth. Thus it is important to know under what conditions the pellet growth rate could be impeded and by what factor. Apart from inhibition, for bioreactors operated in continuous mode the dilution rate used should be less than the maximum growth so as to prevent washout, thus it is important to know the maximum growth rate of the pellets. The kinetic study

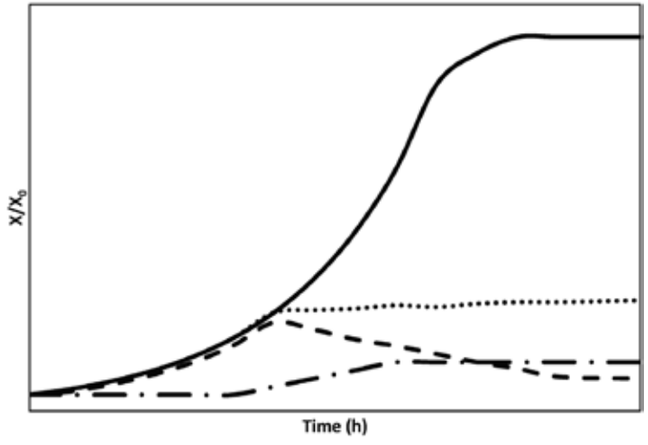

Fig. 1. The deviation from an idealised microbial growth profile (—) when it is affected by aeration limitation (···), product inhibition (– –) and substrate inhibition (– ·) during the growth and stationary phase.

performed in this paper gives information about the growth kinetic parameters of *N. intermedia* in its pellet form, what could inhibit its growth and product formation, how inhibitory conditions can be avoided and how optimal conditions can be maintained.

4.1. Pellet growth rate under normal conditions

To eliminate the effect of oxygen mass transfer limitations, substrate and product inhibition on the growth kinetics of *N. intermedia* pellets, a series of shake flask experiments were performed with low inoculum concentration (0.2 g L^{-1}), low glucose concentration (10–30 g L^{-1}) and pH 3.5. The specific growth rate (μ) for different substrate concentrations (S) was determined by plotting $\ln(X/X_0)$ against time for the experimental data obtained during the exponential growth phase. From the Lineweaver-Burk plot of $1/\mu$ versus 1/S (Fig. 2) the maximum growth rate of the pellets (μ_{max}) was 0.318 h^{-1}, while the substrate saturation constant (K_s) was 54.305 g L^{-1} (R^2 = 0.993). To confirm that there was no aeration mass transfer limitation affecting the growth rate results obtained, aeration rate of 0.71 vvm ($volume_{air}/volume_{media}$/min), much higher than the oxygen transfer rate into the shake flask was used in a lab scale airlift reactor. After 24 h, the specific growth rate of the fungal pellet in the airlift reactor was 0.042 h^{-1}, while the estimated specific growth from the model equation was 0.049 h^{-1}, indicating that the fungal pellet growth rate parameters in Fig. 2 could be used to estimate the pellet growth rate when aeration does not limit the growth rate.

When operating a bioreactor that uses *N. intermedia* pellets as the fermenting organism for a substrate that consists mainly of glucose, if the bioreactor is well mixed and does not have any pellet retention device in it, using a dilution rate exceeding maximum specific growth rate of *N. intermedia* pellets (0.318 h^{-1}) would result in pellets wash out.

4.2. Aeration and pellet growth

For strict aerobe such as *N. intermedia* oxygen must be present in a form that can be used for growth to occur, thus both the oxygen transfer rate (OTR) and the oxygen uptake rate (OUR) are essential for optimal growth, substrate consumption and product formation [31]. The OUR as defined in section 3.1 consists of the specific oxygen uptake rate (q_o) which is unique for each microorganism and can be assumed constant during the exponential growth phase [31], and the biomass concentration. The OTR is affected by several factors such as the geometrical parameters of the bioreactor, the operating conditions in the bioreactor, the physical properties of the fermentation media and any other factor that affects the volumetric mass transfer coefficient [26]. Hence, the kinetic study in this paper was done in shake flasks with air entering only from the cotton plug, thus the same fixed maximum OTR (OTR_{max}) can be assumed [30]. Additionally, at low pellet concentrations the fermentation media properties can be assumed as that of water so it would not affect the OTR. OTR_{max} from Eq. (5) is 2.299 mmol-O_2 L^{-1} h^{-1}, which is similar to the OTR in shake flask bioreactors that were reported by different authors [27,28].

Table 1
Specific oxygen uptake rate of *N. intermedia* pellets.

S_0 (gL^{-1})	X_t (gL^{-1})	q_o (mmol-O_2 g-biomass$^{-1}h^{-1}$)	Average pellet diameter (mm)
20	2.57	0.90	1.02 ± 0.33
30	3.74	0.62	1.92 ± 0.33
50	5.73	0.40	4.22 ± 0.41
70	6.01	0.38	4.22 ± 0.51
100	6.65	0.35	6.52 ± 0.62
200	8.52	0.27	6.54 ± 0.82

As the OTR is fixed in the shake flask, the OUR would increase with increasing pellet concentration. In the absence of any other inhibition, aeration mass transfer limitation in the flask can be observed by the reduction or stagnation of substrate consumption rate in the midst of unconverted substrates at that particular pellet concentration. This was observed for substrate concentrations from 20 to 200 gL^{-1} (shown in Fig. 3 for 20–50 gL^{-1} glucose concentration) and the corresponding q_o was calculated using Eq. (7) prior to when aeration limitation began (Table 1). The calculated q_o was between 0.270–0.896 mmol-O_2 g-biomass$^{-1}h^{-1}$ which is similar to reported q_o of *G. lucidum* [38,39] and *P. chpsogenum* [40] fungal pellets. As the substrate concentration increased, the average diameter of the pellets increased, with fur-like fluffy pellets (which consist of loosely packed mycelium hyphae) observed for pellet with average diameter of 4.22 ± 0.41 mm upwards. The increase in pellet diameter resulted in a reduction in the specific oxygen uptake rate (Table 1), as fur-like fluffy pellet poses little resistance to molecular oxygen transport than the densely packed hyphae, so the smaller densely packed pellet would require more oxygen to grow than larger loose pellets [41].

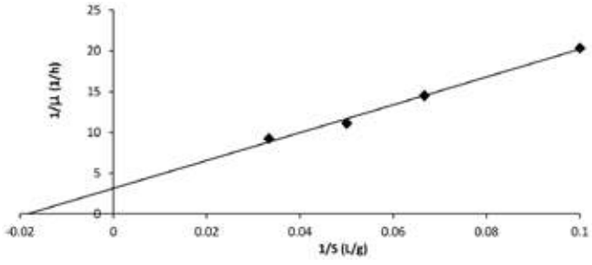

Fig. 2. Lineweaver-Burk plot of pellet growth rate against substrate concentration.

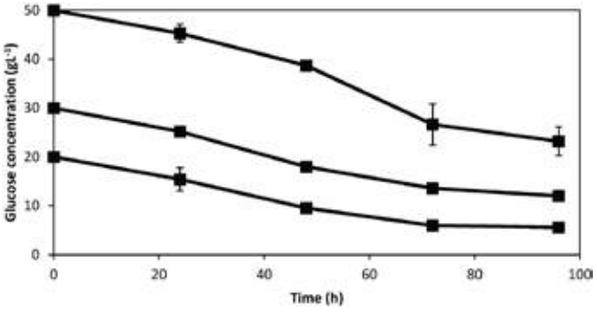

Fig. 3. Substrate consumption rate by *N. intermedia* pellets indicating the onset of aeration limitation.

4.3. Substrate and product concentration influence on pellet growth

Substrate inhibition was not observed for *N. intermedia* pellets for the range of glucose concentration examined (10–200 gL^{-1}), however the average pellet diameter increased with substrate concentration (Table 1), but the number of pellets decreased with substrate concentration. The number pellet was highest at 20 gL^{-1} glucose concentration (70 ± 5 pellets). A possible reason why high substrate concentration did not inhibit pellet growth could be because the core of the pellet is shielded by the outer hyphae from the effect the high substrate concentration would have if the fungus grow as filaments and by the high substrate saturation constant (K_s of 54.305 gL^{-1}). However, the growth of the *N. intermedia* pellets was affected by ethanol, which is the major product of the interest in this paper. The effect of ethanol concentration on pellet growth was investigated by adding ethanol (10–100 gL^{-1}) to the prepared standard shake flask fungi cultivation (section 2.2). The model parameters associated with ethanol inhibition (Eq. (9)) from the experimental results were; no growth ethanol concentration (P*) 70 gL^{-1}, the degree of product inhibition (a) 0.270 and observed maximum specific growth rate (μ'_m) 0.260 h^{-1}. Ethanol influencing the growth rate of the pellets could be attributable to the antimicrobial property of ethanol at high concentration.

For the Luedeking-Piret model (Eq. (11)), the non-growth associated parameter (β) for ethanol production by the pellets was evaluated using data from the stationary phase (where dX/dt is zero). Using similar analogy, the growth associated parameter (α) for ethanol production from the pellets was also determined. α was found to be 3.189 while β was 0.077 h^{-1}. Ethanol production by the pellets is more associated with pellet growth, which as seen by the higher value of the growth parameter, thus providing the nutrients and environmental conditions needed for pellet growth is essential if ethanol is to be produced optimally.

4.4. pH and pellet growth

N. intermedia pellets and filamentous growth optimal pH were previously reported as 3.5 and 5.5 respectively, with pellets formation occurring at pH 3–4 [13]. The best pellet formation was found to be at pH 3.5 with distinctly uniform and separated pellets (2–3 mm in diameter). At pH 3.0, the pellets were smaller (with an average diameter of 2.38 ± 0.12 mm) than at pH 3.5 (with an average diameter of 2.86 ± 0.38 mm). The substrate consumption rate and product formation rate for *N. intermedia* at different pH is shown in Fig. 4. Ethanol production rate is higher for the pellet formation pH range but biomass formation has been reported to be higher for the filamentous form of *N. intermedia* in the pH investigated [13]. This can be attributable to the formation of anoxic environment by the pellets, which is favours the formation of ethanol than biomass. The μ_{max} for Eq. (12) at the optimal ethanol production pH was 0.318 h^{-1}. During the growth phase the observed growth rate at pH 5.5 was 1.42 times faster than that at

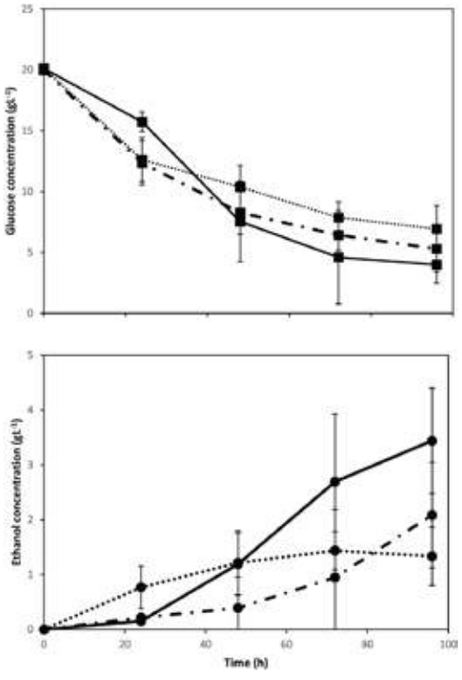

Fig. 4. Glucose consumption rate (■) and ethanol production rate (●) by *N. intermedia* at pH 3.5 (—), pH 4 (– ·) and pH 5.5 (···).

pH 3.5, while that at pH 4 was 1.17 times faster than that at pH 3.5. The observed production of less biomass and more ethanol agrees with pH reduction agrees with the reported higher production of lactic acid by *Rhizopus oryzae* R1021 pellets [42] and more product formation from *G. lucidum* fungi when the pH of the culture medium was reduced [43].

4.5. *Importance of the kinetic findings for* N. intermedia *applications*

When *N. intermedia* is used in biotechnology, apart from its application in genetics study, the goal is usually for specific product(s) production such as ethanol, treating waste streams while creating valuable products alongside [24], for food processing or use as food [44] etc. The goal from any of the previously mentioned applications can be achieved by optimizing the process for more biomass production and or more product formation using the kinetic parameters in Table 2. More biomass production can be achieved by using aeration rate which makes the OTR to be much greater than OUR. Using aeration rates that makes OTR much greater than OUR would mean that substrate would be used a lot more for cellular respiration than for biomass or product formation [11]. If the goal is to produce anaerobic product(s) such as ethanol, optimal ethanol production can be achieved by steadily increasing the aeration rate in such a way that the OTR in slightly above or equal to the OUR as the pellets grow. If the goal is to produce fur-like fluffy pellets, this could be achieved by combined use of aeration rate that makes OTR equal or slightly higher than OUR with high substrate concentration.

Table 2
Summary of growth, product formation and inhibition kinetic parameters of *N. intermedia* pellets.

Parameters	Average pellet diameter (mm)
μ_{max}	0.318 h^{-1}
Ks	54.305 g L^{-1}
α	3.189
β	0.077 h^{-1}
P*	70 g L^{-1}
a	0.270
μ'_m	0.260 h^{-1}
q_o	0.27–0.9 mmol-O_2 g-biomass^{-1} h^{-1}

5. Conclusion

Kinetic study of *N. intermedia* showed that aeration, substrate, product concentration and pH influence its pellet formation. The maximum growth rate of the pellets at pH 3.5 was 0.318 h^{-1}, while the substrate saturation constant was 54.305 gL^{-1}. The specific oxygen uptake rate of the pellets was between 0.27–0.9 mmol-O_2 g-biomass^{-1} h^{-1}. Ethanol production by *N. intermedia* was found to be highly growth dependent, with growth associated growth associated parameter of 3.189 and non-growth associated parameter of 0.077 h^{-1}. The kinetic parameters of *N. intermedia* from this study can be used for designing, operating and optimizing *N. intermedia* fermentation processes.

Acknowledgement

The authors are grateful for the financial support from the Swedish Research Council Formas.

References

[1] J. Zhang, J. Zhang, The filamentous fungal pellet and forces driving its formation, Crit. Rev. Biotechnol. (2015) 1–12.
[2] A. Saraswathy, R. Hallberg, Mycelial pellet formation by Penicillium ochrochloron species due to exposure to pyrene, Microbiol. Res. 160 (2005) 375–383.
[3] J.L. Casas López, J.A. Sánchez Pérez, J.M. Fernández Sevilla, E.M. Rodríguez Porcel, Y. Chisti, Pellet morphology, culture rheology and lovastatin production in cultures of Aspergillus terreus, J. Biotechnol. 116 (2005).
[4] Y. Liu, W. Liao, C. Frear, S. Chen, Pelletization process to control filamentous fungi morphology for enhanced reactor rheology bioproduct formation, Google Patents, 2013.
[5] A. Koch, The kinetics of mycelial growth, Microbiology 89 (1975) 209–216.
[6] S. Pirt, A kinetic study of the mode of growth of surface colonies of bacteria and fungi, Microbiology 47 (1967) 181–197.
[7] Y.-L. Feng, W.-Q. Li, X.-Q. Wu, J.-W. Cheng, S.-Y. Ma, Statistical optimization of media for mycelial growth and exo-polysaccharide production by Lentinus edodes and a kinetic model study of two growth morphologies, Biochem. Eng. J. 49 (2010) 104–112.
[8] J. Nielsen, Modelling the morphology of filamentous microorganisms, Trends Biotechnol. 14 (1996) 438–443.
[9] S. Marın, V. Sanchis, R. Saenz, A. Ramos, I. Vinas, N. Magan, Ecological determinants for germination and growth of some Aspergillus and Penicillium spp. from maize grain, J. Appl. Microbiol. 84 (1998) 25–36.
[10] L. Hellendoorn, H. Mulder, J. Van den Heuvel, S. Ottengraf, Intrinsic kinetic parameters of the pellet forming fungus Aspergillus awamori, Biotechnol. Bioeng. 58 (1998) 478–485.
[11] F.C. Michel, E.A. Grulke, C.A. Reddy, A kinetic model for the fungal pellet lifecycle, AIChE J. 38 (1992) 1449–1460.
[12] J. Van Suijdam, H. Hols, N. Kossen, Unstructured model for growth of mycelial pellets in submerged cultures, Biotechnol. Bioeng. 24 (1982) 177–191.
[13] R.B. Nair, P.R. Lennartsson, M.J. Taherzadeh, Mycelial pellet formation by edible ascomycete filamentous fungi, Neurospora intermedia, AMB Express 6 (2016) 1–10.
[14] W. Zhou, Y. Cheng, Y. Li, Y. Wan, Y. Liu, X. Lin, R. Ruan, Novel fungal pelletization-assisted technology for algae harvesting and wastewater treatment, Appl. Biochem. Biotechnol. 167 (2012) 214–228.
[15] Y. Zhou, J. Du, G.T. Tsao, Mycelial pellet formation by rhizopus oryzae ATCC 20344, Appl. Biochem. Biotechnol. 84 (2000) 779–789.

[16] F. Domingues, J. Queiroz, J. Cabral, L. Fonseca, The influence of culture conditions on mycelial structure and cellulase production by Trichoderma reesei Rut C-30, Enzyme Microb. Technol. 26 (2000) 394–401.
[17] T.K. Kirk, E. Schultz, W. Connors, L. Lorenz, J. Zeikus, Influence of culture parameters on lignin metabolism byPhanerochaete chrysosporium, Arch. Microbiol. 117 (1978) 277–285.
[18] W. Liao, Y. Liu, C. Frear, S. Chen, A new approach of pellet formation of a filamentous fungus –Rhizopus oryzae, Bioresour. Technol. 98 (2007) 3415–3423.
[19] C.C. Ho, Identity and characteristics of Neurospora intermedia responsible for oncom fermentation in Indonesia, Food Microbiol. 3 (1986) 115–132.
[20] A.J.F. Griffiths, H. Bertrand, Unstable cytoplasms in Hawaiian strains of Neurospora intermedia, Curr. Genet. 8 (1984) 387–398.
[21] H. Bertrand, A.J.F. Griffiths, D.A. Court, C.K. Cheng, An extrachromosomal plasmid is the etiological precursor of kalDNA insertion sequences in the mitochrondrial chromosome of senescent neurospora, Cell 47 (1986) 829–837.
[22] A.J.F. Griffiths, X. Yang, Senescence in natural populations of Neurospora intermedia, Mycol. Res. 97 (1993) 1379–1387.
[23] R.B. Nair, M. Lundin, P.R. Lennartsson, M.J.C.J.-R. Taherzadeh, Optimizing dilute phosphoric acid pretreatment of wheat straw in the laboratory and in a demonstration plant for ethanol and edible fungal biomass production using Neurospora intermedia, J. Chem. Technol. Biot. (2016).
[24] R.B. Nair, M.J. Taherzadeh, Valorization of sugar-to-ethanol process waste vinasse: a novel biorefinery approach using edible ascomycetes filamentous fungi, Bioresour. Technol. 221 (2016) 469–476.
[25] J.A. Ferreira, P.R. Lennartsson, M.J. Taherzadeh, Production of ethanol and biomass from thin stillage by Neurospora intermedia: a pilot study for process diversification, Eng. Life Sci. (2015).
[26] F. Garcia-Ochoa, E. Gomez, Bioreactor scale-up and oxygen transfer rate in microbial processes: an overview, Biotechnol. Adv. 27 (2009) 153–176.
[27] Y.-S. Liu, J.-Y. Wu, K.-p. Ho, Characterization of oxygen transfer conditions and their effects on Phaffia rhodozyma growth and carotenoid production in shake-flask cultures, Biochem. Eng. J. 27 (2006) 331–335.
[28] U. Maier, J. Büchs, Characterisation of the gas?liquid mass transfer in shaking bioreactors, Biochem. Eng. J. 7 (2001) 99–106.
[29] M.A. Auro, H.M. Hodge, N.G. Roth, Oxygen absorption rates in shaken flasks, J. Ind. Eng. Chem. 49 (1957) 1237–1238.
[30] P.M. Doran, Chapter 10 – Mass Transfer, Bioprocess Engineering Principles, Second Edition, Academic Press London, 2013, pp. 379–444.
[31] F. Garcia-Ochoa, E. Gomez, V.E. Santos, J.C. Merchuk, Oxygen uptake rate in microbial processes: an overview, Biochem. Eng. J. 49 (2010) 289–307.
[32] E. Gomez, V.E. Santos, A. Alcon, A.B. Martin, F. Garcia-Ochoa, Oxygen-uptake and mass-transfer rates on the growth of pseudomonas p utida CECT5279: influence on biodesulfurization (BDS) capability, Energy Fuels 20 (2006) 1565–1571.
[33] K. Han, O. Levenspiel, Extended Monod kinetics for substrate, product, and cell inhibition, Biotechnol. Bioeng. 32 (1988) 430–447.
[34] O. Levenspiel, The Monod equation: a revisit and a generalization to product inhibition situations, Biotechnol. Bioeng. 22 (1980) 1671–1687.
[35] G. Viniegra-González, E. Favela-Torres, C.N. Aguilar, S. de Jesus Rómero-Gomez, G. Diaz-Godınez, C. Augur, Advantages of fungal enzyme production in solid state over liquid fermentation systems, Biochem. Eng. J. 13 (2003) 157–167.
[36] I. Tang, M.R. Okos, S.T. Yang, Effects of pH and acetic acid on homoacetic fermentation of lactate by Clostridium formicoaceticum, Biotechnol. Bioeng. 34 (1989) 1063–1074.
[37] A.P. Zeng, A. Ross, H. Biebl, C. Tag, B. Günzel, W.D. Deckwer, Multiple product inhibition and growth modeling of Clostridium butyricum and Klebsiella pneumoniae in glycerol fermentation, Biotechnol. Bioeng. 44 (1994) 902–911.
[38] Q.H. Fang, J.J. Zhong, Two-stage culture process for improved production of ganoderic acid by liquid fermentation of higher fungus Ganoderma lucidum, Biotechnol. Progr. 18 (2002) 51–54.
[39] Y.-J. Tang, J.-J. Zhong, Role of oxygen supply in submerged fermentation of Ganoderma lucidum for production of Ganoderma polysaccharide and ganoderic acid, Enzyme Microb. Technol. 32 (2003) 478–484.
[40] C.S. Ho, L.K. Ju, R.F. Baddour, Enhancing penicillin fermentations by increased oxygen solubility through the addition of n-hexadecane, Biotechnol. Bioeng. 36 (1990) 1110–1118.
[41] J. Oostra, E.P. Le Comte, J.C. Van den Heuvel, J. Tramper, A. Rinzema, Intra-particle oxygen diffusion limitation in solid-state fermentation, Biotechnol. Bioeng. 75 (2001) 13–24.
[42] D.-M. Bai, M.-Z. Jia, X.-M. Zhao, R. Ban, F. Shen, X.-G. Li, S.-M. Xu, l(+)-lactic acid production by pellet-form Rhizopus oryzae R1021 in a stirred tank fermentor, Chem. Eng. Sci. 58 (2003) 785–791.
[43] Q.-H. Fang, J.-J. Zhong, Effect of initial pH on production of ganoderic acid and polysaccharide by submerged fermentation of Ganoderma lucidum, Process Biochem. 37 (2002) 769–774.
[44] M. Matsuo, Chemical components palatability, antioxidant activity and antimutagenicity of oncom miso using a mixture of fermented soybeans and okara with Neurospora intermedia, J. Nutr. Sci. Vitaminol. (Tokyo) 52 (2006) 216–222.

PAPER V

Cost effective dry anaerobic digestion in textile bioreactors:
Experimental and economic evaluation.
Bioresource Technology Doi.org/10.1016/j.biortech.2017.08.081

Bioresource Technology 245 (2017) 549–559

Contents lists available at ScienceDirect

Bioresource Technology

journal homepage: www.elsevier.com/locate/biortech

Cost effective dry anaerobic digestion in textile bioreactors: Experimental and economic evaluation

Regina J. Patinvoh[a,b,*], Osagie A. Osadolor[a], Ilona Sárvári Horváth[a], Mohammad J. Taherzadeh[a]

[a] Swedish Centre for Resource Recovery, University of Borås, SE 501 90 Borås, Sweden
[b] Department of Chemical and Polymer Engineering, Faculty of Engineering, Lagos State University, Lagos, Nigeria

ARTICLE INFO

Keywords:
Dry anaerobic digestion
Textile bioreactor
Solid waste management
Digestate
Economic evaluation

ABSTRACT

The aim of this work was to study dry anaerobic digestion (dry-AD) of manure bedded with straw using textile-based bioreactor in repeated batches. The 90-L reactor filled with the feedstocks (22–30% total solid) and inoculum without any further treatment, while the biogas produced were collected and analyzed. The digestate residue was also analyzed to check its suitability as bio-fertilizer. Methane yield after acclimatization increased from 183 to 290 NmlCH_4/gVS, degradation time decreased from 136 to 92 days and the digestate composition point to suitable bio-fertilizer. The results then used to carry out economical evaluation, which shows dry-AD in textile bioreactors is a profitable method of handling the waste with maximum payback period of 5 years, net present value from $7,000 to $9,800,000 (small to large bioreactors) with internal rate of return from 56.6 to 19.3%.

1. Introduction

Solid wastes from agricultural, municipal and industrial activities are major sources of environmental pollution. Large volumes of these wastes are being generated and are increasing immensely due to population growth and high consumption rate. Currently, people generate globally about 17 billion tonnes of total solid wastes annually (Chattopadhyay et al., 2009) and it is estimated to reach 27 billion tonnes in 2050 (Karak et al., 2012). These wastes streams usually have a solid content between 15% and 50%. Landfilling is a major practice of disposing solid wastes resulting in emissions of methane and nitrous oxides which contribute to greenhouse effect. Composting and incineration are also common methods of treating these wastes; composting results in emissions of volatile compounds (ketones, aldehydes, ammonia and methane) (Mata-Alvarez et al., 2000) while incineration can lead to significant release of dioxin to the environment (Strange, 2002) if the exhaust gas is not treated properly. There are regulations and standards for management of these wastes, but in addition to this it is essential that other waste management options which are both environmentally friendly and economical are explored. Biogas production through anaerobic digestion is an interesting waste management option for handling the organic fraction of solid waste, as biogas production usually leads to reduced pollution and increased energy production. Studies have shown that anaerobic digestion of these wastes is sustainable and has a great advantage over aerobic treatment because of its improved energy balance (Mata-Alvarez et al., 2000). In addition to biogas production, digestate residue from anaerobic digestion usually contains high content of phosphate and nitrogen, especially in the form of ammonium which is available for plants; it also contains other macro-nutrients and trace elements essential for plant growth (Makádi et al., 2012).

Anaerobic digestion of organic wastes is carried out generally through wet (feedstock with solid concentration between 0.5% and 15%) (Li et al., 2011) and dry (feedstock with solid concentration greater than 20%) (Bolzonella et al., 2003) anaerobic digestion processes. When treating solid wastes in wet anaerobic digestion processes, fresh and recycled water must be added while large reactor volume, high energy for heating and costly dewatering process of the digestate is required. Therefore, processing of solid wastes for biogas production through dry-AD is a better option since they usually have low moisture content. However, for enhanced performance of dry-AD process, a suitable reactor is required; considering the substrate composition, amount of substrate to be treated, and process economy of the reactor (Patinvoh et al., 2017). It also requires an appropriate technology for operation. In this vein, several continuous and batch reactors for dry-AD processes have been employed such as plug flow reactors (Deng et al., 2016; Patinvoh et al., 2017) for continuous dry-AD processes, and completely mixed reactor (Guendouz et al., 2010) for batch dry-AD processes. However, some of these reactors required expert design and constructions, constant monitoring, high capital and operational cost.

* Corresponding author at: Swedish Centre for Resource Recovery, University of Borås, SE 501 90 Borås, Sweden.
E-mail address: regina.jijoho_patinvoh@hb.se (R.J. Patinvoh).

http://dx.doi.org/10.1016/j.biortech.2017.08.081
Received 30 June 2017; Received in revised form 11 August 2017; Accepted 14 August 2017
Available online 19 August 2017
0960-8524/

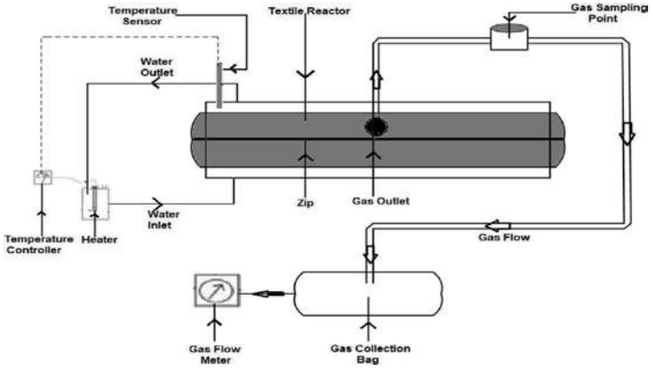

Fig. 1. Schematic sketch of the experimental set up.

The most commonly used reactors in developing countries are fixed-dome reactors, floating-drum reactors and polyethylene tubular reactors (usually modelled as plug flow reactors) (Rowse, 2011). The cost of a fixed-dome reactor is relatively low and the reactor is usually constructed underground which makes it less sensitive to seasonal temperature changes but this reactor requires high technical skill for construction (Kossmann et al., 1999). It is also prone to leakages (Kossmann et al., 1999; Rajendran et al., 2013) (porosity and cracks) and utilization of gas produced is less effective as the gas pressure fluctuates substantially. Floating-drum reactor is easy to operate, it provides gas at constant pressure but the steel drum is relatively expensive and requires rigorous maintenance (Kossmann et al., 1999). It requires constant removal of rust and regular painting to avoid gas leakage, this reactor is not also suitable for fibrous substrates because the gas-holder can get stuck in the resulting floating scum (Kossmann et al., 1999). Hence, there is a need for reactors that are robust in nature, easy to maintain, suitable for dry digestion processes and cost effective. An innovative textile-based bioreactor which is durable, cost effective and easy-to-operate was developed for biogas production, and it was found to be effective and economical for wet anaerobic digestion of organic fraction of municipal solid wastes (Rajendran et al., 2013).

In this work, the potential of dry anaerobic digestion in the textile-based bioreactor was studied in batch process, and its technical and economic aspects were evaluated. Manure bedded with straw was used as an example of the substrate abundantly available at farms. Repeated batch digestion processes were investigated, the TS in the reactor was gradually increased in order to acclimatize the inoculum to the substrates under solid state condition and thereafter increase the amount of wastes treated. The residue after biogas production was analysed to check its suitability as bio-fertilizer. Additionally, the economic analysis was carried out to evaluate this technology.

2. Materials and methods

2.1. Bioreactor

A new design of innovative textile reactor at laboratory scale was developed and supplied by FOV Fabrics AB (Borås, Sweden). It was made of advanced textiles and sophisticated coated polymers which makes the bioreactor durable, resistant to digesting bacteria and chemicals, easily transportable and highly resistant to UV light and high temperature (up to 80 °C) (Rajendran et al., 2013). The reactor is made of high quality polyester PVC coated fabrics; it is a horizontal bioreactor of 184 cm length, 54 cm breadth and had a total volume of about 90 L. The bioreactor was maintained at 25 °C by circulating water through water jacket. This bioreactor had an air tight zip which was opened for feeding and closed after feeding; it also had an opener for gas outlet. The reactor was examined for leakages by filling with water and air before starting the experiment. Fig. 1 shows the schematic sketch of the experimental set up together with other accessories, such as gas collection bag, sampling point for biogas compositional analysis and the gas flow meter (Drum-type gas meter, TG 05 Model 5, Ritter, Germany) for measuring the produced biogas volume.

2.2. Substrate and inoculum preparation

Cattle manure bedded with straw and untreated wheat straw was obtained from a farm outside Borås (Rådde Gård, Sweden). During the experimental period, two different batches of the substrates were obtained; the amount of straw in manure was higher in the second batch collected compared to the first batch. The first batch was used for first experiment while second batch was used for the second and third experiments. The manure was shredded manually to reduce the particle size of straw in the manure. The untreated wheat straw was milled to particle size of 0.5–2 mm, after which the feedstocks were characterized.

Inoculum was obtained from a digester treating wastewater sludge and operating at mesophilic conditions (Vatten and Miljö i Väst AB, Varberg, Sweden). The inoculum was filtered through a 2-mm porosity sieve to remove sand, plastic and other unwanted particles after which it was acclimatized for five days prior to use. The inoculum was centrifuged at 7,600 × *g* using continuous centrifuge to obtain a TS content of 7.0 ± 0.24%. The inoculum from wet fermentation with TS content of 3.53 ± 0.01% was centrifuged in order to reduce its water content since the textile reactor is studied under dry anaerobic digestion. The inoculum after centrifuge having TS and VS content of 7% and 4% respectively was then used for the first batch experiment.

2.3. Experimental procedure

Manure bedded with straw was mixed with required amount of untreated wheat straw to increase the C/N ratio; the C/N ratio was kept between 20:1 and 25:1 throughout the experiment. The amount of untreated straw needed to increase the C/N was calculated according to Eq. (1) (AAFRD, 2005) and the required amount added is shown in Table 3. During the first digestion process (unacclimatized inoculum), the total feedstock with 22% TS was inoculated with the initial inoculum (7%TS and 4%VS) keeping a volatile solids (VS) ratio ($VS_{inoculum}$ to $VS_{substrate}$) at 1:1 thereby having total TS of 10% in the reactor. A nutrient solution with composition according to Angelidaki et al. (2009) was added only at this start-up period and the pH of the mixture was adjusted to 7.45 using 2 M HCl solution. The reactor was maintained at 25 °C by circulating water through water jacket arranged under the reactor as shown in Fig. 1 and there was no mixing inside the reactor during the digestion process. The biogas produced was collected in a gas bag and volume was measured once the gas collection bag was filled. Biogas samples were taken through the gas sampling point for compositional analysis. The first digestion process lasted for 136 days. In order to increase the TS in the textile reactor and investigate the response of bacteria after acclimatization, the second batch digestion (acclimatized low TS) was performed. Second digestion process was performed the same way as in the first one, except that the digestate residue from the first digestion was used as inoculum (7.97%TS and 5.19%VS) and no nutrient was added. The volatile solids (VS) ratio ($VS_{inoculum}$ to $VS_{substrate}$) was kept at 1:1 and TS of the substrate was increased to 27% thereby increasing the TS in the reactor to 12%. To further increase the TS in the reactor thereby treating more wastes, a third batch digestion process (acclimatized high TS) was also performed. The digestate residue from the second digestion was used as inoculum (9.6%TS and 6.2%VS). The volatile solids (VS) ratio ($VS_{inoculum}$ to $VS_{substrate}$) was reduced to 0.5 and TS of the substrate was increased to 30% thereby increasing the TS in the reactor to 17%. The compositions in different batch digestion setup are summarized in Table 2.

$$a = \frac{\%N_b}{\%N_a} \times \frac{R - R_b}{R_a - R} \times \frac{1 - M_b}{1 - M_a} \quad (1)$$

where:

a = total weight of straw
b = total weight of manure with straw
M_a = moisture content of straw
M_b = moisture content of manure with straw
% N_a = % nitrogen of straw on dry basis
% N_b = % nitrogen of manure with straw on dry basis
R_a = C/N ratio of straw
R_b = C/N ratio of manure with straw
R = desired C/N of mixture

2.4. Analytical methods

Moisture content, pH, total nitrogen, TS and VS were determined according to biomass analytical procedures (APHA-AWWA-WEF, 2005). Total nitrogen contents were measured using the Kjeldahl method, and the protein content was estimated by multiplying the Kjeldahl nitrogen content with a factor of 6.25 according to Gunaseelan (2009). The total carbon was obtained by correcting the total dry weight carbon value for the ash content (Haug, 1993; Zhou et al., 2015). The bulk density was determined according to Zhang et al. (2012).

Extractives in untreated straw samples were determined according to NREL protocols (Sluiter et al., 2008) using Soxhlet method with water and ethanol extraction for 24 h. Total carbohydrate and lignin content of extractive free straw samples were determined according to NREL protocols (Sluiter et al., 2011). The extractive free straw samples were air-dried until moisture content was less than 10%. Samples were then hydrolyzed using 72% H_2SO_4 in a water bath at 30 °C for 60 min while samples were stirred every 5 min to ensure uniform hydrolysis, and then a second hydrolysis was performed using 4% H_2SO_4 in an autoclave at 121 °C for 60 min. Monomeric sugars obtained during the hydrolysis were determined by HPLC. Mannose, glucose, galactose, xylose and arabinose were analyzed using Aminex HPX-87 P column (Bio-Rad) at 85 °C and 0.6 mL/min ultrapure water as eluent. Acid soluble lignin (ASL) was determined using a UV spectrophotometer (Libra S60, Biochrom, England) at 320 nm. Acid insoluble lignin (AIL) was gravimetrically determined as residual solid after hydrolysis corrected with ash content. The ash content was determined as the remaining residue after keeping the samples in the muffle furnace at 575 °C for 24 h.

The biogas volume was measured with Drum-type gas meter (TG 05 Model 5, Ritter, Germany), and then it was corrected for reporting at standard temperature and pressure (0 °C, and 1 bar) using ideal gas law. The methane composition of the produced biogas was determined using a GC (Perkin-Elmer, USA) equipped with a packed column (6′ × 1.8″ OD, 80/100, Mesh, Perkin Elmer, USA), and a thermal conductivity detector (Perkin-Elmer, USA), with an inject temperature of 150 °C. The carrier gas was nitrogen operated with a flow rate of 20 ml/min at 60 °C. A 250-µl pressure-lock gas syringe (VICI, precious sampling Inc., USA) was used for taking samples for the gas composition analysis. The degree of digestion was calculated using Eq. (2) according to Schnürer and Jarvis (2010);

$$Degree\ of\ Digestion = (((TS_{in} * VS_{in}) - (TS_{out} * VS_{out}))/(TS_{in} * VS_{in})) * 100 \quad (2)$$

2.5. Digestate analysis

The digestate residue was centrifuged at 5,000 × *g* for 10 min and the liquid fraction was passed through 0.2 µm filter prior to analysis. 0.2*g* of the solid fraction was dissolved in 2 ml concentrated HNO_3 (65%), 6 ml concentrated HCl (37%), 1 ml concentrated HF (48%) and 1 ml H_2O_2 (30%). Thereafter, it was digested at 200 °C (800 W) for 20 min in the microwave oven. Dissolved samples were then diluted with milli-Q water to 25 ml. The available heavy metals, trace elements and macro-nutrients in both the liquid and solid fraction of the digestate were quantified using microwave plasma-atomic emission spectrometer (Agilent Technologies 4200 MP-AES). The liquid fraction of the digestate was analyzed for ammonium nitrogen concentration using Ammonium 100 test kit (Nanocolor, MACHEREY-NAGEL GmbH & Co. KG. 10 Germany) and concentration measured using Nanocolor 500D Photometer (MACHEREY-NAGEL GmbH & Co. KG. Germany).

2.6. Economic analysis

The annual cost of producing biogas or any of the fermentative biofuels in US$/Volume can be estimated using Eq. (3) (Bergeron, 1996). A 15-year biogas production lifetime was assumed for the textile bioreactor (Rajendran et al., 2013). The interest rate (i) used for the analysis was 7.8% which is the average deposit interest rate in Nigeria (a tropical country) from 2010 to 2016 (World Bank, 2017a).

$$Annual\ biogas\ production\ cost\ (ACBP) = FC/Y + (ACC + OC) - Ye.\ EC \quad (3)$$

where FC = feedstock cost ($/tonne), Y = yield ($Nm^3$/tonne), ACC = annual capital cost ($/$Nm^3$), CC = Capital cost, i = interest rate, OC = operating cost ($/$Nm^3$), Ye = electricity yield (kWh/L), EC = -electricity credit ($/kWh), n = 15 (years).

Economic analysis was performed on the cost of replacing agricultural solid waste generation by collection through waste management providers and by composting with dry-AD at three different dry-AD scenarios which are; no acclimatization of the inoculum using solid waste with a density of 907 kg/m^3 (scenario A), short acclimatization (136 days) of the inoculum using solid waste with a density of 542 kg/m^3 (scenario B) and longer acclimatization (232 days) of the inoculum using solid waste with a density of 542 kg/m^3 (scenario C). The calculations were performed at three different waste generation levels; 3 tons/year for a typical small scale farm with animal husbandry and vegetable cultivation or 2 mature cows (Ho et al., 2013), 5200 tons/year for a medium mechanized farm or over 100 mature cows and 51,000 tons/year for a large scale mechanised farm or over 1000 mature cows (Chen, 2016; Hoornweg et al., 1999). The unit cost of compositing from a study in Taiwan (which is similar to many tropical or

subtropical country) was $67/ton for highly mechanised privatized large scale compost production facility, $97/ton for mid scale and $404/ton for small scale manual government affiliated composting facility or farms (using a conversion factor of 1 NT$ = $0.033 and 53% conversion of waste to compost) (Chen, 2016; Hoornweg et al., 1999). For the waste collection by waste managers option, the estimated cost of collecting waste for lower mid income countries in 2010 was between $30–$75 per ton of solid waste (World Bank, 2016). Additionally farms that employ waste disposal by waste managers also have to purchase compost or organic fertilizer (Ruggieri et al., 2009) and this cost an additional $211–$356 per ton (Chen, 2016), making the total cost handling solid waste by waste managers to be from $241 to $431 per ton.

The annual profit (AP) was calculated by substracting the annual cost of biogas production (Eq. (3)) from the annual cost of handling waste through other means plus the revenue generated from biogas sales as shown in Eq. (4);

$$AP = Annual\ expenditure\ on\ waste\ management - ACBP + Revenue \quad (4)$$

The revenue (R) from biogas was gotten by multiplying the current commercial selling price of natural gas of $0.222/1000-Nm^3 (Selling price in Febrauary 2017) by the annual methane production from the dry anearobic digestion divided by the methane fraction in natural gas (95%) (EIA, 2017). The revenue calculations (Eq. (5)) were done using the methane production values for the experiments performed.

$$R = \text{"\$"}0.000234\ (Nm^3) \times Vol\ of\ methane\ produced\ (Nm^3) \quad (5)$$

The payback period (PBP) was calculated using Eq. (6), where the initial project delay time was the time needed for completing the first anaerobic digestion batch. The net present value (NPV) was calculated using Eq. (7), with the profit from the first year different from those of the other years, and the internal rate of return which makes the NPV zero was also calculated.

$$PBP = CC/AP + initial\ project\ delay\ time \quad (6)$$

$$NPV = -C_0 + \sum_{n=1}^{n} \frac{AP}{(1+i)n} \quad (7)$$

where C_0 = the initial capital investment.

The capital cost for the biogas production was based on the volume of the textile bioreactor needed for biogas production per year and the cost of other auxiliary equipment such as shredders, shovels and tractors (for mid and large scale). The volumes of the textile bioreactors needed for the different scenerious investigated were calculated using the data from the experimental section by dividing the mass of the waste and innoculum by their respective densities while accounting for duration of the dry-AD, feedstock storage, gas storage and digestate storage. Details on how to perform this kind of calculations and optimal reactor sizing can be found elsewhere (Mähnert and Linke, 2009). Using 3 tons/year waste generation without acclimatization as an example, the digestion period is 136 days so storage for 1.12 tons (i.e. 3 tons × 136/365) of waste is needed as the waste is produced continuously. The reactor volume needed for storing the daily produced waste is 1.23 m^3 (i.e. mass/density). This is also going to be the volume needed for storing the digestate as the amount digestate removed from the reactor would be equal to the amount of waste to be feed to the reactor. The volume needed for the digestion will be equal to the sum of 1.23 m^3 (the volume of the waste needed for the dry-AD), 5.24 m^3 for the inoculum (i.e. inoculum mass/density) and 2 m^3 to provide some air space which gives 8.47 m^3. Using the assumption that the produced biogas will be sold monthly, the textile bioreactor volume needed for one month storage is 8 m^3 making the total required volume for all activities to be 19 m^3. Calculations similar to this where performed for the other scenarios and scales, and the required reactor volume are shown in Table 2.

The annual operating cost associated with the textile reactor was assumed to be 5% of its capital cost (Rajendran et al., 2013), while that for the auxiliary equipment were; $1.95/ton for shredders, $0.12/ton for tractors and $0.14/ton for shovels (using 1€ = 1.09 $) (Ruggieri et al., 2009). The investment cost for the first year for the shredders, shovels and tractors were $20/ton, $1.5/ton and $1.2/ton respectively accounting for the work-time used only feedstock preparation related to biogas production (Ruggieri et al., 2009) and they were assumed to last through the 15 years of the project.

2.7. Sensitivity analysis

To determine the flexibility of the results of the economic evaluation, sensitivity analysis were carried out using cost of the textile reactor, cost of auxiliary equipment and annual tons of waste produced. For the cost of the textile reactor and auxiliary equipment, a ± 20% change in the investment and operation cost were used to determine how the calculated NPV and IRR would vary, while a ± 20% change in the annual tons of produced waste was used to determine the effect of varying amount of waste generation on NPV and IRR. For the textile reactor cost, in the base case, the investment cost of the textile reactor was $150/volume for small scale (in volume of 2 m^3) (Rajendran et al., 2013), $100/volume for mid-scale (volume in 100s of m^3) and $70/volume for large-scale (volume in 1000s of m^3) (Osadolor et al., 2014), while the operation cost was 5% of the investment cost. For the cost of the auxiliary equipment, in the base condition, the investment cost for the shredders, shovels and tractors were $20/ton, $1.5/ton and $1.2/ton respectively, while the operation cost was $1.95/ton for shredders, $0.12/ton for tractors (used only mid and large scale evaluations) and $0.14/ton for shovels. For the amount of produced waste, in the base case, 3 tons/y was used for small scale, 5200 tons/y for mid-scale and 51,000 tons/y for large scale.

3. Results and discussion

The batch dry anaerobic digestion (dry-AD) of manure bedded with straw was carried out in a textile-based bioreactor. The reactor is built from textile (Rajendran et al., 2013) and has undergone drag, tears and pressure testing prior to the experimental study and was found very durable. It was used successfully for over 324 days without any gas leakage or major maintenance. The first batch anaerobic digestion of the feedstock took longer degradation time and the methane yield was slightly lower. Subsequent batch digestion processes resulted to improved methane yield and reduced degradation time. The digestate after biogas production was analyzed as supplement for soil deficient of major nutrients. Then economic analysis of replacing waste collection by waste managers or composting with dry-AD in a textile bioreactor was carried out using payback period, net present value and internal rate of return as profitability criteria. A sensitivity analysis of what effect changes in key cost and waste generation factors could have on the profitability of dry-AD in the textile bioreactor was also investigated.

3.1. An industrial concept for dry-AD in rural areas

The results obtained in this work would be beneficial for rural areas, farmers, some industrial applications and developing countries where a cost-effective and simple solution is needed. The solid waste with higher TS is treated while generating energy and bio-fertilizer. Dry-AD of solid wastes in the textile-based bioreactors function on a simple principle (Fig. 2a) as a few reactors should run in parallel. Fresh solid wastes are mixed with inoculum (needed only at the initial stage), fed to the bioreactor (with shovel for small scale or tractor/pumps for large scale) and then the bioreactor is closed. As the materials inside the bioreactor have higher TS, and it is not mixed, it has low heat transfer so it can perform better than wet digestion in colder climates. However, it can be heated underneath to attain desired temperature in cold

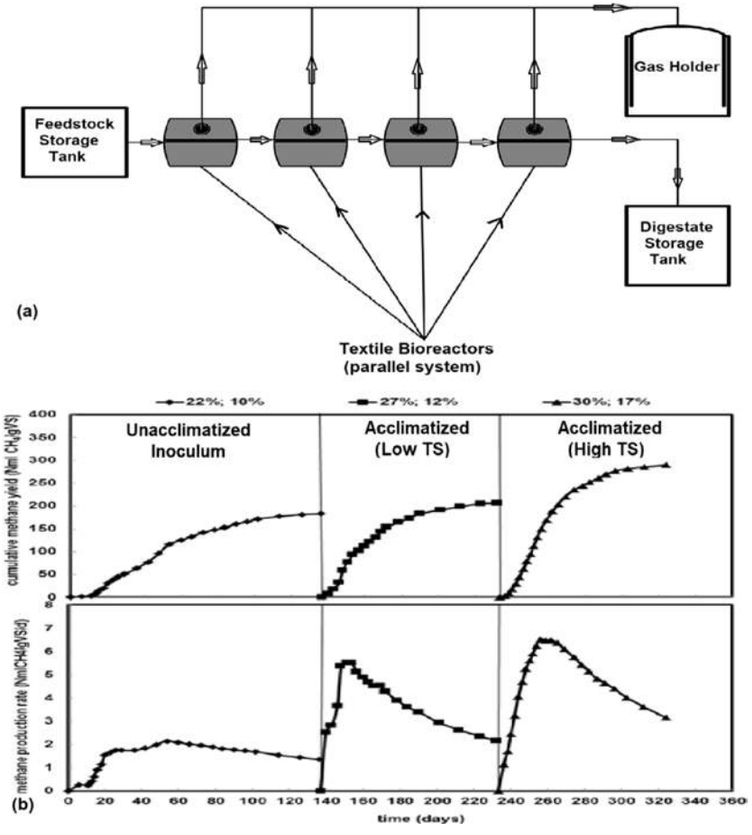

Fig. 2. (a) Typical dry-AD technology in textile bioreactors – industrial concept for rural areas. (b) Cumulative methane production and methane production rate obtained during digestion process with gradual increase of total solid (TS) content of the feedstock and reactor mixture. 22%, 27% and 30% (TS of feedstock); 10%, 12% and 17% (TS in reactor).

regions, but this is not needed for tropical regions. The bioreactor is closed until degradation time is completed while gas produced is collected continuously in a gas holder. When there is no more gas production, the bioreactor is opened and a portion of the digestate will be pumped or moved for storage in a separate bioreactor, while a portion of the digestates remains inside the bioreactor, mixed with fresh wastes and the bioreactors is closed and sealed for the next run of gas production. The number of the bioreactors needed in parallel depends on the feeding time and the gas production duration in each batch. For example, if 3 months would be the gas production period in each batch and 15 days would be enough for emptying, and refilling the bioreactors, 6 bioreactors can work in parallel to fulfil continuous receiving of the fresh wastes. The volume of the textile bioreactor needed to handle different amount of waste is shown in Table 2, and they can be arranged as shown in Fig. 2a.

3.2. Feedstock characterization

The characteristics of the feedstocks used in this work are shown in Table 1. The result showed that the substrates have different moisture content at different batches, probably because they were collected under different storage conditions. The C/N of the manure bedded with straw was the same but the C/N ratio of wheat straw was considerably different from one batch to another. The variation in the C/N ratio of wheat straw could be due to the age of the straw; the younger the tissues of the straw, the lower the C/N ratio (Hicks, 1928). Cellulose and hemicellulose content of wheat straw were similar for the two batches. The cellulose was between the range of 39–43% and hemicellulose was between the ranges of 28–32% but not all these carbon will be accessible during the anaerobic digestion process. The manure bedded with straw collected has a total solid content between 18% and 26% which makes it suitable for dry digestion compared to other means of handling. This waste also has a C/N of 19:1 which means it can be used directly by farmers for the digestion process; the C/N can also be adjusted slightly using untreated wheat straw to enhance the buffer capacity of the process and also reduce the possibility of substrate or product inhibition (Wang et al., 2011).

Table 1
Characteristics of substrates used during the experiments.

Parameters	Manure bedded with straw	Wheat straw
First Batch		
Total solids (%)	17.81 ± 0.16	91.77 ± 0.02
Volatile solids (%)*	80.23 ± 0.55	92.89 ± 0.11
Moisture (%)	82.19 ± 0.16	8.23 ± 0.02
Ash (%)*	19.77 ± 0.55	7.11 ± 0.11
Total Carbon (%)*	44.57 ± 0.31	51.60 ± 0.06
Total Nitrogen (%)*	2.33 ± 0.03	0.37 ± 0.15
Protein content (%)	14.56 ± 0.03	2.31 ± 0.15
C/N	19	139
Bulk density (kg/m^3)	907.1 ± 7.83	89.5 ± 2.89
Extractives (%)*	ND	12.17
Total Lignin (%)*	ND	15.27 ± 0.71
Cellulose (%)*	ND	39.25 ± 0.03
Hemicellulose (%)*	ND	31.99 ± 0.08
Second Batch		
Total solids (%)	25.84 ± 0.92	89.07 ± 0.08
Volatile solids (%)*	77.21 ± 2.74	94.96 ± 0.14
Moisture (%)	74.16 ± 0.92	10.93 ± 0.08
Ash (%)*	22.79 ± 2.74	5.04 ± 0.14
Total Carbon (%)*	42.89 ± 1.52	52.76 ± 0.08
Total Nitrogen (%)*	2.26 ± 0.04	0.77 ± 0.01
Protein content (%)	14.13 ± 0.04	4.81 ± 0.01
C/N	19	69
Bulk density (kg/m^3)	542 ± 26.87	190.47 ± 6.93
pH	8.72 ± 0.83	ND
Extractives (%)*	ND	8.27
Total Lignin (%)*	ND	16.52 ± 0.38
Cellulose (%)*	ND	42.74 ± 0.06
Hemicellulose (%)*	ND	27.99 ± 0.01

Standard deviation based on at least duplicate measurements.
* Dry basis; ND = Not determined; C/N = carbon nitrogen ratio.

3.3. Methane yield and production rate

Fig. 2b shows the cumulative methane production for the three (3) batch digestion processes during the whole experiment and the methane production rates were estimated from the cumulative methane production as shown. For the first digestion process (22% TS of feedstock; 10% TS in reactor), there was a lag phase of 10 days and afterwards the methane production increased steadily indicating the beginning of the exponential growth. The digestion process lasted for 136 days and methane yield of 183 NmlCH_4/gVS was obtained. Patinvoh et al. (2017) reported yield of 163 NmlCH_4/gVS using plug flow reactor when manure bedded with straw at 22%TS and C/N of 16.8 was used. However, in the current study using textile reactor there was slight increase of 12% in the methane yield obtained, probably due to increase in C/N by addition of untreated wheat straw. Wang et al. (2013) also indicated that addition of even small amounts of co-substrates altered the bacteria communities within the reactors, and thereafter increased the yield. This shows that increasing the C/N ratio slightly with addition of fresh wheat straw is more favorable to the digestion process. During the second digestion process (27% TS and 12% TS in feedstock and reactor respectively), the digestion started almost immediately (no lag phase) showing the acclimatization of microbial communities to the feedstock resulting in an increase in methane yield by about 13% compared to that during the first digestion, while the degradation time was reduced from 136 days to 96 days. After a long-term acclimatization of 232 days (first and second digestion), the VS ratio for inoculum to feedstock was reduced from 1 to 0.5 thereby increasing the TS in the reactor to 17%. The biogas production started almost immediately even here, although there was a slight reduction in the methane yield at the beginning compared to that during the second digestion. Then, there was steady increase in the methane yield resulting in about 58% increase compared to that obtained in the first digestion. Accordingly, the degradation time was reduced from 136 days to 92 days. Furthermore, the methane production rates increased with gradual increase in the TS which shows gradual acclimatization of microbial communities to the conditions in the reactor and probably new predominant microbial community for high solid-state digestion were formed (Li et al., 2013). However, the degree of digestion was low; only 29% of the organic matter was broken down and converted to biogas during the digestion period. This could be due to lack of internal mixing and slow degradation rate of the feedstocks (manure with straw and untreated wheat straw). An approximate degree of digestion of 35% has been reported for cattle manure (Schnürer & Jarvis, 2010) which is low compared to readily degradable substrates. The residue can undergo post storage stage where biogas production can continue over a long period of time.

The results showed that farmers can only treat small volume of wastes at the beginning which will also result to low biogas yield and longer degradation time. Then, the volume of wastes can be increased and subsequent digestion processes will results to higher methane yield and shorter degradation time.

Table 2
Composition and experimental results at different batch digestion setup Volume and cost of textile reactor needed for the different scenarios and scales.

Setup	Feedstock (g)		Inoculum (g)	Total Feedstock		Reactor Mixture TS (%)		Reactor Mixture VS (%)*		Cumulative Methane yield (Nml/gVS)
	Manure with straw	Wheat straw		TS (%)	C/N	In	Out	In	Out	
Unacclimatized inoculum	3478	235	17425	22	25	10	7.97 ± 0.02	66	65.10 ± 0.15	182.94
Acclimatized (Low TS)	5000	86	20617	27	20	12	9.60 ± 0.12	69.2	64.60 ± 0.06	207.03
Acclimatized (High TS)	7021	473	14516	30	25	17	13.39 ± 1.15	72.4	65.5 ± 0.16	289.86
	Volume of textile reactor (m^3)						Cost of textile reactor ($)			
Scenario	3 tons/year	5200 tons/year	51000 tons/year				3 tons/year	5200 tons/year	51000 tons/year	
Unacclimatized inoculum	19	33 687	330 392				2 915	3 368 698	23 127 405	
Acclimatized (Low TS)	14	24 202	237 367				2 094	2 420 208	16 615 659	
Acclimatized (High TS)	9	14 871	145 853				1 287	1 487 124	10 209 675	

* Dry basis.

Table 3
Analysis of digestate from dry anaerobic digestion.

Parameter	Digestate residue		
pH		8.01–8.06	
Total carbon (%)*		34.36–36.23	
TS (%)*		7.97–13. 39	
VS (%)*		61.84–65.15	
	Unit	Liquid fraction[a]	Solid fraction[a]
Total Nitrogen	g/L	2.45–2.8	6.77–9.22 (mg/g)
Ammonium nitrogen	g/L	1.25–1.55	ND
Potassium	g/L	1.19–4.29	0.025–0.051
Phosphorus	mg/L	10.03–30.54	14.71–36.52
Calcium	mg/L	15–50.50	48.33–64.33
Magnesium	mg/L	3.35–60	13.4–16.73
Copper	mg/L	0.13–0.19	0.14–0.35
Iron	mg/L	3–5.5	ND
Zinc	mg/L	0.11–0.19	0.33–0.69
Nickel	mg/L	0.28–0.37	0.01
Chromium	mg/L	< 0.001	0.02–0.05
Cadmium	mg/L	< 0.001	< 0.001

[a] Fresh matter; ND = not determined.
* Dry basis.

3.4. Digestate quality

The pH of the digestate was slightly alkaline as shown in Table 3; this will increase the buffering capacity of the soil as many agricultural lands are mostly acidic. The liquid fraction of the digestate has higher nitrogen and potassium content compared to the solid fraction as shown in Table 3. Möller et al. (2010), also reported high nitrogen and potassium content in liquid fraction after separation of the biogas effluent. The digestate (liquid fraction) contains an average of 2.63 g/L of total nitrogen and 1.4 g/L of ammonium nitrogen which is a major benefit of using digestate as bio-fertilizer because the ammonium nitrogen can be directly taking up by the plants for their growth (Börjesson & Berglund, 2007; Svensson et al., 2004). The digestate (liquid fraction) contain a higher amount of potassium (an average of 2.74 g/L) which is also a major macronutrient needed for plant growth. However, the phosphorus content of the digestate is low probably part of the phosphorus has been lost during the digestion process (Möller & Müller, 2012) and as such phosphorus or phosphate can be added as supplement to avoid phosphorus deficiency in the soil or the digestate supplied to soil lacking majorly nitrogen and potassium. Additionally, concentration of heavy metals (Cadmium, Chromium, Nickel, Zinc and Copper) in the digestate is low; the concentration did not exceed the quality standards (Al Seadi & Lukehurst, 2012) and as such the digestate could be used as bio-fertilizer. The solid fraction can as well be used on the soil to improve the soil structure; retain nutrients and avoid leaching. Therefore, the whole digestate can be used as bio-fertilizer or the solid fraction post treated using aerobic composting process thereby closing the production cycle (Fouda, 2011; Meissl & Smidt, 2007; Poggi-Varaldo et al., 1999).

3.5. Economic evaluation

For biogas to be used as a means for handling manure and straw waste, it has to be more profitable than other possible methods of handling the waste. Several techno-economic analysis have been done in comparing the profitability of biogas production against other methods such as; replacing kerosene or LPG utilization with biogas at household level (Rajendran et al., 2013), biogas for electricity generation (Gebrezgabher et al., 2010), biogas for combined heat and power generation (Trendewicz & Braun, 2013). However, economic analysis of replacing composting or waste collection by waste managers with dry-AD has not yet been reported in literature. In this work, economic profitability was measured by the payback period, net present value and the internal rate of return. The economics associated with replacing composting and waste collection by waste managers with dry anaerobic digestion was investigated for three different dry digestion scenarios; no acclimatization of the inoculum and solid waste with a density of 907 kg/m^3 (scenario A), short acclimatization of the inoculum and solid waste with a density of 542 kg/m^3 (scenario B) and longer acclimatization of the inoculum and solid waste with a density of 542 kg/m^3 (scenario C). The analyses were performed at three different scales corresponding to solid waste generation from typical small, mid and large scale farms.

The volume of the textile bioreactors needed for the different scales and scenarios were calculated as discussed in Section 2.6 and are shown in Table 2. How the reactor volumes can be used for gathering waste, dry-AD, digestate storage and biogas storage is shown in Fig. 2a and was discussed in Section 3.1. Building on that, this is how the reactor volumes will be allocated for different purposes: For the first anaerobic digestion batch; 6 % (scenario A), 16% (scenario B), 32% (scenario C) of the total reactor volume is needed for storing the daily produced farm waste prior to dry anaerobic digestion at all scales, while 6% (scenario A), 10% (scenario B), 16% (scenario C) of the total reactor volume is needed for storing the digestate after the completion of the dry-AD. For the subsequent batches 6% (scenario A), 10% (scenario B), 16% (scenario C) of the total reactor volume would be needed for storing the daily produced waste, while 6% (scenario A), 10% (scenario B), 16% (scenario C) of the total reactor volume would be needed for storing the digestate after the dry-AD. Details on how to perform this kind of calculations and optimal reactor sizing can be found in literature (Mähnert & Linke, 2009). The investment cost of the textile bioreactor (Table 2) were calculated using; $150/volume for small scale (in volumes of 2 m^3) (Rajendran et al., 2013), $100/volume for mid-scale (volume in 100s of m^3) and $70/volume for large-scale (volume in 1000s of m^3) (Osadolor et al., 2014). The total capital investment needed for dry-AD for the different scenarios and scales with the annual cost associated with managing the waste either through composting or through waste managers is shown in Table 4.

Table 4
Cost associated different waste management option for handling solid waste and revenue from biogas sales.

Cost associated with different solid waste management approach			
Total Investment cost needed for biogas production ($)			
Scenario	Small scale	Mid-scale	Large-scale
A	2980	3 518 040	24 257 700
B	3032	3 518 040	24 957 700
C	1967	2 318 040	16 557 700
Total annual operation cost needed for biogas production ($)			
Scenario	Small scale	Mid-scale	Large-scale
A	152	170 007	1 155 007
B	155	170 007	1 190 007
C	102	110 007	770 007
Revenue from biogas sales ($)			
Scenario	Small scale	Mid-scale	Large-scale
A	0	42	409
B	0	53	519
C	0	83	817
Annual composting cost	1200	504000	3417000
Annual cost when waste managers are used	1300	1250000	12300000

A dense substrate without innoculum acclimatization; B less dense substrate with short innoculum acclimatization; C less dense substrate with long innoculum acclimatization.

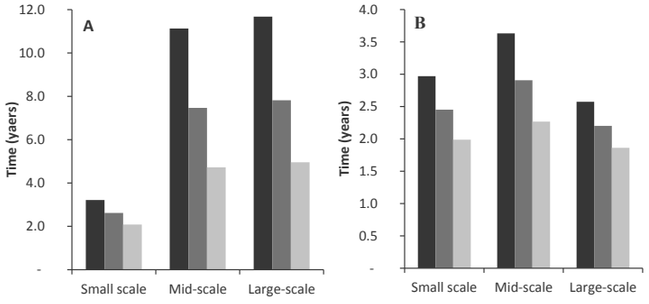

Fig. 3. Payback period if dry anaerobic digestion is used to replace compost (A) or waste collection by waste managers (B) when there is; no inoculum acclimatization and dense feedstock (■), short inoculum acclimatization with less dense feedstock (■) and long inoculum acclimatization with less dense feedstock (■).

3.5.1. Payback period

The payback period for replacing composting and using waste managers are shown in Fig. 3 for the different scenarios considered. The initial project delay time for the first anaerobic digestion batch completion for scenario A was 0.37 years (calculated by dividing the number of needed for batch completion by 365), 0.64 for scenario B and 0.89 for scenario C. Replacing composting or the use of waste managers by dry-AD in the textile reactor always resulted in a payback period less than the proposed project life of 15 years. In addition, it can be observed that the longer the acclimatizing time of the inoculum, the shorter the payback period. Another possible explanation for the reduction in the payback period is that more amount of waste per year is processed in scenario B compared to A, and scenario C processes the most amount of waste per year. Considering the result for small scale, the payback period for all dry anaerobic digestion scenarios considered were all less than 3.5 years, indicating that using the textile bioreactor for dry digestion is more profitable than composting or waste collection by waste managers for small scale farmers. As the farm scale increased, dry anaerobic digestion in the textile bioreactor would still be the most profitable method of handling solid waste, particularly dry anaerobic digestion after long inoculum acclimatization which had a payback period of 5 years or less for all cases considered.

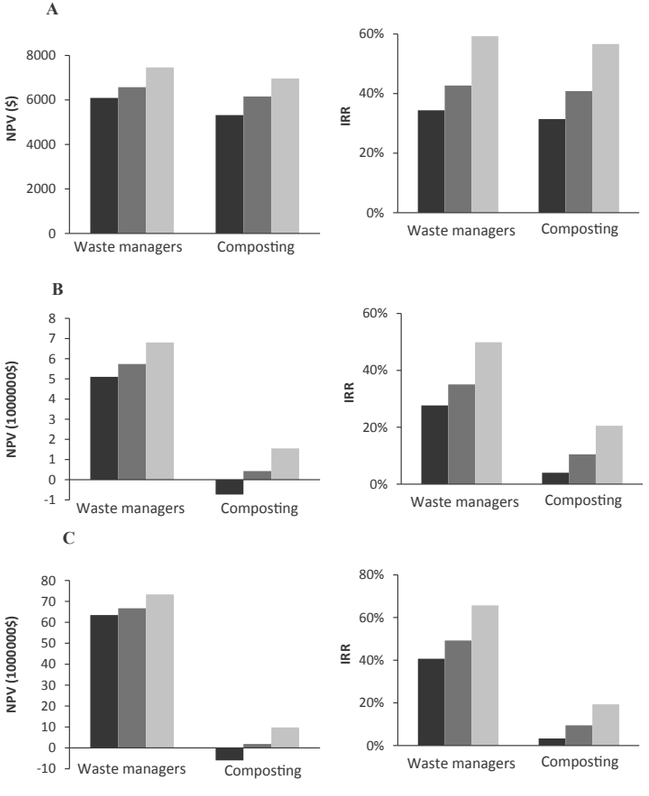

Fig. 4. The net present value and the corresponding internal rate of return analysis for replacing waste collection by waste managers and composting with dry anaerobic digestion for; small scale (A), mid-scale (B) and large-scale(C) when is; no inoculum acclimatization and dense feedstock (■), short inoculum acclimatization with less dense feedstock (■) and long inoculum acclimatization with less dense feedstock (■).

3.5.2. Net present value and internal rate of return

The result for the net present value (NPV) and internal rate of return (IRR) calculated for the different scenarios using an interest rate of 7.8% are shown in Fig. 4. For the first year, the annual profit was multiplied by 0.627 for scenario A (1 – delay fraction used for PBP

Table 5
Sensitivity analysis on replacing composting with dry anaerobic digestion.

	Replacing composting with dry anaerobic digestion					
	Base case					
	Net present value (NPV) ($)			Internal rate of return (IRR) (%)		
	Small scale	Mid-scale	Large scale	Small scale	Mid-scale	Large scale
Scenario A	5320	−733,125	−5,948,401	31.44	4.00	3.32
Scenario B	6152	428,723	1,874,533	40.83	10.47	9.48
Scenario C	6959	1,553,297	9,783,711	56.62	20.53	19.31
	20% less textile reactor cost					
	NPV ($)			IRR (%)		
	Small scale	Mid-scale	Large scale	Small scale	Mid-scale	Large scale
Scenario A	6086	151,842	127,233	39.86	8.7	7.91
Scenario B	6698	1,059,041	6,373,146	50.09	15.38	14.37
Scenario C	7291	1,937,377	12,420,569	67.1	26.02	24.48
	20% more textile reactor cost					
	NPV ($)			IRR (%)		
	Small scale	Mid-scale	Large scale	Small scale	Mid-scale	Large scale
Scenario A	4555	−1,618,091	−12,024,036	25.47	0.26	−0.37
Scenario B	5607	−201,595	−2,281,603	34.2	6.68	5.95
Scenario C	6627	1,169,216	7,146,853	48.95	16.37	15.35
	20% less auxiliary equipment cost					
	NPV ($)			IRR (%)		
	Small scale	Mid-scale	Large scale	Small scale	Mid-scale	Large scale
Scenario A	5343	−693,487	−5,559,649	31.61	4.20	3.60
Scenario B	6174	467,841	2,429,422	41.09	10.72	10.00
Scenario C	6981	1,591,915	10,162,472	57.09	20.97	19.91
	20% more auxiliary equipment cost					
	NPV ($)			IRR (%)		
	Small scale	Mid-scale	Large scale	Small scale	Mid-scale	Large scale
Scenario A	5298	−772,762	−6,337,153	31.26	3.81	3.05
Scenario B	6130	389,606	1,662,121	40.57	10.21	9.29
Scenario C	6937	1,514,678	9,404,950	56.15	20.11	18.73
	20% less waste generation					
	NPV ($)			IRR (%)		
	Small scale	Mid-scale	Large scale	Small scale	Mid-scale	Large scale
Scenario A	4331	−584,030	−4,758,721	31.8	4.02	3.32
Scenario B	4994	345,376	1,636,617	41.24	10.49	9.64
Scenario C	5637	1,244,965	7,826,969	57.1	20.55	19.31
	20% more waste generation					
	NPV ($)			IRR (%)		
	Small scale	Mid-scale	Large scale	Small scale	Mid-scale	Large scale
Scenario A	6496	−876,045	−7,138,081	31.8	4.02	3.32
Scenario B	7491	518,064	2,454,926	41.24	10.49	9.64
Scenario C	8456	1,867,448	11,740,453	57.1	20.55	19.31

A dense substrate without innoculum acclimatization; B less dense substrate with short innoculum acclimatization; C less dense substrate with long innoculum acclimatization.

calculation), 0.36 for scenario B and 0.11 for scenario C. Considering waste disposal through waste managers, irrespective of inoculum acclimatization, dry anaerobic digestion is more profitable as evident by the positive NPV's. In addition, the IRR for all scales and scenarios considered were from 30.1 to 69.6%, implying that dry anaerobic digestion using the textile reactor would remain the most profitable option for all farm scale with or without inoculum acclimatization until the interest rate in that country exceeds the IRR. Currently there are only three countries in the world where the interest rate exceeds 30%, and there is no country with an interest rate greater than 50% (World Bank, 2017b) so the odds of solid waste management by using waste managers becoming more profitable than dry anaerobic digestion in the textile reactor is rear.

Comparing dry-AD to composting (Fig. 4), both the scale of waste generation and the duration inoculum acclimatization influences what option is more profitable. For small scale, irrespective of inoculum acclimatization or the nature of the feed, dry-AD is more profitable than composting as evident by the positive NPV's and IRR greater than 33%. As the scale of waste generation increases, the profitability of dry-AD in the textile reactor over composting increases with the duration of the acclimatization of the inoculum used, as evident by the increasing positive NPV's and the increasing IRR from short to long inoculum acclimatization time at all scales. The minimum IRR for replacing composting with dry anaerobic digestion when long acclimatization is used was 19.3%, this indicates that the NPV would remain positive over a high interest rate range, with it only becoming negative when the interest rate in that country exceeds the IRR. In the cases where composting was found to be a better option than anaerobic digestion because of negative NPV, the IRR were 4% or less indicating that the NPV at those cases is sensitive to the interest rate assumed for the calculations, if an interest rate of 3% was used for the calculations all the NPV's will be positive. A 3% interest rate is feasible because there are many countries whose current interest rate are 3% or less (World Bank, 2017b), using the interest rate of any of those countries would make NPV of replacing composting with dry anaerobic digestion positive for all scale with or without inoculum acclimatization.

3.6. Sensitivity analysis

The result from the sensitivity analysis calculations for replacing composting with dry-AD is shown in Table 5. At small scale, the NPVs were insensitive to a ± 20% change in reactor cost, equipment cost and the amount of waste generated. For cases that had a positive or negative NPV in the base scenario, a ± 20 % change in the cost of equipment and amount of waste generated was not sufficient in changing the sign notation of the NPV of any of the base cases. So, the profitability criteria were not sensitive to a ± 20% change in the cost of equipment and amount of waste generated.

The profitability criteria for replacing composting with dry anaerobic digestion at mid and large scale was sensitive to changes in the cost of the textile reactor when short or no inoculum acclimatization time was used. For the base case, the NPV of using scenario A for replacing composting with dry anaerobic digestion were negative at mid (IRR = 4 %) and large scale (IRR = 3.32%), however, a 20% reduction in the cost of the textile reactor made the NPV positive for both mid (IRR = 8.7%) and large scale (IRR = 7.91%) scenarios. A 20% increase in the cost of the textile reactor resulted in the positive NPV at the base case of scenario B at mid (IRR = 10.47) and large scale (IRR = 9.48) becoming negative for both mid (IRR = 6.68%) and large scale (IRR = 5.95%). The sensitivity of the textile reactor cost for mid- and large-scale scenario A and B cases would mean that using other reactors more expensive than the textile reactor for dry-AD would not be economical when compared with composting. However, replacing composting with dry anaerobic digestion after long acclimatization (scenario C) was not sensitive to a 20% change in the cost of the textile reactor at all scales, as seen from the positive NPV in all cases and high IRR values ranging from 15.35% to 67.1%. This indicates that dry anaerobic digestion of solid farm waste in the textile reactor after a long period of inoculum acclimatization is a more economical way of handling the waste than composting.

4. Conclusion

Textile-based bioreactor is a cost-effective solution and the technology is simple to operate. It can be accessed easily by developing countries where required expertise may not be available. For small scale farm, irrespective of inoculum acclimatization or the nature of the feed, dry-AD is more profitable than composting as evident by the positive NPV's and IRR greater than 33%. A long acclimatization period makes dry-AD in the textile reactor more profitable than composting for small, mid and large scale farms when handling solid waste as evident by the positive NPV's and IRR greater than 19%.

Acknowledgements

This work was financially supported by Västra Götaland Region (Sweden), Smart textile (Sweden) and FOV Fabrics, AB (Sweden). The authors acknowledge Mostafa Jabbari for assisting in making the heat exchanger for the reactor.

References

AAFRD, 2005. Manure Composting Manual. Alberta Agriculture, Food and Rural Development. Edmonton, Alberta, Canada T6H 5T6. http://www1.agric.gov.ab.ca/$department/deptdocs.nsf/all/agdex8875/$file/400_27-1.pdf?OpenElement, Accessed 2015/09/21.
Al Seadi, T., Lukehurst, C., 2012. Quality management of digestate from biogas plants used as fertiliser. IEA Bioenergy 4–36.
Angelidaki, I., Alves, M., Bolzonella, D., Borzacconi, L., Campos, J.L., Guwy, A.J., Kalyuzhnyi, S., Jenicek, P., Van Lier, J.B., 2009. Defining the biomethane potential (BMP) of solid organic wastes and energy crops: a proposed protocol for batch assays. Water Sci. Technol. 59 (5), 927–934.
APHA-AWWA-WEF, 2005. Standard Methods for the Examination of Water and Wastewater 21st ed, American Public Health Association (APHA), American Water Works Association (AWWA), Water Environment Federation (WEF), Washington DC.
Bergeron, P., 1996. Bioethanol market forces. In: Wyman, C. (Ed.), Handbook on bioethanol: production and utilization. CRC Press, pp. 61–88.
Bolzonella, D., Innocenti, L., Pavan, P., Traverso, P., Cecchi, F., 2003. Semi-dry thermophilic anaerobic digestion of the organic fraction of municipal solid waste: focusing on the start-up phase. Bioresour. Technol. 86 (2), 123–129.
Börjesson, P., Berglund, M., 2007. Environmental systems analysis of biogas systems—Part II: the environmental impact of replacing various reference systems. Biomass Bioenergy 31 (5), 326–344.
Chattopadhyay, S., Dutta, A., Ray, S., 2009. Municipal solid waste management in Kolkata, India–a review. Waste Manage. 29 (4), 1449–1458.
Chen, Y.-T., 2016. A cost analysis of food waste composting in Taiwan. Sustainability 8 (11), 1210.
Deng, L., Chen, C., Zheng, D., Yang, H., Liu, Y., Chen, Z., 2016. Effect of temperature on continuous dry fermentation of swine manure. J. Environ. Manage. 177, 247–252.
Fouda, S.E.-S., 2011. Nitrogen availability of biogas residues (PhD Dissertation), Technical University of München.
Gebrezgabher, S.A., Meuwissen, M.P.M., Prins, B.A.M., Lansink, A.G.J.M.O., 2010. Economic analysis of anaerobic digestion—a case of Green power biogas plant in The Netherlands. NJAS-Wagen. J. Life Sci. 57 (2), 109–115.
Guendouz, J., Buffière, P., Cacho, J., Carrère, M., Delgenes, J.P., 2010. Dry anaerobic digestion in batch mode: Design and operation of a laboratory-scale, completely mixed reactor. Waste Manage. 30 (10), 1768–1771.
Gunaseelan, N.V., 2009. Biomass estimates, characteristics, biochemical methane potential, kinetics and energy flow from Jatropha curcus on dry lands. Biomass Bioenergy 33 (4), 589–596.
Haug, R.T., 1993. Feed conditioning – physical and chemical. In: The Practical Handbook of Compost Engineering. Taylor & Francis, pp. 247–257.
Hicks, P.A., 1928. Distribution of carbon/nitrogen ratio in the various organs of the wheat plant at different periods of its life history. New Phytol. 27 (2), 108–116.
Ho, T.L.T., Cao, T.S., Luong, D.A., Vu, D.T., Kurosawa, K., Egashira, K., 2013. Evaluation of water pollution caused by different pig–farming systems in Hungyen province of Vietnam. Kyushu Univ. Int. Reposit 58, 159–165.
Hoornweg, D., Thomas, L., Otten, L. 1999. Composting and its applicability in developing countries. World Bank working paper series, 8.
Karak, T., Bhagat, R.M., Bhattacharyya, P., 2012. Municipal solid waste generation, composition, and management: the world scenario. Crit. Rev. Environ. Sci. Technol. 42 (15), 1509–1630.
Kossmann, W., Pönitz, U., Habermehl, S., Hoerz, T., Krämer, P., Klingler, B., Kellner, C., Wittur, W., Klopotek, F., Krieg, A. 1999. Biogas Digest, Volume II–Biogas–Application and Product Development. Information and Advisory Service on Appropriate Technology, Eschborn.
Li, A., Chu, Y., Wang, X., Ren, L., Yu, J., Liu, X., Yan, J., Zhang, L., Wu, S., Li, S., 2013. A pyrosequencing-based metagenomic study of methane-producing microbial community in solid-state biogas reactor. Biotechnol Biofuels 6.
Li, Y., Park, S.Y., Zhu, J., 2011. Solid-state anaerobic digestion for methane production from organic waste. Renew. Sustainable Energy Rev. 15 (1), 821–826.
Makádi, M., Tomócsik, A., Orosz, V., 2012. Digestate: a new nutrient source – review. In: Kumar, D.S. (Ed.), Biogas. InTech.
Mata-Alvarez, J., Macé, S., Llabrés, P., 2000. Anaerobic digestion of organic solid wastes. An overview of research achievements and perspectives. Bioresour. Technol. 74.
Meissl, K., Smidt, E., 2007. High quality composts by means of cocomposting of residues from anaerobic digestion. Compost Sci. Util. 15 (2), 78–83.
Mähnert, P., Linke, B., 2009. Kinetic study of biogas production from energy crops and animal waste slurry: effect of organic loading rate and reactor size. Environ. Technol. 30 (1), 93–99.
Möller, K., Müller, T., 2012. Effects of anaerobic digestion on digestate nutrient availability and crop growth: a review. Eng. Life Sci. 12 (3), 242–257.
Möller, K., Schulz, R., Müller, T., 2010. Substrate inputs, nutrient flows and nitrogen loss of two centralized biogas plants in southern Germany. Nutr. Cycl. Agroecosys. 87 (2), 307–325.
Osadolor, O.A., Lennartsson, P.R., Taherzadeh, M.J., 2014. Introducing textiles as material of construction of ethanol bioreactors. Energies 7 (11), 7555–7567.
Patinvoh, R.J., Kalantar Mehrjerdi, A., Sárvári Horváth, I., Taherzadeh, M.J., 2017. Dry fermentation of manure with straw in continuous plug flow reactor: reactor development and process stability at different loading rates. Bioresour. Technol. 224, 197–205.
Poggi-Varaldo, H.M., Trejo-Espino, J., Fernandez-Villagomez, G., Esparza-Garcia, F., Caffarel-Mendez, S., Rinderknecht-Seijast, N., 1999. Quality of anaerobic compost from paper mill and municipal solid wastes for soil amendment. Water Sci. Technol. 40 (11–12), 179–186.
Rajendran, K., Aslanzadeh, S., Johansson, F., Taherzadeh, M.J., 2013. Experimental and economical evaluation of a novel biogas digester. Energy Convers. Manage. 74, 183–191.
Rowse, L.E., 2011. Design of small scale anaerobic digesters for application in rural developing countries. University of South Florida.
Ruggieri, L., Cadena, E., Martínez-Blanco, J., Gasol, C.M., Rieradevall, J., Gabarrell, X., Gea, T., Sort, X., Sánchez, A., 2009. Recovery of organic wastes in the Spanish wine industry. Technical, economic and environmental analyses of the composting process. J. Clean. Prod. 17 (9), 830–838.
Schnürer, A., Jarvis, A. 2010. Microbiological Handbook for Biogas Plants. Swedish Waste Management U2009:03.
Sluiter, A., Hames, B., Ruiz, R., Scarlata, C., Sluiter, J., Templeton, D., Crocker, D., 2011. Determination of structural carbohydrates and lignin in biomass. laboratory analytical procedure. NREL/TP-510-42618.
Sluiter, A., Ruiz, R., Scarlata, C., Sluiter, J., Templeton, D., 2008. Determination of Extractives in Biomass. Laboratory Analytical Procedure (LAP). NREL/TP-510-42619.
Strange, K., 2002. Overview of waste management options: their efficacy and acceptability. Issues Environ. Sci. Technol. 18, 1–52.
Svensson, K., Odlare, M., Pell, M., 2004. The fertilizing effect of compost and biogas residues from source separated household waste. J. Agric. Sci. 142 (4), 461–467.
Trendewicz, A.A., Braun, R.J., 2013. Techno-economic analysis of solid oxide fuel cell-based combined heat and power systems for biogas utilization at wastewater treatment facilities. J. Power Sources 233, 380–393.
U.S Energy Information Administration. 2017. U.S. Price of Natural Gas Sold to Commercial Consumers. https://www.eia.gov/dnav/ng/hist/n3020us3m.htm, Accessed 2017/05/02.
Wang, W., Xie, L., Chen, J., Luo, G., Zhou, Q., 2011. Biohydrogen and methane production by co-digestion of cassava stillage and excess sludge under thermophilic condition. Bioresour. Technol. 102 (4), 3833–3839.
Wang, W., Xie, L., Luo, G., Zhou, Q., 2013. Enhanced fermentative hydrogen production from cassava stillage by co-digestion: The effects of different co-substrates. Int. J. Hydrogen Energy 38 (17), 6980–6988.
World Bank Deposit interest rate: Nigeria, 2017. http://data.worldbank.org/indicator/FR.INR.RINR?end=2015&locations=NG&page=3&start=2008&view=chart, Accessed 2017/05/01.
World Bank, 2016. A Global Review of Solid Waste Management; Annex E: Estimated Solid Waste Management Costs. http://siteresources.worldbank.org/INTURBANDEVELOPMENT/Resources/336387-1334852610766/AnnexE.pdf, Aceesed 2017/05/02.
World Bank. 2017b. Rear interest rate. http://data.worldbank.org/indicator/FR.INR.RINR?end=2015&start=1997&view=map, Accesed 2017/05/05.
Zhang, Y., Ghaly, A.E., Li, B., 2012. Physical properties of wheat straw varieties cultivated under different climatic and soil conditions in three continents. Am. J. Eng. Appl. Sci. 5 (2), 98–106.
Zhou, C., Liu, Z., Huang, Z.-L., Dong, M., Yu, X.-L., Ning, P., 2015. A new strategy for co-composting dairy manure with rice straw: Addition of different inocula at three stages of composting. Waste Manage. 40, 38–43.

PAPER VI

Effect of media rheology and bioreactor hydrodynamics on filamentous fungi fermentation of lignocellulosic and starch-based substrates under pseudoplastic flow conditions.

Effect of media rheology and bioreactor hydrodynamics on filamentous fungi fermentation of lignocellulosic and starch-based substrates under pseudoplastic flow conditions

Osagie A. Osadolor [1,*], Mostafa Jabbari [1], Ramkumar B. Nair [2], Patrik R. Lennartsson [1] and Mohammad J. Taherzadeh [1]

[1] Swedish Centre for Resource Recovery, University of Borås, SE 501 90 Borås, Sweden; Emails: mostafa.jabbari@hb.se; patrik.lennartsson@hb.se; mohammad.taherzadeh@hb.se

[2] Mycorena AB, Stena Center 1A, 411 92, Gothenburg, Sweden
Email: ram@mycorena.com

* Corresponding author
alex.osagie@hb.se
Tel.: +46-33-435-4620
Fax: +46-33-435-4008

Abstract

Reported rheology models are based on substrates that are Newtonian. However, several polymeric substrates used for fermentation display a pseudoplastic flow behavior at high solid content, with media rheology and bioreactor hydrodynamics influencing the fermentation effectiveness. This was investigated using a 1:1 mixture of hydrolyzed wheat straw and wheat-based thin stillage and filamentous fungi as inoculum in bubble column, airlift and a horizontal hybrid tubular/bubble column (textile bioreactor) bioreactors. During the growth phase, the rheological models showed that the consistency index was mainly dependent on biomass growth (R^2 0.99) while the flow behavior index depended on both biomass growth and the suspended solid in the fermentation broth (R^2 0.99). Oxygen transfer rate above 0.356 mmol-O_2/L/h was needed for growing fungi in the media with a cube-root growth rate constant of 0.03 $g^{1/3}/L^{1/3}$/h. At 1.4 VVM aeration rate the textile bioreactor performed better than the other bioreactors with minimal foaming, ethanol yield of 0.22 ± 0.01 g/g, substrate consumption rate of 0.38 g/L/h and a biomass yield of 0.47 ± 0.01 g/g after 48 h of fermentation. Operating the bioreactors with air flowrate to cross-sectional area ratio of 8.75×10^{-3} ($m^3/s/m^2$) or more led to sustained foaming.

Keywords: Foaming; Oxygen transfer rate; Rheology model; Fungi growth kinetics; Viscosity;

1. Introduction

The properties of the media in a bioreactor, such as temperature or concentration, can only be changed as a result of the motion of components in the media or the entire media. Hence the nature of fluid flow (rheology) in the bioreactor is important both in providing process conditions for optimizing productivity and in efficient bioreactor design (Doran, 2013b; Gögus et al., 2006; Papagianni, 2004; Verma et al., 2007). In addition to rheology, the prevailing bioreactor hydrodynamic conditions also influences the efficiency of the bioreactor (Olmos et al., 2013; Papagianni, 2004), as it influences the mass transfer rate in the bioreactor, which in turn affects the product yield (Koutinas et al., 2003). A proper understanding of the rheological and hydrodynamic behavior during fermentation is important because rheological and hydrodynamic conditions can change with changes in substrate composition, biomass concentration and growth pattern, process conditions and process scale-up which in turn can affect the efficiency of the fermentation process.

For several fermentative-based production processes such as biogas or bioethanol production, the bioreactor content is usually composed of solid liquid and gases. For proper mixing, mass transfer or aeration to be attained in those bioreactors, the resistance to flow (viscosity) has to be accounted for. The viscosity during the fermentation process could be constant or change with time. For bioreactor with filamentous microorganisms, the media viscosity change with time following the pseudoplastic model, while bioreactors with other microorganisms become pseudoplastic after exceeding a biomass concentration threshold (Núñez-Ramírez et al., 2012; Olmos et al., 2013; Serrano-Carreón et al., 2015). The consistency index (K) and the flow behavior index or power law index (n) is used for describing the rheological behavior of pseudoplastic fluid. As the media viscosity change with biomass concentration, several authors report the consistency index and flow behavior index in the bioreactor as a function of the biomass concentration (Kumar & Dubey, 2017; Pamboukian & Facciotti, 2005; Queiroz et al., 1997). The reported rheology models were

based on substrates that were Newtonian, however, several polymeric substrates used for fermentation display a pseudoplastic flow from the beginning, which needs to be factored into the rheological models.

Several bioreactor designs such as the continuous stirred tank bioreactor, the bubble column bioreactor, the airlift bioreactor with unique hydrodynamic conditions have been introduced overtime to aid both in overcoming the resistance due to high media viscosity of the pseudoplastic fermentation broth and to provide good conditions for microbial growth (Doran, 2013b). The airlift and bubble column bioreactors were introduced for fermentation applications with shear sensitive microorganisms such as filamentous fungi were mixing is carried out without mechanical stirrers (Kadic & Heindel, 2014). For fungi biomass production, aerobic fermentation is needed and a high oxygen transfer rate (OTR) is needed to eliminate the possibility of oxygen mass transfer limitation. Increasing the oxygen transfer rate into bioreactors also increases the tendency of foam formation and stabilization in the bioreactor which can affect productivity and yield (Delvigne & Lecomte, 2010). Overcoming this challenge is important as several important fermentation substrates such lignocellulosic or starch-based feedstock would have high viscosity at high solid content (Nair et al., 2018).

In this work, rheological and hydrodynamic studies were carried out on the fermentation of a pseudoplastic substrate composed of hydrolyzed wheat straw and thin stillage using a filamentous fungi. The effect of the pseudoplastic nature of the substrate on the conventional rheological model was examined. Fermentation experiment were scaled up in three different bioreactor designs; a bubble column bioreactor, an airlift bioreactor and a bioreactor hybrid design between a horizontal tubular bioreactor and a bubble column (hereafter referred to as a textile bioreactor) which previously introduced and developed (Osadolor et al., 2015; Osadolor et al., 2014). Bioreactor hydrodynamic conditions for efficient OTR with minimized foaming for a fungal based fermentation of a pseudoplastic substrate was reported for the first time.

2. Materials and Methods

2.1. Microbial culture

A fungal strain *Neurospora intermedia* CBS 131.92 (Centraalbureau voor Schimmelcultures, Netherlands), an edible ascomycete, was used in this study (Nair & Taherzadeh, 2016). The fungal strain was maintained and inoculum preparation was followed using the methodology that was previously described elsewhere (Osadolor et al., 2017). Inoculation was carried out either as fungal spores or as fungal biomass. A fungal spore concentration of $5.7 \pm 1.8 \times 10^5$ spores/mL was used for inoculating shake flask media using 3-5 mL spore suspension per L medium, while mycelial filamentous fungi biomass concentration 0.3 ± 0.1 g/L (dry weight) was used for inoculating the airlift, bubble column and textile bioreactor.

2.2. Substrate

Wheat straw was pretreated in a 30 L one-step vertical plug-flow continuous reactor using acid concentration of 1.75 % (w/V), residence time of 10 min and temperature of 190 ± 2 °C at Biorefinery Demo Plant (BDP, Örnsköldsvik, Sweden) and stored as previously described (Nair et al., 2017) before the experiments. The composition of the pretreated straw (g/g, dry basis) was; arabinan 0.048 ± 0.013, galactan 0.0053 ± 0.0015, glucan 0.315 ± 0.061, mannan 0.0047 ± 0.0011, and xylan 0.24 ± 0.08. Using cellulase enzyme Cellic CTec2 (Novozymes, Denmark) with 134 FPU /mL activity, the pretreated wheat straw, was hydrolysed using 7 % solid loading, pH of 5.0 ± 0.3, temperature of 50.0 ± 0.2 °C and an enzyme loading of 10 FPU/g substrate dry weight in a water bath.

Thin stillage used for the experiments were supplied from a wheat-based dry mill ethanol plant (Lantmännen Agroetanol, Norrköping, Sweden). This stillage with an initial pH of 3.5, was characterized with the composition of total solids (% w/v) 9.2 ± 0.4 and suspended

solids (% w/v) 2.2 ± 0.6 and (g/L) total nitrogen 4.8 ± 0.5; xylose 0.8 ± 0.1; arabinose 1.5 ± 0.1; glycerol 7.0 ± 0.; lactic acid 1.8 ± 0.1; acetic acid 0.21 ± 0.01 and ethanol 1.2 ± 0.2.

2.3. Fermentation in shake flask

Hydrolyzed wheat straw at solid loading rate of 7.0 % was mixed with thin stillage (total solids 8%) at ratio 1:1 to form the fermentation slurry. The pH of the integrated media was adjusted to 5.5 with either 2 M HCl or 2 M NaOH and the media was autoclaved. Fermentation experiments were carried out using 50 and 100 ml integrated media volume in 250 ml Erlenmeyer flasks for 120 h in an orbital shaking water bath (Grant OLS-Aqua pro, UK) at 150 rpm (with an orbital shaking radius of 9 mm and a flask diameter of 85 mm) at 35 °C. Samples were taken every 24 h, centrifuged and the supernatant frozen at -20°C until analyzed.

2.4. Fermentation in bioreactors

Fermentation experiments were carried out aerobically in a bubble column bioreactor, an airlift bioreactor and a textile bioreactor using the fungus as fermenting microorganism to compare the effect of different bioreactor design on the media fermentation. The air supplied to the bioreactors was filtered using a polytetrafluoroethylene (PTFE) membrane filter (0.1 µm pore size, Whatman, Florham Park, NJ, USA). For the airlift and bubble column bioreactors; fermentation of the media was carried out in a 4.5-L bench scale bioreactor (Belach Bioteknik, Sweden), with a working volume of 3.5 L. To make the bioreactor function as an airlift bioreactor, an internal loop with cylindrical geometry with a diameter 58 mm, height 400 mm and thickness 3.2 mm was put in it. The bioreactor had a sintered stainless-steel air-sparger with a pore size of 90µm at its bottom, which was used for aerating the bioreactor at 1.4 VVM (volume per volume per minute) throughout the duration of the fermentation unless otherwise stated. To maintain the airlift and bubble column bioreactor liquid volume, distilled water equal to the volume of the liquid volume lost due to foaming was added to the bioreactors.

A textile bioreactor with working volume of 3.5 L previously described elsewhere was used for fermentation experiments (Jabbari et al., 2017; Osadolor et al., 2015; Osadolor et al., 2014). A schematic representation of the textile based bioreactor is shown in Fig.1. The diameter of the perforations in the aeration tubing was 0.1 mm. The aeration tubing was coiled into six wounds at the bottom of the bioreactor to maximize oxygen transfer through the bioreactor and increase bubble collision frequency. The details of how this mixing strategy works has previously been described elsewhere (Osadolor et al., 2015).

A schematic representation of the air bubbling pattern in the airlift, bubble column and textile bioreactors is shown in Fig. 2 with the arrows in the figure pointing to the direction the gas bubbles follow in the bioreactors

2.5. Analytical methods

The content of total solids (TS), suspended solids (SS), ash, starch, lignin, and sugars present in the lignocellulosic materials were quantified according to NREL (National Renewable Energy Laboratory) protocols [23-28]. Spore concentration was measured using a Bürker counting chamber (with a depth of 0.1 mm) under light microscope (Carl Zeiss Axiostar plus, Germany). The spore solution was diluted ten times before the measurement, and the spores were counted in a volume of 1/250 µl each. HPLC (Waters 2695, Waters Corporation, U.S.A.) was used to analyze all liquid fractions. A hydrogen-based ion-exchange column (Aminex HPX-87H, Bio-Rad Hercules, CA, U.S.A.) at 60°C with a Micro-Guard cation-H guard column (Bio-Rad) and 0.6 mL/min 5 mM H_2SO_4, used as eluent, was used for the analyses of glucose, ethanol, glycerol and acetic acid. Fungal biomass concentration (dry weight) was determined, at the end of the cultivation, by washing

the fungi biomass with deionized water followed by drying at 105 °C for 24 h before weight measurement. For the kinetic study, biomass was harvested daily to determine the biomass concentration. Error bars were calculated from the standard deviation of two experimental replicates.

2.6. Fungi growth kinetics

Under non-limiting conditions the growth-rate of any microorganism can be described using equation 1 where X is the dry weight of cells (g/L), t is time (h) and μ is the specific growth rate (1/h).

$$dX/dt = \mu X, \tag{1}$$

The specific growth rate can be defined in terms of the maximum specific growth rate μ_m (1/h), saturation constant K_s (g/L) and the substrate concentration S (g/L) using the Monod kinetic model (equation 2).

$$\mu = \mu_m \frac{S}{S + K_S} \tag{2}$$

However, filamentous fungi growth conditions tend to be limiting and the growth kinetics is then best represented using the cube root law (Feng et al., 2010) as shown in equation 3, where X_0 is the starting biomass concentration (g/L), t is time (h) and k_x is a constant ($g^{1/3}/L^{1/3}/h$).

$$X^{1/3} = k_x t + X_0^{1/3} \tag{3}$$

2.7. Rheological studies

Viscosity was measured offline using a Brookfield digital viscometer-model DV-E (Chemical Instruments AB, Sweden). The spindle rotational speed of the viscometer was varied at least four times between 30 and 100 rpm for every viscosity measurement. The spindles used for the analysis were SSA-18 (with a shear rate ranging from 0 – 330 1/s, with apparent viscosity readings ranging from 1.3 to 30000 cP) and SSA-31 (with a shear rate ranging from 0 to 85 1/s, with apparent viscosity readings ranging from 12 and 30000 cP). The rheological parameters (the consistency index K ($Pa.s^n$) and flow behavior index n) were calculated from the apparent viscosity μ_a (Pa.s) using the pseudoplastic power law relationship as shown in equations 4 and 5, where γ is the shearing rate (1/s) and τ is the shear stress (Pa).

$$\mu_a = K\gamma^{n-1} = \frac{\tau}{\gamma} \tag{4}$$

$$Log\ \mu_a = Log\ K + (n-1)\ Log\ \gamma \tag{5}$$

For SSA-18 and SSA-31 spindles the shearing rate can be calculated using equation 6, where ω is the spindle rotational speed (RPM) (Durgueil, 1987).

$$\gamma = \omega\pi/10 \tag{6}$$

2.8. Hydrodynamics study

Using the assumption that oxygen transfer into microorganisms occur through molecular diffusion (Garcia-Ochoa & Gomez, 2009), the oxygen transfer rate (OTR) in mmol-O_2/L/h into a bioreactor can be determined using equation 7, where k_La is the volumetric oxygen mass transfer coefficient (1/h), C^* is the saturated oxygen concentration in the liquid phase (mmol-O_2/L) and C_o is dissolved oxygen concentration in the bulk liquid (mmol-O_2/L).

$$OTR = k_La\ (C^* - C_o) \tag{7}$$

For shake flask, the OTR can be calculated using a modified version of the OTR empirical relationship (equation 8) developed by Auro et al. (1957) when viscosity and shake flask frequency are factored in (Garcia-Ochoa & Gomez, 2009; Liu et al., 2006). Where f is the shake flask frequency (rpm), f_o is the reference shake flask frequency (96 rpm), bi = 1.468, mi = 7.9 × 10-5, V_F is the volume of the flask (mL), ms = - 0.94, V_L is the liquid volume in the flask (mL), bs = 1.657, μ_{ao} is viscosity of the media at reference condition (1 cP), and c is a constant number between -0.7 to -0.4.

$$OTR = 8.46(\mu_a / \mu_{ao})^c (f/f_o)^{0.88} [bi (10^{miV_F}) \quad (10^{-bsV_L V_F^{ms}})] \tag{8}$$

As there are no stirrers to break foams formed in the bioreactors examined, the foam rise velocity (V_{foam}) out of the liquid in the bioreactor is a function of the gas rise velocity (V_g) as shown in equation 8, where G is the air flow rate (m^3/s) and S is the bioreactor cross-sectional area (Delvigne & Lecomte, 2010).

$$V_{foam} = f(V_g) = f(G/S), \tag{9}$$

The oxygen transfer rate to the bioreactor is highly associated with foam formation tendencies in a bioreactor. The relationship between the volumetric oxygen mass transfer coefficient and the operating conditions (air flow rate) in the bioreactors without mechanical stirrers is shown in equation 10, where C and α are constants based on the bioreactor geometry and the hydrodynamic conditions in the bioreactor

$$k_L a = C (G/S)^{\alpha}, \tag{10}$$

3. Results and Discussion

The rheological and hydrodynamic conditions in a bioreactor can affect the productivity and product yield from a bioreactor particularly for bioreactors with viscous media, microbial growth resulting in pseudoplastic flow conditions and under aerobic conditions (Garcia-Ochoa & Gomez, 2009; Núñez-Ramírez et al., 2012; Olmos et al., 2013; Serrano-Carreón et al., 2015). In addition, as the rheological and hydrodynamic conditions in a bioreactor changes during the fermentation process, researchers have used rheological models to describe how the consistency index and the behavior index changes with the biomass concentration (Kumar & Dubey, 2017; Pamboukian & Facciotti, 2005; Queiroz et al., 1997). However, the reported models for fermentation in bioreactors have been for substrates that were Newtonian from the beginning (Pamboukian & Facciotti, 2005; Queiroz et al., 1997). As several polymeric fermentation substrate such as lignocellulosic or starch based feedstocks would follow a pseudoplastic flow model at high solid content or in the presence of several metabolites (Baudez & Coussot, 2001; Um & Hanley, 2008), it is important that this is factored into the rheological models. In terms of bioreactor hydrodynamics, the design of the bioreactor can be used in improving the efficiency of pseudoplastic fermentation processes. The results gotten from rheological and hydrodynamic studies that were carried out on a pseudoplastic media substrate composed of hydrolyzed wheat straw and thin stillage using a filamentous fungus in an airlift, bubble column and textile bioreactor were discussed in the subsequent subsections.

3.1. Viscosity and Fungi growth profile in the integrated media

An important rheological parameter in any bioreactor is the apparent viscosity of the fermentation broth. Knowing the viscosity profile during fermentation can help in maintaining optimal process conditions during fermentation. This is because changes in

viscosity of the fermentation media would affect mass and heat transfer, mixing efficiency, pumping requirement, product and substrate distribution, aeration and the overall economics of the fermentation process (Doran, 2013a). The viscosity and fungi growth profile during the fermentation of the integrated media is shown in Fig. 3. From the figure, it can be observed that increase in biomass concentration increases the viscosity of the media, with the media viscosity declining during the lag phase and the stationary phase.

The growth kinetics of the fungus was investigated using 50 ml and 100 ml filling volume in shake flask cultivations as described in section 2.3. Fungi growth occurred for the 50 ml flask while no fungi growth was observed for the 100 ml shake flask indicating that a high oxygen transfer rate (OTR) was needed to grow the fungi in the media. This can be attributable to the high initial viscosity of the media (Fig. 3a) as there is an inverse relationship between media viscosity and OTR (see equation 7). Using equation 3, the growth rate constant of the filamentous fungus in an integrated media of wheat straw and thin stillage was 0.03 $g^{1/3}/L^{1/3}/h$ with an R^2 of 0.973, which was similar to reported R^2 value of 0.948 when the cube root law model was used elsewhere (Feng et al., 2010).

3.2. Rheology of the fermentation of the integrated media

The consistency index (K) and the flow behavior index (n) are rheological parameters that can be used to understand how easy or difficult it is to control bioreactor process conditions related to fluid flow, such as mixing and oxygen transfer rate. Fig. 4 shows how the consistency index and flow behavior index changed with time during the fermentation of the media. The fermentation media exhibited a pseudoplastic flow behavior before the fermentation started (n = 0.52, K = 0.34 $Pa.s^n$) which continued through the fermentation process. The consistency index increased while the flow behavior index decreased up till 72 h, afterwards the trend was reversed. The increase in the consistency index can be linked to fungi growth occurring during the growth phase. The change in the flow behavior index can be linked to both biomass growth and the absorption of some of the solid particles from the fermentation liquid medium into the fungi. Filamentous fungi growth decreased the flow behavior index, while the absorption of the solid particles increased it. Hence the flow behavior index was increasing towards 1 from the 72^{nd} h, when the fungi growth was approaching the stationary phase (Fig. 3b).

Several authors have proposed that the consistency index (K) and flow behavior index (n) can be correlated with biomass concentration (X) using the relationship shown in equation 11 and 12 (Kumar & Dubey, 2017; Pamboukian & Facciotti, 2005; Queiroz et al., 1997). The model parameters in equation 11 for the consistency index using experimental data for *N. intermedia* during the growth phase were $A1$ = 0.59 and $B1$ = 0.90 with R^2 of 0.99, higher than the reported R^2 of 0.94 for the model relationship for another ascomycete fungi *Aspergillus awamori* (Queiroz et al., 1997). For the flow behavior index, the model (equation 12) had a poor correlation with the experimental data (R^2 = 0.60), while a linear model (shown in equation 13) had a better correlation (R^2 = 0.99) with the experimental data. The deviation of the observed flow behavior index from the model equation (equation 12) that has been used in literature could be explained considering that the substrate used by those authors were Newtonian at the beginning (Pamboukian & Facciotti, 2005; Queiroz et al., 1997), while the fermentation media used in this study was pseudoplastic, which agrees with the findings reported by Riley et al. (2000).

$$K = A_1 X^{B1} \quad (11)$$

$$n = E_1 X^{F1} \quad (12)$$

$$n = 0.539 - 0.062X \quad (13)$$

Substituting the equation for biomass growth (equation 3) into equation 11, the consistency index for the fungal growth in a pseudoplastic media can be estimated with time in a bioreactor during the growth phase. Similar analogy applies to the flow behavior index when equation 3 is put into equation 13. Doing this for a bioreactor with an initial biomass concentration of 0.3 g/L gave consistency index values from 0.2 to 3.8 $Pa.s^n$ and flow behavior index from 0.52 to 0.02, which were similar to the reported consistency and flow behavior index during the growth phase and pseudoplastic flow behavior pattern of the fermentation media of another ascomycete fungi (Queiroz et al., 1997).

3.3. Hydrodynamics of the fermentation of the integrated media

Several factors such as stirring rate, aeration rate, gas hold-up time or volume, geometry of the bioreactor, media viscosity, sparger design affect the hydrodynamic conditions in a bioreactor (Olmos et al., 2013; Serrano-Carreón et al., 2015). For filamentous fungi, the use of stirrers increases the shear force in the bioreactor which could damage the cell wall (Serrano-Carreón et al., 2015). To eliminate this, mixing was carried out only via aeration in this study. Hence only hydrodynamic factors related to aeration (oxygen transfer rate and foam formation) were investigated using shake flask and bioreactor cultivations.

For shake flask fermentation of the media, the oxygen transfer rate (OTR) was calculated using equation 8. Using the reported values of the viscosity exponent (c) in literature which ranged from -0.4 to -0.7, the OTR on the commencement of the fermentation of the integrated media when a filling volume of 100 mL was used in 250 mL flask would be from 0.088 to 0.356 mmol-O_2/L/h. However, no fungi growth was observed after 96 h of cultivation for that range of OTR. Under similar conditions growth was observed when 50 mL filling volume was used for the fermentation in shake flasks. This could indicate that OTR values higher than 0.356 mmol-O_2/L/h would be needed for growing the fungus in the pseudoplastic media. This is because for growth to occur, the oxygen uptake rate (OUR) should be less than or equal to the OTR, and the reported OTR for shake flask where fungi growth was recorded were higher than 0.356 mmol-O_2/L/h (Osadolor et al., 2017; Tang & Zhong, 2003). Different OTR was calculated using different values of viscosity exponent and it summarized in Table 1. As the OTR should be higher than 0.356 mmol-O_2/L/h for *N. intermedia* growth to occur in the pseudoplastic media, only viscosity exponents -0.5 and -0.4 can be used in equation 8 to estimate the OTR into the fermentation media as the fungal growth was observed up to 96 h (Fig. 3b).

For the same aeration rate of 1.4 volume per volume per minute (VVM), hydrodynamics effect was investigated in three different bioreactors designs namely; an airlift bioreactor, a bubble column bioreactor and a textile bioreactor. This high aeration rate was used because the reported average OUR in aerobic bioreactors to prevent oxygen mass transfer limitation is 200 mmol-O_2/L/h and also because of the high initial viscosity of the media (Benz, 2011). For the airlift and bubble column bioreactor foaming was observed throughout the duration of the fermentation despite the continual addition of antifoam. This led to a loss of 1.5 L and 1.9 L of the fermentation media from the airlift bioreactor and bubble column bioreactor respectively. For the textile bioreactor, foaming was only observed during startup, antifoam was added and the bioreactor functioned without foaming. The better performance of the textile bioreactor than the airlift or bubble column bioreactor (with regards to foaming) can be explained using the foam rise velocity (equations 9 and 10). As the textile bioreactor had a higher cross-sectional area (0.050 m^2) than the airlift and bubble column bioreactors (0.008 m^2), the gas rise velocity for the textile bioreactor was 6.25 times less than those from the airlift and bubble column bioreactors. The higher the gas rise velocity the higher the foam rise velocity (equation 9). Another explanation for the minimized foaming in the textile

bioreactor was the design of the sparger or aeration tubing in the bioreactor (Osadolor et al., 2015). The aeration tubing was coiled into six wounds which increased the randomness of bubbles coming out of the aeration tubing (Fig. 2c), which would increase the bubble collision rate, increase bubble size, reduce the rising rate of the bubble and minimize foam stabilization (Delvigne & Lecomte, 2010). This also explained why there was less liquid medium loss (due to foaming) from the airlift bioreactor than the bubble column as the airlift bioreactor design has a down-comer liquid and gas stream which increases its bubble collision rate than the bubble column bioreactor.

For a specific liquid up flow velocity, there tend to be a gas rise velocity above which foam formation and stabilization occurs (Guitian & Joseph, 1998). Because of the high viscosity of the fermentation media (with viscosity approximately 100 cP), the liquid up flow velocity would be lower than that for other non-viscous media, hence there would be higher tendencies for foam formation to occur in it at high aeration rate than other non-viscous media (Flores-Cotera & García-Salas, 2005). To investigate the aeration rate from which foam formation and stabilization began during the fermentation of the integrated media, fermentation was carried out using different aeration rate (from 0.8 VVM to 1.4 VVM) in the airlift bioreactor. Foam formation and stabilization occurred when the aeration rate had increased up to 1.2 VVM. So for a volumetric air flowrate to cross-sectional area ratio of 8.75×10^{-3} ($m^3/s/m^2$) or higher foam formation and stabilization would occur during the fermentation of the media.

3.4. Effect of rheology and hydrodynamics on substrate consumption and product formation

As the rheological and hydrodynamic conditions during the fermentation of the media affected the media composition and fungi growth, they also influenced how well the fermentation process proceeded. Fig. 5 shows the product formation and substrate consumption in shake flask and three bioreactor designs. In the shake flask cultivations where there was no foaming there was an ethanol yield of 0.26 ± 0.01 g/g after 48 h and a biomass yield of 0.42 ± 0.01 g/g after 72 h. For the bioreactors, the textile bioreactor without foaming challenge had a better performance with highest ethanol yield of 0.22 ± 0.01 g/g, while it had a substrate consumption rate of 0.38 ± 0.01 g/L/h and a biomass yield of 0.47 ± 0.01 g/g during the growth phase (fermentation period of 48 h). The high biomass yield could be attributed to the ability of the fungi to produce enzymes that aid it to assimilated some of the un-hydrolyzed solid into its cell wall (Ferreira et al., 2013).

As an OTR higher than 0.356 mmol-O_2/L/h was needed for growing the fungus and the substrate and product formation profile for both the shake flask cultivation and textile bioreactor cultivation were similar (Fig.5 a and b), so the OTR in the textile bioreactor was adequate at an aeration rate of 1.4 VVM. A high initial media viscosity meant that high aeration rate would be needed for fungi growth in the media. High aeration rate increased the gas rise velocity (equation 9), which increased the foam formation and stabilization tendencies as experienced in the airlift and bubble column bioreactor at an aeration rate of 1.4 VVM. Continual addition of antifoam to a bioreactor reduces the OTR in bioreactors which could lead to oxygen mass transfer limitations (Hoeks et al., 2003; Yasukawa et al., 1991). Also, the loss of media from the bioreactors could also be a reason for the lower ethanol productivity from airlift and bubble column bioreactors. Despite that, the biomass yield from the airlift and bubble column bioreactors were 0.48 ± 0.01 g/g and 0.44 ± 0.02 g/g respectively after 48 h. Using an aeration rate of 1 VVM in the airlift bioreactor minimized

foam stabilization. This led to increased ethanol productivity by 34 % after 48 h but it resulted in reduced biomass yield of 0.43 g/g ± 0.01 after 72 h.

4. Conclusions

The rheological properties of a fermentation media composed of a 1:1 mixture of hydrolyzed wheat straw and thin stillage and the bioreactor hydrodynamics condition influenced the ethanol productivity, biomass concentration and substrate consumption rate. The high initial viscosity (93 ± 4 cP) of the fermentation media meant that an oxygen transfer rate higher than 0.356 mmol-O2/L/h was needed for fungi growth. High aeration rate resulted in foaming the bioreactors examined. The textile bioreactor with a gas rise velocity 6.25 times less than the airlift and bubble column bioreactor had the best performance with minimal foaming, an ethanol yield of 0.22 ± 0.01 g/g, substrate consumption rate of 0.38 ± 0.01 g/L/h and a biomass yield of 0.47 ± 0.01 g/g after 48 h of fermentation.

Acknowledgments

The authors acknowledge Lantmännen Agroetanol Sweden for providing the thin stillage used for the experiments performed in this article. The authors also appreciate Research Institute of Sweden (RISE) whose Biorefinery Demo Plant at Örnsköldsvik, was used for pretreating the wheat straw used for the experiments in this article.

References

Auro, M.A., Hodge, H.M., Roth, N.G. 1957. Oxygen absorption rates in shaken flasks. *Industrial & Engineering Chemistry*, **49**(8), 1237-1238.

Baudez, J.-C., Coussot, P. 2001. Rheology of aging, concentrated, polymeric suspensions: application to pasty sewage sludges. *Journal of Rheology*, **45**(5), 1123-1139.

Benz, G.T. 2011. Bioreactor design for chemical engineers. *Chem. Eng. Prog*, **107**(2126), 13.

Delvigne, F., Lecomte, J.p. 2010. Foam formation and control in bioreactors. *Encyclopedia of Industrial Biotechnology*.

Doran, P.M. 2013a. Chapter 7 - Fluid Flow. in: *Bioprocess Engineering Principles (Second Edition)*, Academic Press. London, pp. 201-254.

Doran, P.M. 2013b. Chapter 14 - Reactor Engineering. in: *Bioprocess Engineering Principles (Second Edition)*, Academic Press. London, pp. 761-852.

Durgueil, E.J. 1987. Determination of the consistency of non-Newtonian fluids using a Brookfield HBT viscometer. *Proceedings of the annual congress-South African Sugar Technologists' Association*.

Feng, Y.-L., Li, W.-Q., Wu, X.-Q., Cheng, J.-W., Ma, S.-Y. 2010. Statistical optimization of media for mycelial growth and exo-polysaccharide production by Lentinus edodes and a kinetic model study of two growth morphologies. *Biochemical Engineering Journal*, **49**(1), 104-112.

Ferreira, J.A., Lennartsson, P.R., Edebo, L., Taherzadeh, M.J. 2013. Zygomycetes-based biorefinery: Present status and future prospects. *Bioresource Technology*, **135**, 523-532.

Flores-Cotera, L.B., García-Salas, S. 2005. Gas holdup, foaming and oxygen transfer in a jet loop bioreactor with artificial foaming media and yeast culture. *Journal of biotechnology*, **116**(4), 387-396.

Garcia-Ochoa, F., Gomez, E. 2009. Bioreactor scale-up and oxygen transfer rate in microbial processes: an overview. *Biotechnology advances*, **27**(2), 153-176.

Gögus, N., Tari, C., Oncü, S., Unluturk, S., Tokatli, F. 2006. Relationship between morphology, rheology and polygalacturonase production by Aspergillus sojae ATCC 20235 in submerged cultures. *Biochemical Engineering Journal*, **32**(3), 171-178.

Guitian, J., Joseph, D. 1998. How bubbly mixtures foam and foam control using a fluidized bed. *International Journal of Multiphase Flow*, **24**(1), 1-16.

Hoeks, F.W.J.M.M., Boon, L.A., Studer, F., Wolff, M.O., van der Schot, F., Vrabél, P., van der Lans, R.G.J.M., Bujalski, W., Manelius, Å., Blomsten, G., Hjorth, S., Prada, G., Luyben, K.C.A.M., Nienow, A.W. 2003. Scale-up of stirring as foam disruption (SAFD) to industrial scale. *Journal of Industrial Microbiology and Biotechnology*, **30**(2), 118-128.

Jabbari, M., Osadolor, O., Nair, R., Taherzadeh, M. 2017. All-Polyamide Composite Coated-Fabric as an Alternative Material of Construction for Textile-Bioreactors (TBRs). *Energies*, **10**(11), 1928.

Kadic, E., Heindel, T.J. 2014. Concluding Remarks. in: *An Introduction to Bioreactor Hydrodynamics and Gas-Liquid Mass Transfer*, John Wiley & Sons, Inc., pp. 263-266.

Koutinas, A.A., Wang, R., Kookos, I.K., Webb, C. 2003. Kinetic parameters of Aspergillus awamori in submerged cultivations on whole wheat flour under oxygen limiting conditions. *Biochemical Engineering Journal*, **16**(1), 23-34.

Kumar, P., Dubey, K.K. 2017. Mycelium transformation of Streptomyces toxytricini into pellet: Role of culture conditions and kinetics. *Bioresource technology*, **228**, 339-347.

Liu, Y.-S., Wu, J.-Y., Ho, K.-p. 2006. Characterization of oxygen transfer conditions and their effects on Phaffia rhodozyma growth and carotenoid production in shake-flask cultures. *Biochemical engineering journal*, **27**(3), 331-335.

Nair, R.B., Kabir, M.M., Lennartsson, P.R., Taherzadeh, M.J., Horváth, I.S. 2018. Integrated process for ethanol, biogas, and edible filamentous fungi-based animal feed production from dilute phosphoric acid-pretreated wheat straw. *Applied biochemistry and biotechnology*, **184**(1), 48-62.

Nair, R.B., Lundin, M., Lennartsson, P.R., Taherzadeh, M.J. 2017. Optimizing dilute phosphoric acid pretreatment of wheat straw in the laboratory and in a demonstration plant for ethanol and edible fungal biomass production using Neurospora intermedia. *Journal of Chemical Technology & Biotechnology*, **92**(6), 1256-1265.

Nair, R.B., Taherzadeh, M.J. 2016. Valorization of sugar-to-ethanol process waste vinasse: a novel biorefinery approach using edible ascomycetes filamentous fungi. *Bioresource technology*, **221**, 469-476.

Núñez-Ramírez, D.M., Medina-Torres, L., Valencia-López, J.J., Calderas, F., López-Miranda, J., Medrano-Roldán, H., Solís-Soto, A. 2012. Study of the rheological properties of a fermentation broth of the fungus Beauveria bassiana in a bioreactor under different hydrodynamic conditions. *Journal of microbiology and biotechnology*, **22**(11), 1494-1500.

Olmos, E., Mehmood, N., Husein, L.H., Goergen, J.L., Fick, M., Delaunay, S. 2013. Effects of bioreactor hydrodynamics on the physiology of Streptomyces. *Bioprocess and biosystems engineering*, **36**(3), 259-272.

Osadolor, O., Lennartsson, P., Taherzadeh, M. 2015. Development of Novel Textile Bioreactor for Anaerobic Utilization of Flocculating Yeast for Ethanol Production. *Fermentation*, **1**(1), 98.

Osadolor, O.A., Lennartsson, P.R., Taherzadeh, M.J. 2014. Introducing Textiles as Material of Construction of Ethanol Bioreactors. *Energies*, **7**(11), 7555-7567.

Osadolor, O.A., Nair, R.B., Lennartsson, P.R., Taherzadeh, M.J. 2017. Empirical and experimental determination of the kinetics of pellet growth in filamentous fungi: A case study using Neurospora intermedia. *Biochemical Engineering Journal*, **124**, 115-121.

Pamboukian, C.R.D., Facciotti, M.C.R. 2005. Rheological and morphological characterization of Streptomyces olindensis growing in batch and fed-batch fermentations. *Brazilian Journal of Chemical Engineering*, **22**(1), 31-40.

Papagianni, M. 2004. Fungal morphology and metabolite production in submerged mycelial processes. *Biotechnology Advances*, **22**(3), 189-259.

Queiroz, M.C.R., Facciotti, M.C.R., Schmidell, W. 1997. Rheological changes of Aspergillus awamori broth during amyloglucosidase production. *Biotechnology Letters*, **19**(2), 167-170.

Riley, G.L., Tucker, K.G., Paul, G.C., Thomas, C.R. 2000. Effect of biomass concentration and mycelial morphology on fermentation broth rheology. *Biotechnology and bioengineering*, **68**(2), 160-172.

Serrano-Carreón, L., Galindo, E., Rocha-Valadéz, J.A., Holguín-Salas, A., Corkidi, G. 2015. Hydrodynamics, fungal physiology, and morphology. in: *Filaments in Bioprocesses*, Springer, pp. 55-90.

Tang, Y.-J., Zhong, J.-J. 2003. Role of oxygen supply in submerged fermentation of Ganoderma lucidum for production of Ganoderma polysaccharide and ganoderic acid. *Enzyme and Microbial technology*, **32**(3-4), 478-484.

Um, B.-H., Hanley, T.R. 2008. A comparison of simple rheological parameters and simulation data for Zymomonas mobilis fermentation broths with high substrate loading in a 3-L bioreactor. *Applied Biochemistry and Biotechnology*, **145**(1-3), 29-38.

Verma, M., Brar, S.K., Tyagi, R.D., Sahai, V., Prévost, D., Valéro, J.R., Surampalli, R.Y. 2007. Bench-scale fermentation of Trichoderma viride on wastewater sludge: Rheology, lytic enzymes and biocontrol activity. *Enzyme and Microbial Technology*, **41**(6), 764-771.

Yasukawa, M., Onodera, M., Yamagiwa, K., Ohkawa, A. 1991. Gas holdup, power consumption, and oxygen absorption coefficient in a stirred-tank fermentor under foam control. *Biotechnology and bioengineering*, **38**(6), 629-636.

Tables and Figures

Table 1. Estimated oxygen transfer rate (mmol-O_2/L/h) during the fermentation of the integrated media in shake flask cultivations

Time (h)	**Oxygen transfer rate using different viscosity exponent** (mmol-O_2/L/h)			
	-0.7	-0.6	-0.5	-0.4
0	0.279	0.438	0.690	1.085
24	0.353	0.537	0.816	1.242
48	0.130	0.228	0.399	0.701
72	0.120	0.212	0.377	0.670
96	0.107	0.193	0.348	0.628

Figures

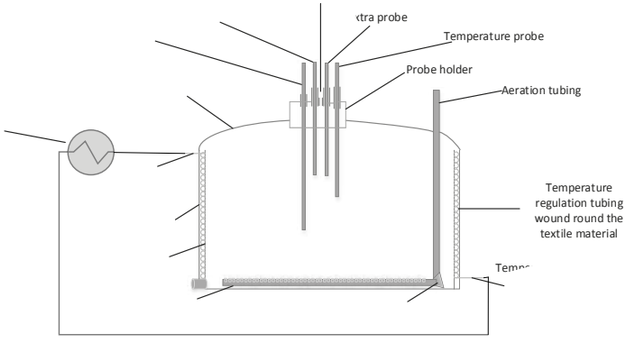

Fig. 1. Schematic representation of the textile bioreactor.

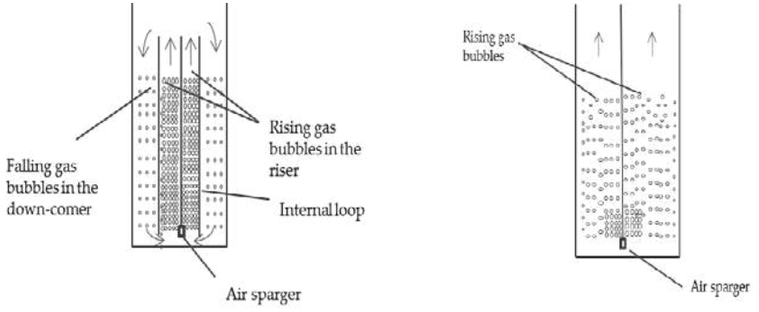

(**a**) (**b**)

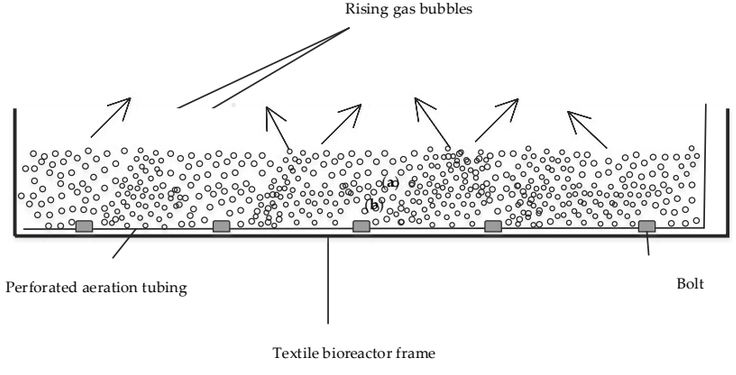

Fig. 2. Schematic representation of bubbling pattern in an airlift bioreactor (**a**), a bubble column bioreactor (**b**) and a textile bioreactor (c)

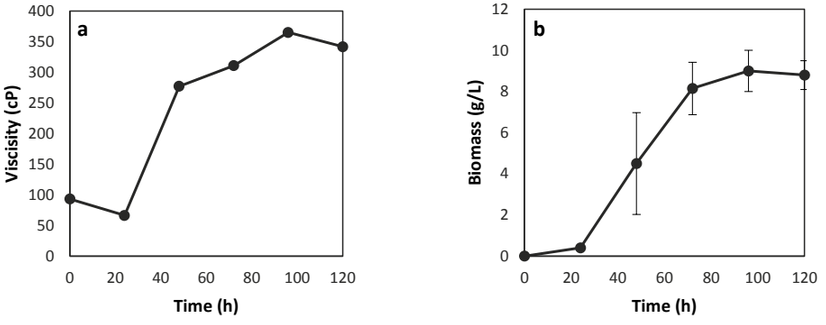

Fig. 3. Viscosity (a) and Fungi growth (b) profile during the fermentation of the integrated media in shake flask.

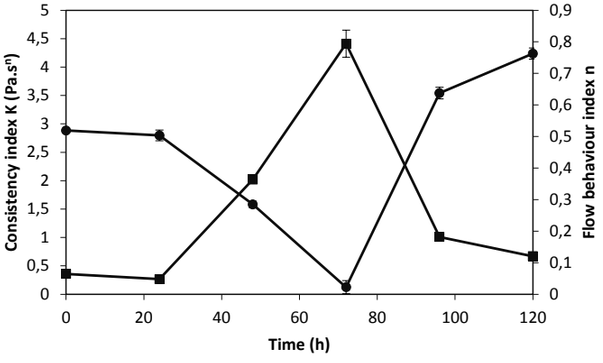

Fig. 4. The consistency index (■) (primary axis) and flow behavior index (●) (secondary axis) profile during the fermentation of the integrated media.

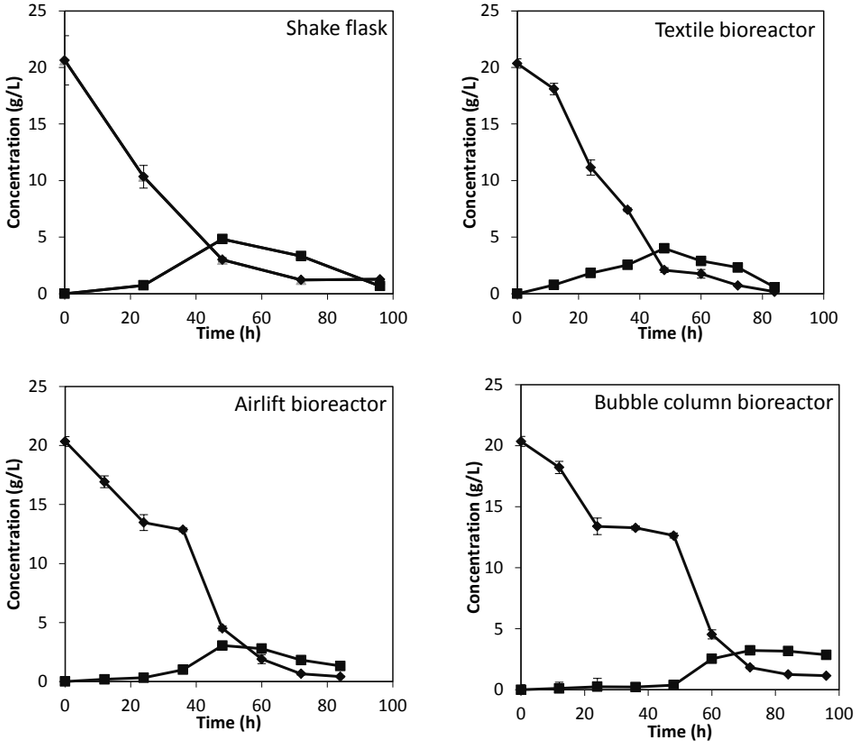

Fig. 5. Combined sugar concentration (♦) and ethanol concentration (■) with time during the fermentation of the integrated media in shake flask, textile bioreactor, airlift bioreactor and bubble column bioreactor.